Gradual evolution of allopolyploidy in *Arabidopsis suecica*

Robin Burns[1], Terezie Mandáková[2], Joanna Gunis[1], Luz Mayela Soto-Jiménez[1], Chang Liu[3], Martin A. Lysak[2], Polina Yu. Novikova[4,5*] and Magnus Nordborg[1*]

[1]Gregor Mendel Institute, Austrian Academy of Sciences, Vienna BioCenter, Vienna, Austria.
[2]CEITEC - Central European Institute of Technology, and Faculty of Science, Masaryk University, Brno, Czech Republic.
[3]Institute of Biology, University of Hohenheim, Garbenstrasse 30, 70599 Stuttgart, Germany.
[4]VIB-UGent Center for Plant Systems Biology, Ghent, Belgium.
[5]Department of Chromosome Biology, Max Planck Institute for Plant Breeding Research, Cologne, Germany.

***Corresponding authors: pnovikova@mpipz.mpg.de, magnus.nordborg@gmi.oeaw.ac.at**

Abstract

The majority of diploid organisms have polyploid ancestors. The evolutionary process of polyploidization (and subsequent re-diploidization) is poorly understood, but has frequently been conjectured to involve some form of "genome shock" — partly inspired by studies in crops, where polyploidy has been linked to major genomic changes such as genome reorganization and subgenome expression dominance. It is unclear, however, whether such dramatic changes would be characteristic of natural polyploidization, or whether they are a product of domestication. Here, we study polyploidization in *Arabidopsis suecica* (n = 13), a post-glacial allopolyploid species formed via hybridization of *A. thaliana* (n = 5) and *A. arenosa* (n = 8). We generated a chromosome-level genome assembly of *A. suecica* and complemented it with polymorphism and transcriptome data from multiple individuals of all species. Despite a divergence of ~6 Mya between the two ancestral species and appreciable differences in their genome composition, we see no evidence of a genome shock: the *A. suecica* genome is highly colinear with the ancestral genomes, there is no subgenome dominance in expression, and transposable element dynamics appear to be stable. We do, however, find strong evidence for changes suggesting gradual adaptation to polyploidy. In particular, the *A. thaliana* subgenome shows upregulation of meiosis-related genes, possibly in order to prevent aneuploidy and undesirable homeologous exchanges that are frequently observed in experimentally generated *A. suecica*, and the *A. arenosa* subgenome shows upregulation of cyto-nuclear related processes, possibly in response to the new cytoplasmic environment of *A. suecica,* with plastids maternally inherited from *A. thaliana*.

Introduction

Ancient polyploidization or whole-genome duplication is a hallmark of most higher-organism genomes[1,2], including our own[3,4]. While most of these organisms are now diploid and show only traces of polyploidy, there are many examples of recent polyploidization, in particular among flowering plants[5–9]. These examples are important because they allow us to study the process of polyploidization, rather than just inferring that it happened and trying to understand its evolutionary importance.

Wide-spread naturally occuring polyploid hybrids (i.e. allopolyploids), such as *Capsella bursa-pastoris* (Shepherd's Purse)[10–12], *Trifolium repens* (white clover)[13], *Brachypodium hybridum*[14,15], *Arabidopsis kamchatica*[16], *Mimulus peregrinus*[17], *Tragopogon miscellus* and *T. mirus*[18], demonstrate that natural polyploid species can quickly become successful, and even be deemed invasive[19]. Regardless of their eventual evolutionary success, new allopolyploid species face numerous challenges, ranging from those on a population level, such as bottlenecks[13,20] and competition with their diploid progenitors[21], to those on a genomic level, such as chromosome segregation[22–24] and changes to hybrid genome structure (e.g. chromosomal structural variants and aneuploidy[25]) and genome regulation (e.g. subgenome expression dominance[26] and the regulation of transposable elements[27]) — phenomena which may be enhanced by genomic conflicts between the newly merged subgenomes, leading to a "genome shock"[28]. In agreement with this, genomic and transcriptomic changes tied to the hybridization of two (or more) diverged genomes have been reported in resynthesized polyploids of wheat[29–35], *Brassica napus*[36–38] and cotton[39,40-37,41,42] (although resynthesized cotton appears genetically stable[43]).

The long-term importance of such rapid changes is less clear . For example, the transposable element transcription and mobilization observed in resynthesized wheat[33,44–46], is not reflected in the genome sequence of cultivated wheat[47]. However, other cultivated crop genomes, for example cotton, show instances of large structural rearrangements[5,48–50], biased gene loss[51], a spreading and proliferation of centromere repeats between subgenomes[52] and changes to the 3D genome structure[53]. Strawberry[6], peanut[8] and the mesopolyploids *B. rapa*[54] and maize[55] show evidence of subgenome dominance, while wheat[56], cotton[51] and *B. napus*[57] do not. The reasons for these differences are not understood.

An even greater source of uncertainty is whether allopolyploid crops are representative of natural polyploidization. Domestication is frequently associated with very strong "artifical" selection, which can dramatically alter the fitness landscape[58–62]. For example, large structural variants have been linked to favourable agronomic traits[63–65]. In addition, polyploid crops are generally quite recent, evolutionarily speaking.

Turning to non-domesticated species, genomic changes have been reported in natural allopolyploids like the ~80 years old *Tragopogon miscellus*[66,67], the ~140 years old *Mimulus pergrinus*[17], and *Spartina anglica*[68] , which likely originated at the end of the 19th century — however, these examples are extremely recent and are more in line with the reported genomic changes in the resynthesized allopolyploids. Older natural allopolyploids, on the other hand, generally do not show signs of genomic changes after allopolyploidy. Examples of these include: white clover[13], *C. bursa-pastoris*[12,69], *A. kamchatica*[16,70], *B. hybridium*[14] and the gymnosperm *Ephedra*[71].

Here we focus on an allopolyploid comparable in age to these examples, the highly selfing[72], *A. suecica* (2n = 4x = 26), formed through the hybridization of *A. thaliana* (2n = 10) and *A. arenosa* (2n = 2x/4x = 16/32), circa 16 kya, during the Last Glacial Maximum[20] and

now widely established in northern Fennoscandia (Fig. 1a). The ancestral species diverged around 6 Mya[73], and, based on mitochondrial and chloroplast sequences, it is clear that *A. thaliana* is the maternal and *A. arenosa* the paternal parent of the hybrid[74], a scenario also supported by the fact that *A. arenosa* itself is a ploidy-variable species, so that *A. suecica* could readily be generated through the fertilization of an unreduced egg cell (2n = 2x) from *A. thaliana* by a sperm cell (n = 2x) from autotetraploid *A. arenosa*[20,75]. We have previously shown that, although *A. suecica* shows clear evidence of a genetic bottleneck[20], it shares most of its variation with the ancestral species, demonstrating that the species was formed through a hybridization and polyploidization process that involved many crosses and individuals. In order to study genomic change in *A. suecica*, we used long-read sequencing to generate a high-quality, chromosome-level assembly of a single individual, taking advantage of the fact that *A. suecica*, like *A. thaliana*, is highly selfing, making it possible to sequence naturally inbred individuals. The genome sequence was complemented by a partial assembly of a tetraploid outcrosser *A. arenosa*, and by short-read genome and transcriptome sequencing data from many individuals of all three species — including "synthetic" *A. suecica* generated *de novo* in laboratory crosses.

Results and discussion

1. The genome is conserved

We assembled a reference genome from a naturally inbred (i.e. the species is self-compatible[20,72]) *A. suecica* accession ("ASS3"), using 50x long-read PacBio sequencing (PacBio RS II). The absence of heterozygosity and the substantial (~11.6%) divergence between the subgenomes greatly facilitated the assembly. In contrast, assembling even a diploid genome of the outcrosser *A. arenosa* is complicated by high heterozygosity (nucleotide diversity around 3.5%[76]) coupled with a relatively high level of repetitive sequences (compared to the gene-rich *A. thaliana* genome). Our attempt to assemble a tetraploid *A. arenosa* individual, the result of which is also included here in addition to the genome of *A. suecica*, led to a very fragmented assembly of 3,629 contigs with an N50 of 331 Kb. In contrast, the *A. suecica* assembly has an N50 contig size of 9.02 Mb. The assembled contigs totaled 276 Mb (~90% of the 305 Mb genome size estimated by flow cytometry — see Supplementary Fig. 1; ~88% of the 312Mb genome size estimated by kmer analysis). Contigs were placed into scaffolds using high-coverage chromosome conformation capture (HiC) data and by using the reference genomes of *A. thaliana* and *A. lyrata* (here the closest substitute for *A. arenosa*) as guides. This resulted in 13 chromosome-scale scaffolds (Supplementary Fig. 2a). The placement and orientation of each contig within a scaffold was confirmed and corrected using a genetic map for *A. suecica* (see Methods, Supplementary Fig. 3, Supplementary Fig. 4). The resulting chromosome-level assembly (Fig. 1b) contains 262 Mb, and has an N50 scaffold size of 19.59 Mb. The five chromosomes of the *A. thaliana* subgenome and the eight chromosomes of the *A. arenosa* subgenome sum to 119 Mb and 143 Mb, respectively.

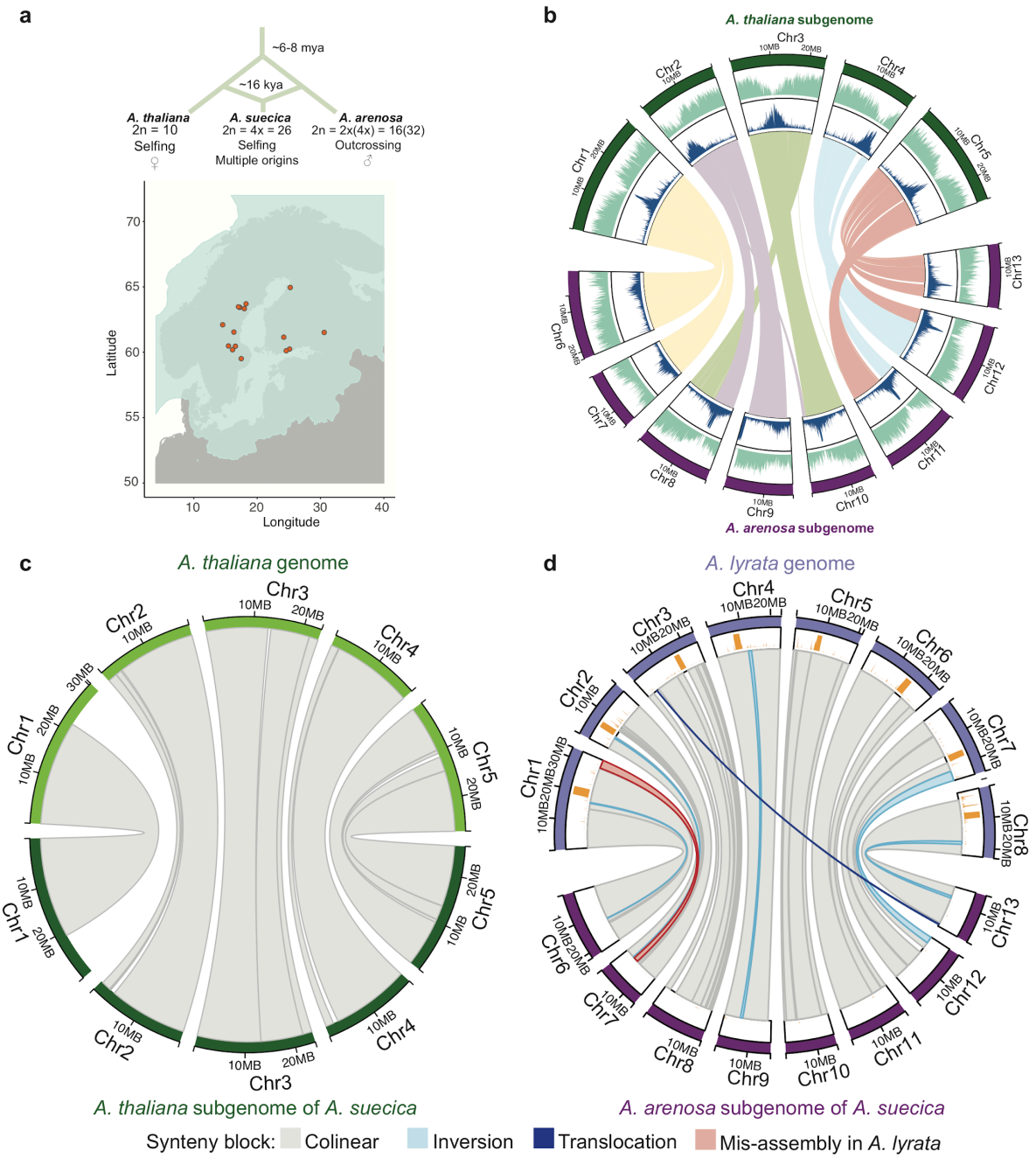

Figure 1. The genome of *A. suecica* is largely colinear with the ancestral genomes. **a** Schematic depicting the origin of *A. suecica* and its current distribution in the relation to the ice cover at the last glacial maximum (LGM). **b** The chromosome-level assembly of the *A. suecica* genome with inner links depicting syntenic blocks between the *A. thaliana* and *A. arenosa* subgenomes of *A. suecica*. The blue histogram represents the distribution of TEs along the genome and the green histogram corresponds to the distribution of protein-coding genes. **c** Synteny of the *A. thaliana* subgenome of *A. suecica* to the *A. thaliana* TAIR10 reference. In total 13 colinear synteny blocks were found. **d** Synteny of the *A. arenosa* subgenome to *A. lyrata*. In total 40 synteny blocks were found, 33 of which were colinear. Of the remaining 7 blocks, 5 represent inversions in the *A. arenosa* subgenome of *A. suecica* compared to *A. lyrata*, 1 is a translocation, and 1 corresponds to a previously reported mis-assembly in the *A. lyrata* genome[77]. Orange bars represent a density plot of missing regions ("N" bases) in the *A. lyrata* genome.

Approximately 108 and 135 Mb of the *A. thaliana* and *A. arenosa* subgenomes of *A. suecica* are in large blocks syntenic to the genomes of the ancestral species: 13 and 40 blocks, respectively (Fig. 1c,d). The vast majority of these syntenic blocks are themselves also colinear, with the exception of five small-scale inversions (~4.5 Mb) and one translocation (~244 Kb) on the *A. arenosa* subgenome— which may well (indeed probably do) reflect differences between *A. lyrata* and *A. arenosa*, two highly polymorphic species separated by about a million years[73,76]. We also corrected for the described[77] mis-assembly in the *A. lyrata* reference genome using our genetic map. Overall we find that approximately 93% of the *A. suecica* genome is syntenic to the ancestral genomes, the 13 chromosomes of *A. suecica* having remained almost completely colinear (Fig. 1c,d). This highlights the conservation of the *A. suecica* genome and contrasts with the major rearrangements that have been observed in several resynthesized polyploids[29,32,34,36] and some crops[48,50,78]. Interestingly, major rearrangements have also been observed in synthetic *A. suecica*[79], and we see clear evidence of aneuploidy in ours — a topic to which we shall return.

A total of 45,585 protein-coding genes were annotated for the *A. suecica* reference, of which 22,232 and 23,353 are located on the *A. thaliana* and *A. arenosa* subgenomes, respectively. We assessed completeness of the genome assembly and annotation with the BUSCO set for eudicots and found 2088 (98.4%) complete genes for both the *A. thaliana* and *A. arenosa* subgenomes (Supplementary Fig. 5c,d). Of the protein-coding genes, 18,023 had a one-to-one orthology between the subgenomes of *A. suecica* and 16,999 genes were conserved in a 1:1:1:1 relationship for both subgenomes of *A. suecica* and the ancestral species (using *A. lyrata* as a substitute for *A. arenosa*) (Supplementary Data 2, Supplementary Fig. 5b). We functionally annotated lineage-specific genes in *A. suecica* (i.e. genes in *A. suecica* without a reciprocal best blast hit to *A. thaliana* or *A. lyrata*) using InterPro, and only found significant enrichment in *A. thaliana* subgenome of *A. suecica* for two GO terms (GO:0008234 and GO:0015074), both of which are associated with repeat content (Supplementary Data 2). Ancestral genes not found in the *A. suecica* genome annotation were overrepresented for functional categories of plant defense response. However, checking coverage for these genes by mapping the raw *A. suecica* whole-genome resequencing data to the ancestral genomes did not confirm their loss, suggesting rather misassembly or misannotation, which is expected due to the repetitive and highly polymorphic nature of R-genes in plants.

2. The rDNA clusters are highly variable

In eukaryotic genomes, genes encoding ribosomal RNA (rRNA) occur as tandem arrays in rDNA clusters. The 45S rDNA clusters are particularly large, containing hundreds or thousands of copies, spanning millions of base pairs[80]. The nucleolus, the site of pre-ribosome assembly, forms at these clusters, but only if they are actively transcribed, and it was observed long ago that only one parent's rDNA tended to be involved in nucleolus formation in inter-specific hybrids, a phenomenon known as "nucleolar dominance"[81–84]. In *A. suecica,* it was observed that the rDNA clusters inherited from *A. thaliana* were silenced[85–87], and structural changes associated with these clusters were also suggested[88].

Given this, we examined the composition of 45S rDNA repeats as well as their transcription. While the large and highly repetitive 45S rDNA clusters are not part of the genome assembly, it is possible to measure the copy number of *A. thaliana* and *A. arenosa* 45S rRNA genes using sequencing coverage (see Methods), and we find three accessions to

have experienced massive loss of the *A. thaliana* rDNA loci (Fig. 2a), which we confirmed for one of the accessions ("AS90a") by FISH analysis (Fig. 2b,c). However, there is massive copy number variation for 45S rRNA genes in *A. suecica* (Fig. 2a), and some accessions (e.g., the reference accession "ASS3") have higher *A. thaliana* than *A. arenosa* 45S rRNA copy number (Fig. 2d,e).

Turning to expression, we also find nucleolar dominance to be variable in *A. suecica* (see Methods and Supplementary Fig. 6), with the majority of accessions expressing both 45S rRNA alleles, five exclusively expressing *A. arenosa* 45S rRNA, and one exclusively expressing *A. thaliana* 45S rRNA (Fig. 2a).

This extensive variation in 45S cluster size and expression is reminiscent of the genetically controlled intraspecific variation seen in *A. thaliana* (where different accessions express either the chromosome 2 or chromosome 4 rDNA cluster, or both[89,90]), and is in agreement with a previous observation made in natural *A. suecica* that both rDNA clusters can be expressed[91]. This suggests that the phenomenon of nucleolar dominance can at least partly be explained by retained ancestral variation. However, the large-scale decrease in rDNA cluster size observed in some accessions may be a direct consequence of allopolyploidization itself, as synthetic *A. suecica* sometimes shows immediate loss of 45S rDNA (even as early as the F1 stage) and this too varies between siblings and generations (Supplementary Fig. 6a). Elimination of rDNA loci has also been previously observed in synthetic wheat[92], and loss of rDNA sites has been reported at higher ploidy levels in strawberry[93].

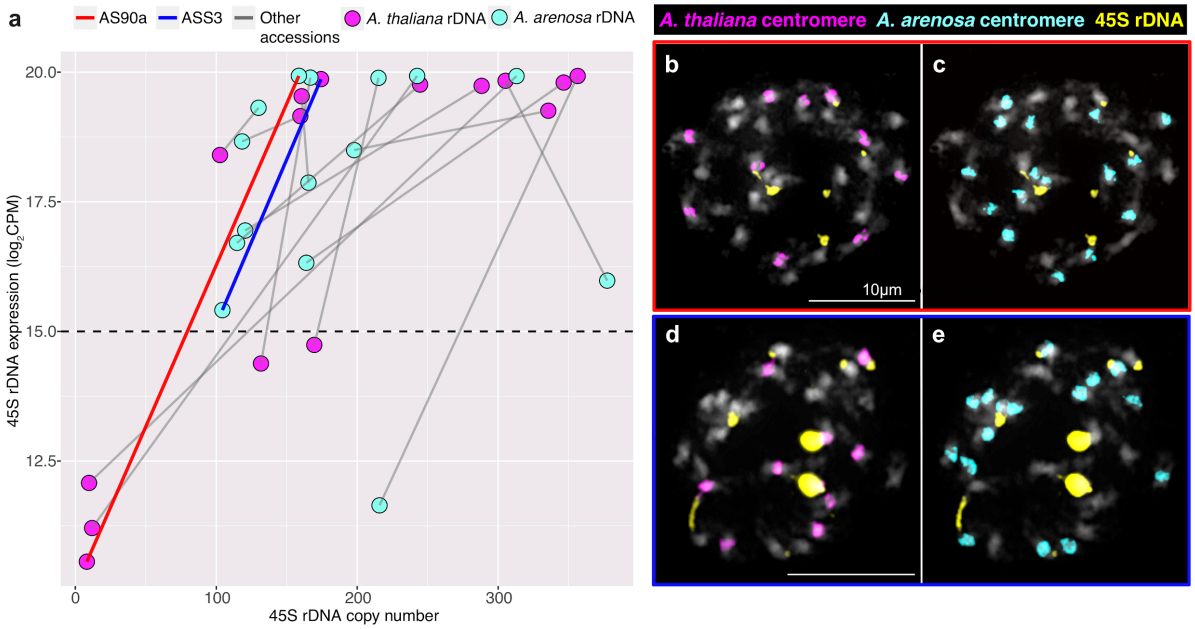

Figure 2. Expression and copy number variation of 45S rDNA in *A. suecica*. a The relationship between expression levels ($\log_2$ CPM) and copy number of 45S rDNA shows extensive variation of 45S rDNA copy number and varying direction of "nucleolar dominance". Grey lines connect subgenomes of the same accession. Values above the dashed line are taken as evidence for the expression of a particular 45S rDNA allele, as this is above the maximum level of mis-mapping seen in the ancestral species here used as a control (see Supplementary Figure 6b). **b** and **c** FISH results of a natural *A. suecica* accession AS90a that has largely lost the rDNA cluster of the *A.thaliana* subgenome (8 copies calculated for the *A. thaliana* 45S rDNA and 159 copies of the *A. arenosa* 45S rDNA). **d** and **e** FISH result of a natural accession ASS3 that has maintained both ancestral rDNA loci (174 copies calculated for the *A. thaliana* 45S rDNA and 104 copies of the *A. arenosa* 45S rDNA).

3. No evidence for abnormal transposon activity

The possibility that hybridization and polyploidization leads to a "genome shock" in the form of increased transposon activity has been much discussed[27,28,94,95]. Evidence for TE proliferation following hybridization has been found for *Ty3/gypsy* retrotransposons in hybrid sunflower species[96], though notably the hybrid sunflower species occupy habitats that are abiotically extreme[97] which is also implicated in LTR proliferation[98]. On the other hand, analysis of TE expression in F1 hybrids between *A. thaliana* and *A. lyrata* found strong correlation, even under drought stress, to the parent species, as well as little alteration of the chromatin marks H3K9me2 and H3K27me3[99] — although it remains unclear whether the F1 generation is not too early to study TE misregulation. Here we examine TE dynamics in natural *A. suecica.*

The two subgenomes of *A. suecica* differ massively in transposon content: there are almost twice as many annotated transposons in the *A. arenosa* as in the *A. thaliana* subgenome (66,722 vs 33,420; see Supplementary Figs. 5a and 7), and the true difference is almost certainly greater given that the *A. arenosa* subgenome assembly is less complete (and many of the missing regions are likely to be repeat-rich) and that the transposon annotation is biased towards *A. thaliana.* Has the combination of two such different genomes lead to increased transposon activity?

Our assembled *A. thaliana* subgenome does contain roughly 3,000 more annotated transposons than the TAIR10 *A. thaliana* reference genome, but this could reflect greater transposon number in the *A. thaliana* ancestors of this genome rather than increased transposon activity in *A. suecica.* In order to gain insight into transposon activity in *A. suecica*, we need to identify jumps that occurred after the species separated (and are thus only found in this species). We used the software PopoolationTE2[100] to call presence-absence variation on a population-scale level using genome re-sequencing datasets for 15 natural *A. suecica* accessions, 18 *A. thaliana* accessions genetically close to *A. suecica*, and 9 *A. arenosa* lines. Of the 24,569 insertion polymorphisms called with respect to the *A. thaliana* subgenome, 8,767 were shared between *A. thaliana* and *A. suecica*, 7,196 were only found in *A. thaliana*, and 8,606 were only found in *A. suecica*. Of the 115,336 insertions on the *A. arenosa* subgenome of *A. suecica,* 13,177 were shared with *A. arenosa*, 83,964 were unique to *A. arenosa*, and 18,195 were unique to *A. suecica* (Supplementary Data 1a,b; Supplementary Figs. 8,9). Considering the number of transposons per individual genome (Fig. 3a), we see that most transposon insertions in a typical *A. thaliana* subgenome are also found in *A. thaliana*, and that the slightly higher transposon load in the *A. thaliana* subgenome is mainly due to these. The reason for this is likely a population bottleneck. In contrast, the number of recent insertions (that are unique to the species) is not higher in the *A. thaliana* subgenome, suggesting that transposon activity in this subgenome is not increased.

Turning to the *A. arenosa* subgenome, we see that a typical *A. suecica* contains only about half the number of transposons of a typical *A. arenosa* individual (Fig. 3a). However, the latter is an outcrossing tetraploid, and it is thus fairer to compare with the number of transposons in four randomly chosen *A. arenosa* subgenomes of *A. suecica* (shown as "*A. arenosa* in *A. suecica* (4n)" in Fig. 3a). This largely accounts for the observed difference, but there are still clearly fewer transposons in *A. suecica*. A population bottleneck likely explains much of this, but it is impossible to rule out a contribution of decreased transposon activity in *A. suecica* as well, which might be explained by its transition to self-fertilization, which is often associated with reduced TE activity[101].

To sum up, we see no evidence for a burst of transposon activity accompanying polyploidization in *A. suecica*, a conclusion also supported by a lack of increase in transposon

expression for both synthetic and natural *A. suecica* compared to the *A. thaliana* and *A. arenosa* on both subgenomes (Supplementary Fig. 9), in agreement with observations made in *A. thaliana* and *A. lyrata* F1 hybrids[99]. We do see clear traces of the population bottleneck accompanying the origin of *A. suecica*, however. The frequency distribution of polymorphic transposon insertions private in *A. suecica* is heavily skewed towards zero — almost certainly because of purifying selection because the distribution is more similar to that of non-synonymous SNPs than to that of synonymous SNPs (Fig. 3b,c). However, for both subgenomes, *A. suecica* also contains a large number of fixed or nearly-fixed insertions that are present in the ancestral species at lower frequency (Fig. 3d,e). These are likely to have reached high-frequency as a result of a bottleneck. Shared transposons are enriched in the pericentromeric regions of the genome depleted of protein-coding genes, while unique transposons insertions, which are generally at low frequency, show a more uniform distribution across the genome, consistent with evidence for stronger selection against transposon insertion in the relatively gene-dense chromosome arms[102,103] (Supplementary Fig. 10).

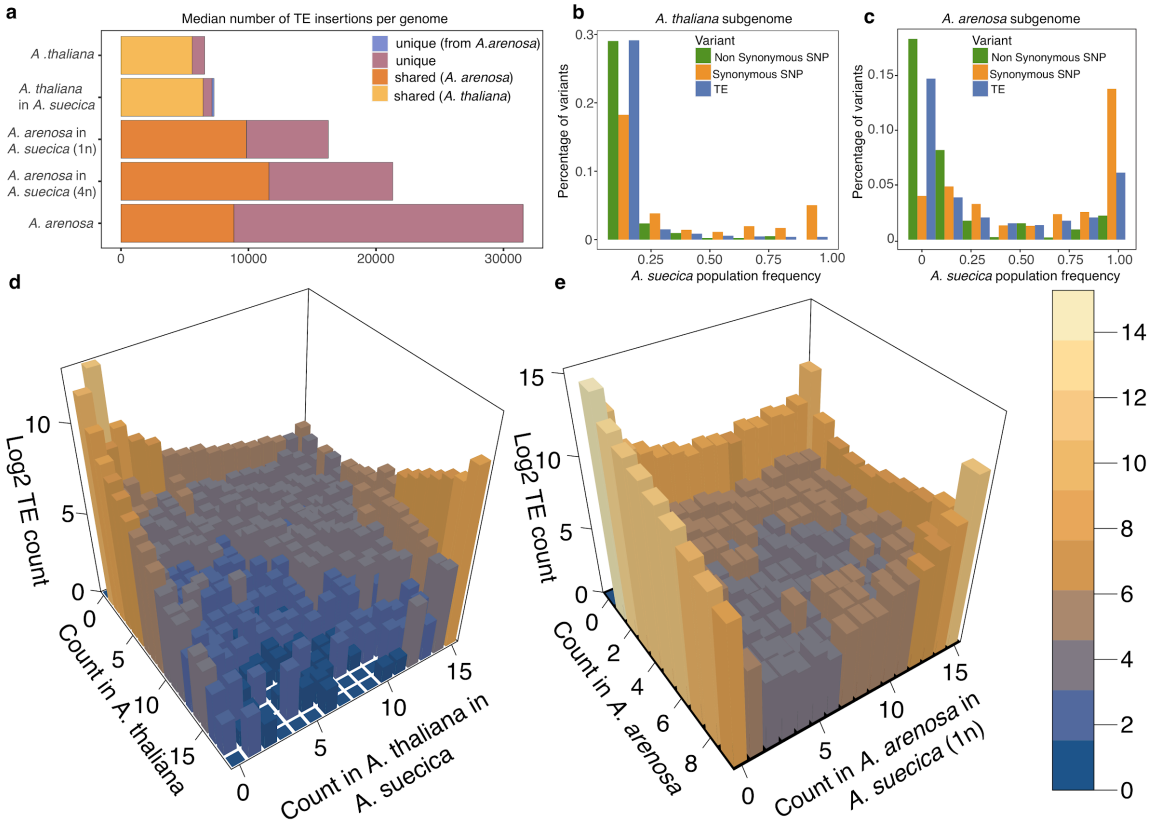

Figure 3. TE dynamics in *A. suecica* reveal no evidence for abnormal transposon activity. a Median TE insertions per genome. As the *A. arenosa* population is an autotetraploid outcrosser, 4 randomly chosen haploid *A. arenosa* subgenomes of *A. suecica* were combined to make a 4n *A. suecica*. *A. suecica* does not show an increase in private TE insertions compared with the ancestral species for both subgenomes, and shared TEs constitute a higher fraction of TEs in *A. suecica* reflecting the strong population bottleneck at its origin. Site-frequency spectra of non-synonymous SNPs, synonymous SNPs and TEs in the **b** *A. thaliana* and **c** *A. arenosa* subgenomes of *A. suecica* suggest that TEs are under purifying selection on both subgenomes. **d** 3D histogram of a joint TE frequency spectrum for *A. thaliana* on the x-axis and the *A. thaliana* subgenome of *A. suecica* on the y-axis **e** 3D histogram of a joint TE frequency spectrum for *A. arenosa* on the x-axis and the *A. arenosa* subgenome of *A. suecica* on the y-axis. **d** and **e** show stable dynamics of private TEs in *A. suecica* and a bottleneck effect on the ancestral TEs (shared) at the origin of the *A. suecica* species.

An interesting subset of recent transposon insertions unique to *A. suecica* are those that have jumped between the two subgenomes. We searched for full-length transposon copies that are present in both subgenomes of *A. suecica* and then assigned the resulting consensus sequences to either the *A. thaliana* or the *A. arenosa* ancestral genome using BLAST (see Methods). We were able to assign 15 and 56 consensus sequences as being specific to the *A. thaliana* and *A. arenosa* ancestral genome, respectively. Using these sequences, we searched our transposon polymorphism data for corresponding polymorphisms, and identified 1,515 *A. arenosa* transposon polymorphisms on the *A. thaliana* subgenome, and 496 *A. thaliana* transposon polymorphisms on the *A. arenosa* subgenome. Like other private polymorphisms, these are skewed towards rare frequencies, and are uniformly distributed across the (sub-)genome. Most of the transposons that have jumped into the *A. thaliana* subgenome are helitrons and LTR elements (Supplementary Fig. 12). LTR (copia) elements also make up most of the *A. thaliana* transposons segregating in the *A. arenosa* subgenome. The fact that roughly three times as many new insertions appear to have resulted from jumps from *A. arenosa* to *A. thaliana* than the other way around is notable. It is suggestive of higher transposon activity in the *A. arenosa* subgenome, but we have to consider differences in genome size and transposon number. If there were no differences in activity, we would expect the number of cross-subgenome jumps to be proportional to the number of potential source elements and the size of the target genome. As we have seen, the *A. arenosa* subgenome contains roughly twice as many transposons as the *A. thaliana* subgenome, but is about 20% larger. We would thus expect a 1.7-fold difference, not a three-fold one.

In conclusion, transposon activity in *A. suecica* appears to be governed largely by the same processes that governed it in the ancestral species.

4. No global dominance in expression between the subgenomes

Over time the traces of polyploidy are erased through an evolutionary process involving gene loss, often referred to as fractionation or re-diploidization[104–108]. Analyses of retained homeologs in ancient allopolyploids such as *A. thaliana*[109], maize[55], *B. rapa*[54] and *Gossypium raimondii*[110] have revealed that one “dominant” subgenome remains more intact, with more highly expressed homeologs compared to the “submissive” genome(s)[109]. This pattern of “biased fractionation” has not been observed in ancient autopolyploids[111], such as pear[112], and is believed to be allopolyploid-specific.

Studying genome expression dominance in contemporary allopolyploids is useful for understanding or predicting which of the subgenomes will likely be refractory to, and which will likely experience this fractionation process more, over time[55]. Subgenome dominance in expression has been reported for a number of more recent allopolyploids such as strawberry[6], peanut[8], *Spartina*[68], *T. miscellus*[113], monkeyflower[17] and synthetic *B. napus*[114]. However, some allopolyploids display even subgenome expression, among them *C. bursa-pastoris*[10,12], white clover[13], *A. kamachatica*[70] and *B. hybridum*[14].

Subgenome dominance is often linked to differences in transposon content[6] and/or large genetic differences between subgenomes[115]. This makes *A. suecica*, with 6 Mya divergence between the gene-dense *A. thaliana* and the transposon-rich *A. arenosa*, a promising candidate to study this phenomenon at unprecedented resolution. Previous reports on

338 subgenome dominance in *A. suecica* are conflicting, suggesting a bias to either the *A.*
339 *thaliana*[116] or the *A. arenosa*[117] subgenome.
340 To investigate the evolution of gene expression in *A. suecica*, we generated RNA-seq data
341 for 15 natural *A. suecica* accessions, 15 closely related *A. thaliana* accessions, 4 *A. arenosa*
342 individuals, a synthetically generated *A. suecica* from a lab cross (the 2nd and 3rd hybrid
343 generations) and the parental lines of this cross. Each sample had 2-3 biological replicates
344 (Supplementary Data 2). On average, we obtained 10.6 million raw reads per replicate, of
345 which 7.6 million reads were uniquely mapped to the *A. suecica* reference genome and 14,041
346 homeologous gene pairs (see Methods, Supplementary Fig. 13).
347 Considering the difference in expression between homeologous genes, we found no
348 general bias towards one or the other subgenome of *A. suecica*, for any sample or tissue,
349 including synthetic *A. suecica* (Fig. 4a and Supplementary Fig. 14a). This strongly suggests
350 that the expression differences between the subgenomes have not changed systematically
351 through polyploidization, and is in contrast to previous studies, which reported a bias towards
352 the *A. thaliana*[116] or the *A. arenosa*[117] subgenome, likely because RNA-seq reads were not
353 mapped to an appropriate reference genome.
354 The set of genes that show large expression differences between the subgenomes
355 appears not to be biased towards any particular gene ontology (GO) category, and is
356 furthermore not consistent between accessions and individuals (Fig. 4b, Supplementary Fig.
357 14b,c). This suggests that many large subgenome expression differences are due to genetic
358 polymorphisms within *A. suecica* rather than fixed differences relative to the ancestral species.
359 Levels of expression dominance were reported to vary across tissues in natural *C. bursa-*
360 *pastoris*[11] and also resynthesized cotton[118]. To test whether expression dominance can vary
361 for tissue-specific genes, we examined homeologous gene-pairs where at least one gene in
362 the gene pair showed tissue specific expression, in whole-rosettes and floral buds. We do not
363 find evidence for dominance between subgenomes in tissue specific expression either (Fig.
364 4b). Interestingly, the 897 genes with significant expression in whole rosettes for both
365 homeologs showed GO overrepresentation that included both photosynthesis and chloroplast
366 related functions (Supplementary Table 1). This result suggests that the *A. arenosa*
367 subgenome has established important cyto-nuclear communication with the chloroplast
368 inherited from *A. thaliana*, rather than being silenced. 2,176 gene pairs with floral bud specific
369 expression for both homeologs were overrepresented for GO terms related to responses to
370 chemical stimuli, such as auxin and jasmonic acid, which may reflect early developmental
371 changes in this young tissue (Supplementary Table 1). Although flowers of selfing *A. thaliana*
372 and *A. suecica* are scentless and are much smaller than those of the outcrosser *A. arenosa*[72],
373 this result suggests the "selfing syndrome"[119] has not hugely impacted the transcriptome of
374 floral buds in *A. suecica*, at least at this stage of development.
375 In summary, we find no evidence that one subgenome is dominant and contributes more
376 to the functioning of *A. suecica*. On the contrary, homeologous gene pairs are strongly
377 correlated in expression across tissues.
378
379
380
381

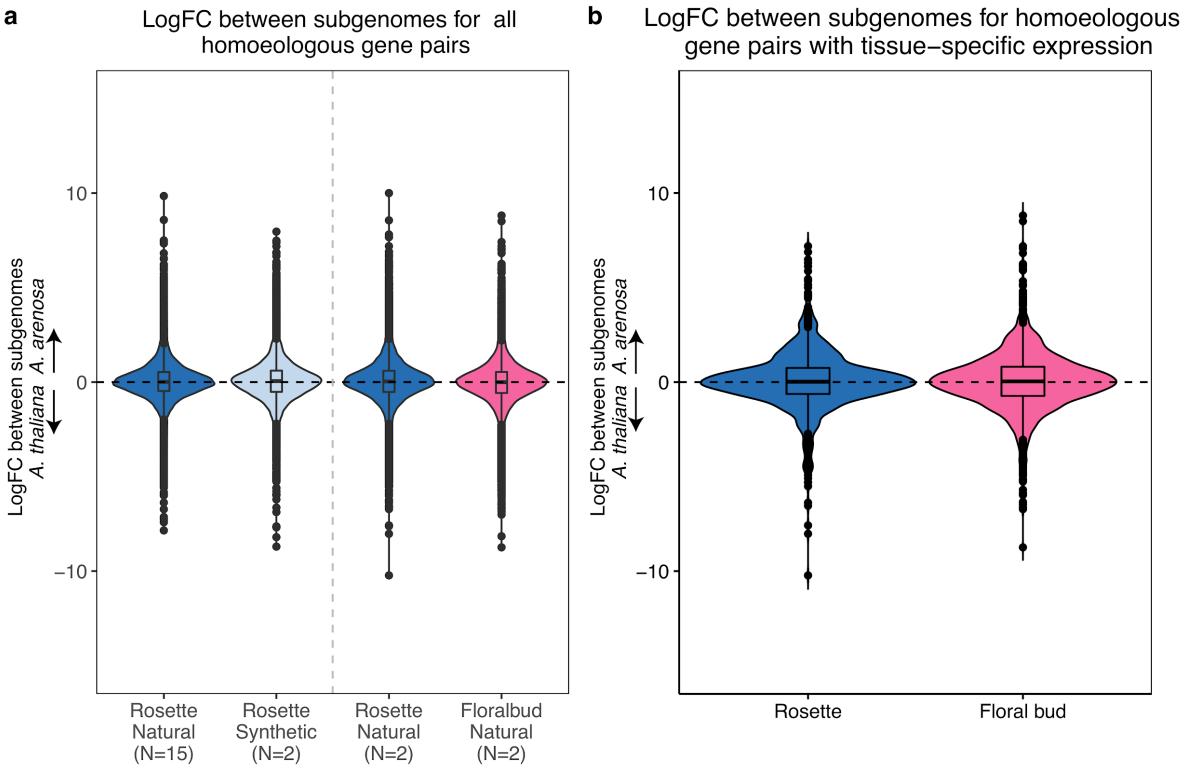

Figure 4. Patterns of gene expression between the subgenomes of *A. suecica* in rosettes and floral buds. **a** Violin plots of the mean log fold-change between the subgenomes for the 15 natural *A. suecica* accessions and two synthetic lines for whole rosettes. Mean log fold-change for the two accessions ("ASS3" and "AS530") where transcriptome data for both whole rosettes and flower buds were available. All the distributions are centered around zero suggesting even subgenome expression. **b** Violin plots for the mean log fold-change between the subgenomes for genes with tissue-specific expression. At least one gene in a homeologous gene pair was required to show tissue-specific expression.

5. Evolving gene expression in *A. suecica*

The previous section focused on differences in expression between the subgenomes, between homeologous copies of the same gene within the same individual. This section will focus on differences between individuals, between homologous copies of genes that are part of the same (sub-)genome. To provide an overview of expression differences between individuals we performed a principal component analysis (PCA) on gene expression separately for each (sub-)genome. For both subgenomes, the first principal component separates *A. suecica* from the ancestral species and the synthetic hybrid (Fig. 5a,b, Supplementary Fig. 15), suggesting that hybridization does not automatically result in large-scale transcriptional changes, and that altered gene expression changes in natural *A. suecica* have evolved over time. Given the limited time involved, and the fact the genes that have changed expression are far from random with respect to function (Fig. 5c), we suggest that the first principal component primarily captures trans-regulated expression changes in *A. suecica* that are likely adaptive.

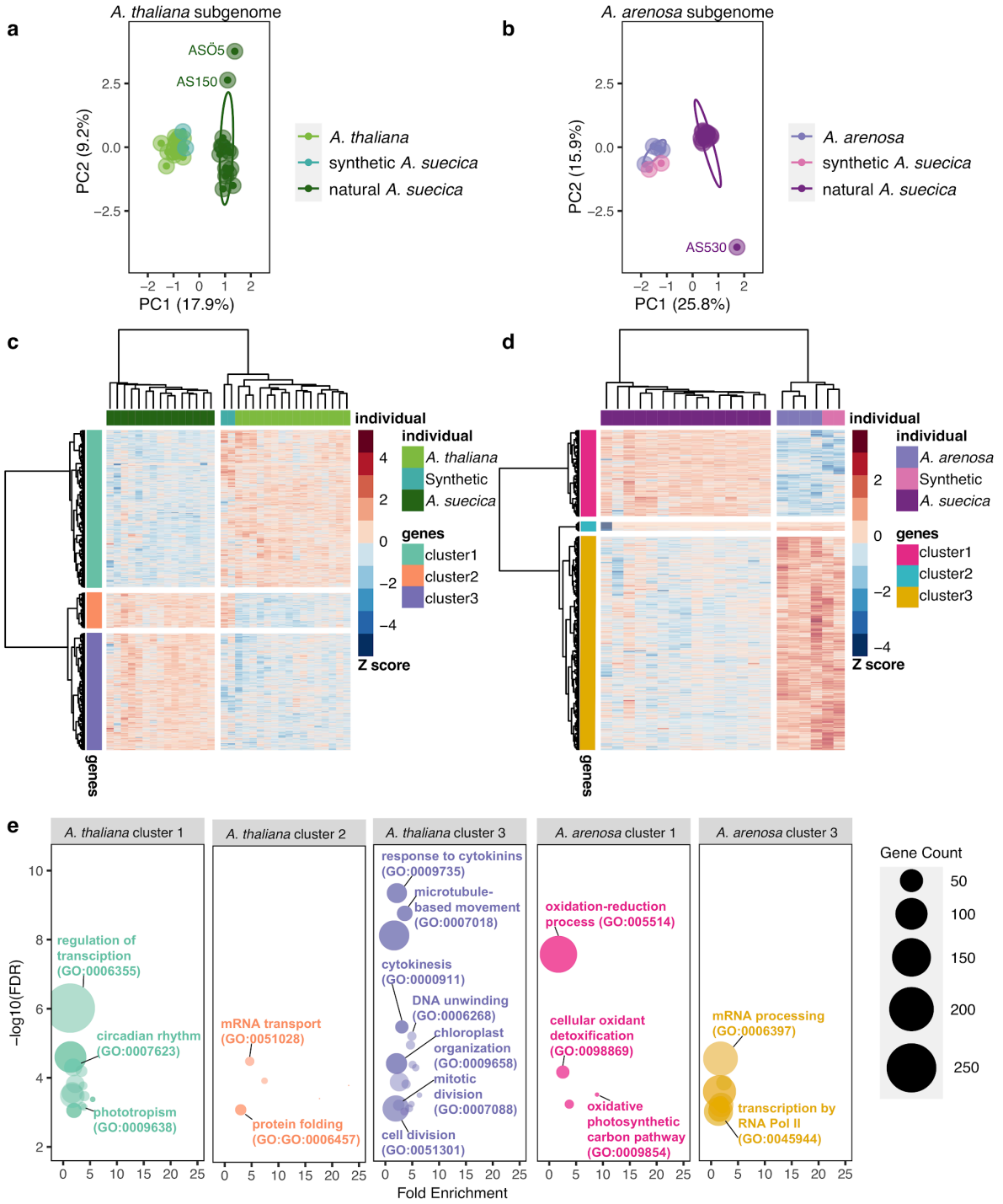

Figure 5. Differential gene expression analysis in *A. suecica*. Patterns of differential gene expression in *A. suecica* support adaptation to the whole-genome duplication for the *A. thaliana* subgenome and adaptation to the new plastid environment for the *A. arenosa* subgenome. **a** PCA for *A. thaliana*, *A. thaliana* subgenome of natural and synthetic *A. suecica* lines. PC1 separates natural *A. suecica* from the ancestral species and the synthetic lines. **b** PCA for *A. arenosa*, *A. arenosa* subgenome of natural and synthetic *A. suecica* lines. PC1 separates natural *A. suecica* from the ancestral species and the synthetic lines, whereas PC2 identifies outlier accessions discussed further below (see Fig. 6). **c, d** Heatmap of differentially expressed genes (DEGs) for the two subgenomes of *A. suecica*. Positive numbers (red color) indicate higher expression. Genes and individuals have been clustered based on similarity in expression, resulting in clusters discussed in the text. **e** Gene ontology enrichment for each cluster in **c** and **d**. Categories discussed in the text are highlighted.

416
417 To further characterize expression changes in natural *A. suecica* we analyzed differentially
418 expressed genes (DEGs) on both subgenomes compared to the corresponding ancestral
419 species. The total number of DEGs was 4,186 and 4,571 genes for the *A. thaliana* and *A.*
420 *arenosa* subgenomes, respectively (see Methods, Supplementary Data 2). These genes were
421 clustered based on the pattern of change across individuals (Fig. 5c,d) and GO enrichment
422 analysis was carried out for each cluster (Fig. 5e, Supplementary Table 2).
423 For the *A. thaliana* subgenome, we identified three clusters. Cluster 1 comprised 2,135
424 genes that showed decreased expression in *A. suecica* compared to *A. thaliana*. These genes
425 are strongly enriched for transcriptional regulation, which may be expected as we are
426 examining DEGs between the species. Also notable are enrichments for circadian rhythm
427 function and phototropism, which may be related to the ecology of *A. suecica* and its post-
428 glacial migration to the Fennoscandinavia region (Fig. 1a).
429 Cluster 2 consisted of 468 genes that are over-expressed in both natural and synthetic *A.*
430 *suecica* relative to *A. thaliana*. These expression changes are thus most likely an immediate
431 consequence of hybridization presumably reflecting trans-regulation. Genes in this cluster are
432 enriched for "mRNA transport" and "protein folding". The importance of the adjustment of
433 protein homeostasis has been reported previously in experimentally evolved stable polyploid
434 yeast[120]. Notably, the synthetic lines used in the expression analysis were selected to be
435 healthy-looking, and did not show signs of aneuploidy (Supplementary Fig. 17).
436 Cluster 3 consisted of 1,583 genes that show increased expression in *A. suecica*
437 compared to *A. thaliana*, and several of the enriched GO categories, such as microtubule-
438 based movement, cytokinesis, meiosis and cell division, suggest that the *A. thaliana*
439 subgenome of *A. suecica* is adapting to polyploidy at the level of basic cell biology. That there
440 has been strong selection for this seems likely given that aneuploidy is frequent in synthetic
441 *A. suecica* (Supplementary Fig. 16), while natural *A. suecica* has a stable and conserved
442 karyotype. Importantly, there is independent evidence for adaptation to polyploidy via
443 modifications of the meiotic machinery in the other ancestor of *A. suecica*, *A. arenosa*, as
444 well[23,121,122], although we see very little overlap in the genes involved (Supplementary Fig. 16).
445 The nature of these changes in the *A. thaliana* subgenome of *A. suecica* will require further
446 investigation, but we note that there is enrichment (see Methods, Supplementary Data 2) for
447 Myb family transcription factor binding sites[123] among upregulated genes in cluster 3.
448 For the *A. arenosa* subgenome, we also found three clusters of DEGs (Fig. 5d) with GO
449 enrichment for two of them (Fig. 5e, Supplementary Table 2). Cluster 1 consisted of 1,278
450 genes that show increased expression in natural *A. suecica* compared to *A. arenosa* and
451 synthetic *A. suecica,* and are enriched for plastid-related functions, including oxidation-
452 reduction and the oxidative photosynthetic carbon pathway. We hypothesize that this may be
453 due to selection on the *A. arenosa* subgenome to restore communication with the new plastid
454 environment as plastid genomes were maternally inherited from *A. thaliana*. We also
455 examined genes that show structural evidence for direct plastid-nuclear interactions in *A.*
456 *thaliana* using CyMIRA[124]. Out of a total of 69 genes, 12 overlap genes identified in Cluster1,
457 more than expected by chance (p-value 0.0072; one-sided Fisher Exact Test, one sided;
458 Supplementary Data 2). Cluster 3 consists of 3,166 genes that show decreased gene
459 expression in *A. suecica* compared to *A. arenosa* and synthetic *A. suecica*. These genes were
460 primarily enriched for mRNA processing and epigenetic regulation of gene expression
461 (Supplementary Table 2) and positive regulation of transcription by RNA polymerase II, which
462 might suggests differences in the epigenetic regulation of expression between *A. arenosa* and

A. suecica. Cluster 2 (127 genes), finally, did not have a GO overrepresentation and showed an intriguing pattern discussed in the next section.

6. Homeologous exchange contributes to variation in gene expression

The second principal component for gene expression identified three outlier-accessions of *A. suecica*, two for the *A. thaliana* subgenome (Fig. 5a) and one for the *A. arenosa* subgenome (Fig. 5b). While closely examining the latter accession, “AS530”, we realized that it is responsible for the cluster of genes with distinct expression patterns but no GO enrichment just mentioned (Fig. 5d, Cluster 2). Genes from this cluster were significantly downregulated on the *A. arenosa* subgenome (Fig. 6a) and upregulated on the *A. thaliana* subgenome (Fig. 6b) — for AS530 only. The further observation that 104 of the 127 genes (Supplementary Fig. 20a) in the cluster are located in close proximity in the genome, pointed to a structural rearrangement. The lack of DNA sequencing coverage on the *A. arenosa* subgenome around these 104 genes and the doubled coverage for their homeologs on the *A. thaliana* subgenome, strongly suggested a homeologous exchange (HE) event resulting in AS530 carrying four copies of the *A. thaliana* subgenome and zero copies of the *A. arenosa* genome with respect to this this, roughly 2.5 Mb region of the genome (Fig. 6c). This explanation was further supported by HiC data, which showed clear evidence for interchromosomal contacts between *A. thaliana* subgenome chromosome 1 and *A. arenosa* subgenome chromosome 6 around the breakpoints of the putative HE in AS530 (Fig. 6 d,e), and by multiple discordant Illumina paired-end reads at the breakpoints between the homeologous chromosomes, which independently support the HE event (Supplementary Fig. 19a-d).

Based on this we examined the two outlier *A. suecica* accessions for the *A. thaliana* subgenome (Fig. 5a; “AS150” and “ASÖ5”), and found that they likely share a single HE event in the opposite direction (four copies of the *A. arenosa* subgenome and no copies of the *A. thaliana* subgenome for a region of roughly 1.2Mb in size, see Supplementary Figure 18). This demonstrates that HE occurs in *A. suecica* and contributes to the intraspecific variation we observed in gene expression (Fig 5a, b). HE in allopolyploids is a main source of diversity, causing phenotypic changes in flower color in synthetic polyploid peanut[9] and extensive phenotypic change in synthetic polyploid rice at a population level[125]. However, the majority of HEs are probably deleterious as they will lead to gene loss: although the *A. thaliana* and *A. arenosa* genomes are largely syntenic, AS530 is missing 108 genes (Supplementary Figure 19) that are only present on the *A. arenosa* subgenome segment that has been replaced by the homeologous segment from the *A. thaliana* subgenome, and AS150/ASÖ5 are missing 53 genes that were only present on the *A. thaliana* subgenome.

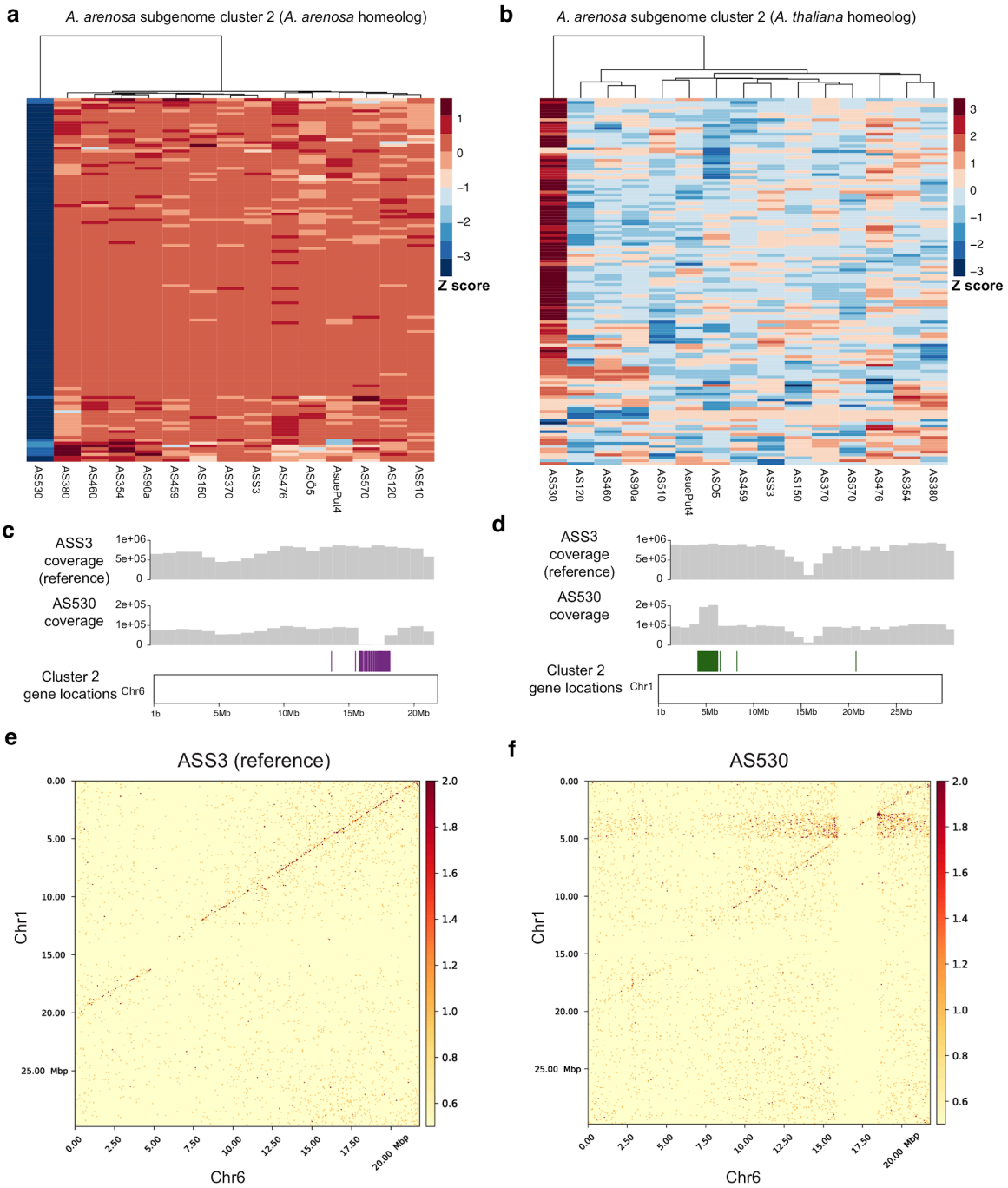

Figure 6. Homeologous exchange contributes to expression variance within *A. suecica*. a Cluster 2 of Fig. 5d explains the outlier accession AS530 which is not expressing a cluster of genes on the *A. arenosa* subgenome. **b** Homeologous genes of this cluster on the *A. thaliana* subgenome of *A. suecica* show the opposite pattern and are more highly expressed in AS530 compared to the rest of the population. **c** 97 of the 122 genes from cluster 3 are located in close proximity to each other on the reference genome but appear to be deleted in AS530 based on sequencing coverage. **d** The *A. thaliana* subgenome homeologs have twice the DNA coverage, suggesting they are duplicated. **e** HiC data show (spurious) interchromosomal contacts at 25 Kb resolution between chromosome 1 and chromosome 6 around the breakpoint of the cluster of 97 genes in AS530 but not in reference accession ASS3.

Conclusion

This study has focused on the process of polyploidization in a natural allotetraploid species, *A. suecica*, generated roughly 16 kya through the hybridization of two species, *A. thaliana* and *A. arenosa*, which differ substantially in everything from genome size and chromosome number to mating system and ecology. Our study is one of a growing number of studies focusing on natural rather than domesticated polyploid, but is unparalleled in its resolution thanks to one of the parents being a major model species.

Our main conclusion from this study is that polyploid speciation, at least in this case, appears to have been a gradual process rather than some kind of "event". We confirmed previous results that genetic polymorphism is largely shared with the ancestral species, demonstrating that *A. suecica* did not originate through a single unique hybridization event, but rather through multiple crosses[20]. We also find no evidence for "genome shock" (i.e. major genomic changes linked to structural and functional changes) that has often been suggested to accompany polyploidization and hybridization. The genome has not been massively rearranged, transposable elements are not out of control, and there is no subgenome dominance in expression. On the contrary, we find evidence of genetic adaptation to "stable" life as a polyploid, in particular changes to the meiotic machinery and in interactions with the plastids. These findings made in natural *A. suecica*, together with the observation that experimentally generated *A. suecica* are often unviable and do exhibit evidence of genome rearrangements, similar to the young allopolyploid species in *Tragapogon* and monkeyflower, suggest that the most important bottleneck in polyploid speciation may be selective. If this is true, domesticated polyploids may not always be representative of natural polyploidization, because of human intervention. Darwin famously argued that "Natura non facit saltum"[126] — we suggest that natural polyploids are no exception from this, but note that many more species will have to be studied before it is possible to draw general conclusions.

Supplemental figures

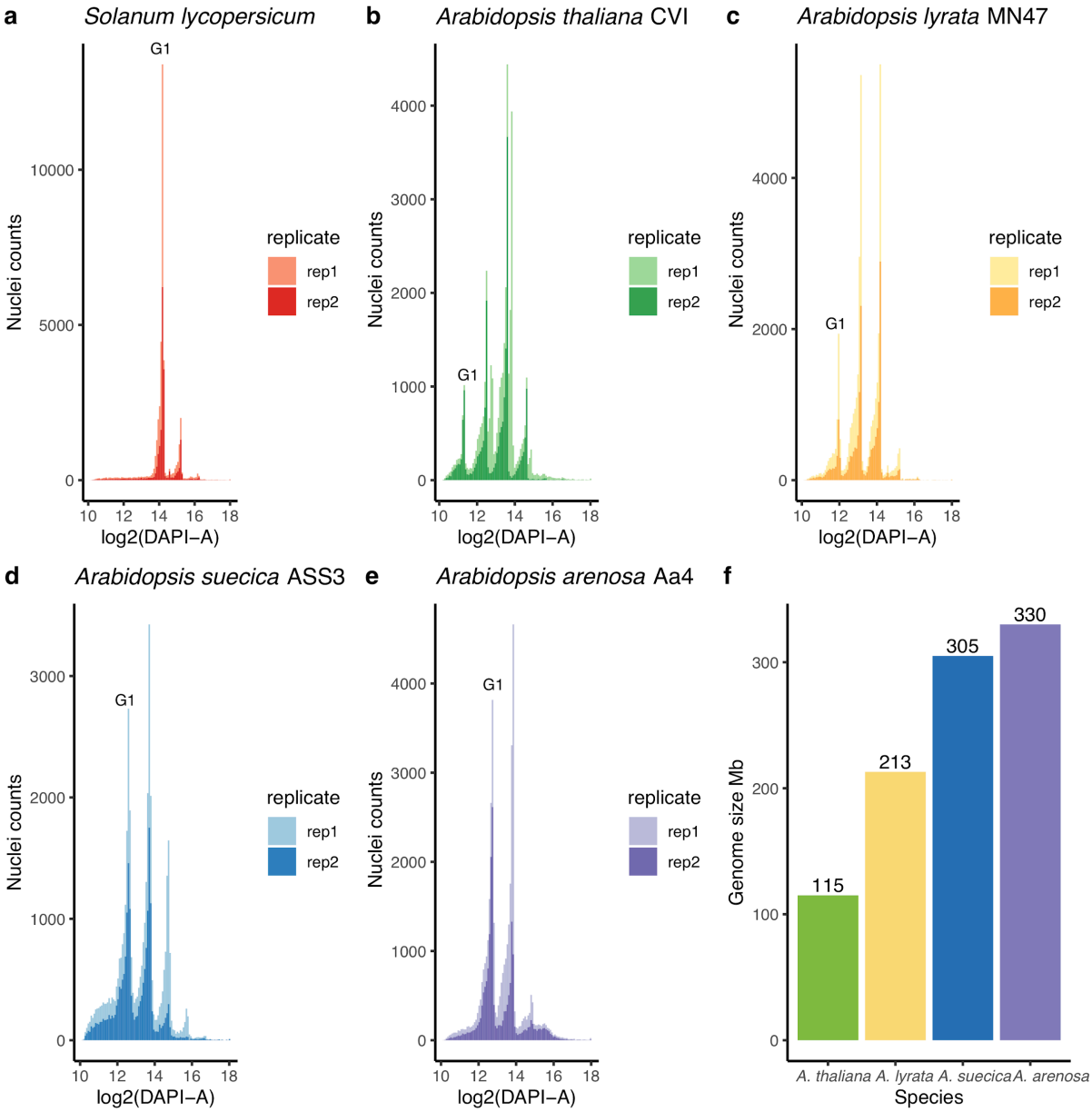

Supplementary Figure 1. Measuring genome sizes of *Arabidopsis* species using flow cytometry. a FACs sorting of *Solanum lycopersicum* cells from 3 week old leaf tissue for two replicates. G1 represents the peak denoting the G1 phase of the cell cycle. Cells in the G1 phase have 2C DNA content (i.e. a 2N genome). **b** *A. thaliana* "CVI" accession **c** *A. lyrata* "MN47" (the reference accession) **d** *A. suecica* "ASS3" (the reference accession) **e** autopolyploid *A. arenosa* accession "Aa4" **f** Bar chart shows calculated genome sizes (rounded to the nearest whole number) for each species using *Solanum lycopersicum* as the standard .

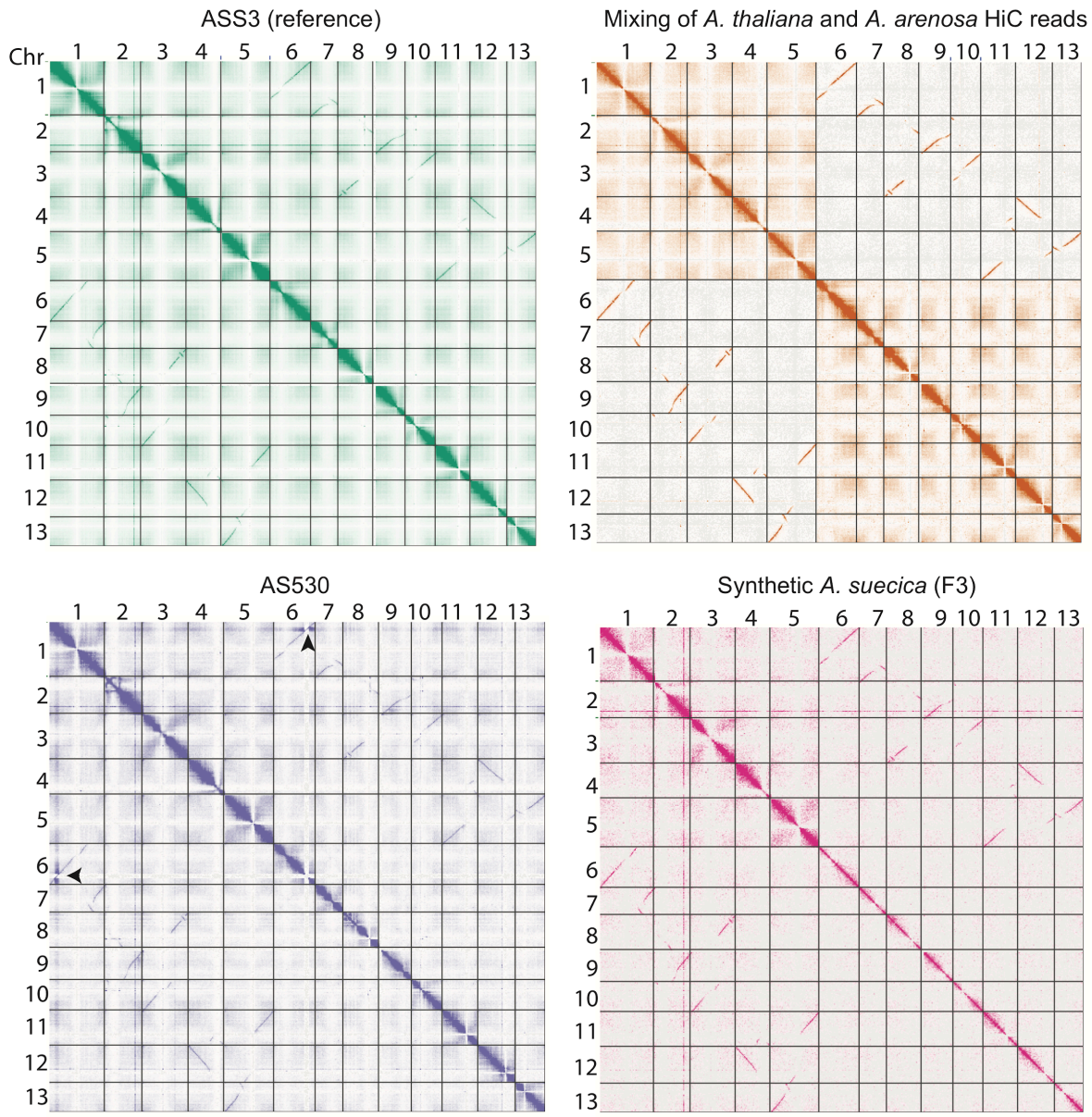

Supplementary Figure 2. HiC as a tool to investigate structural rearrangements. **a** HiC contact map for the full chromosome-level genome assembly of *A. suecica*. **b** Mixing of *A. thaliana* and *A. arenosa* HiC reads suggest interchromosomal contacts between homeologous chromosomes is a result of mis-mapping for HiC reads. Such mis-mapping is typically filtered out in short read DNA and RNA datasets using insert size and proper pairs mapping filters, however in HiC long range chromosomal contacts are not filtered out. **c** Accession "AS530" with the region of homeologous exchange highlighted with an arrow (Figure 6), no other rearrangements were observed. **d** HiC of synthetic *A. suecica* (F3).

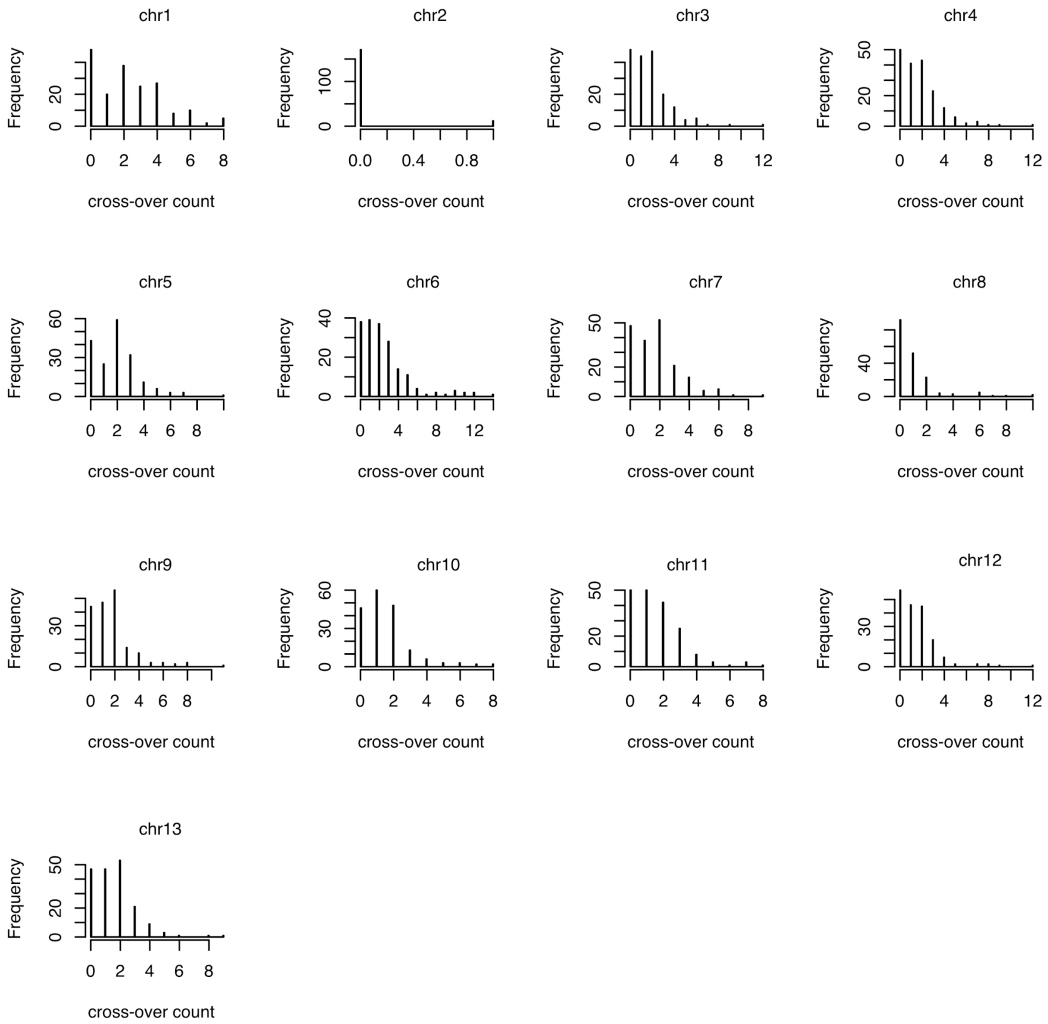

Supplementary Figure 3. Crossover counts in an *A. suecica* F2 population. Per chromosome crossover counts in our F2 population (N=185). Chromosome 2 had too few SNPs to be analysed in our cross due to the recent bottleneck in *A. suecica*[20].

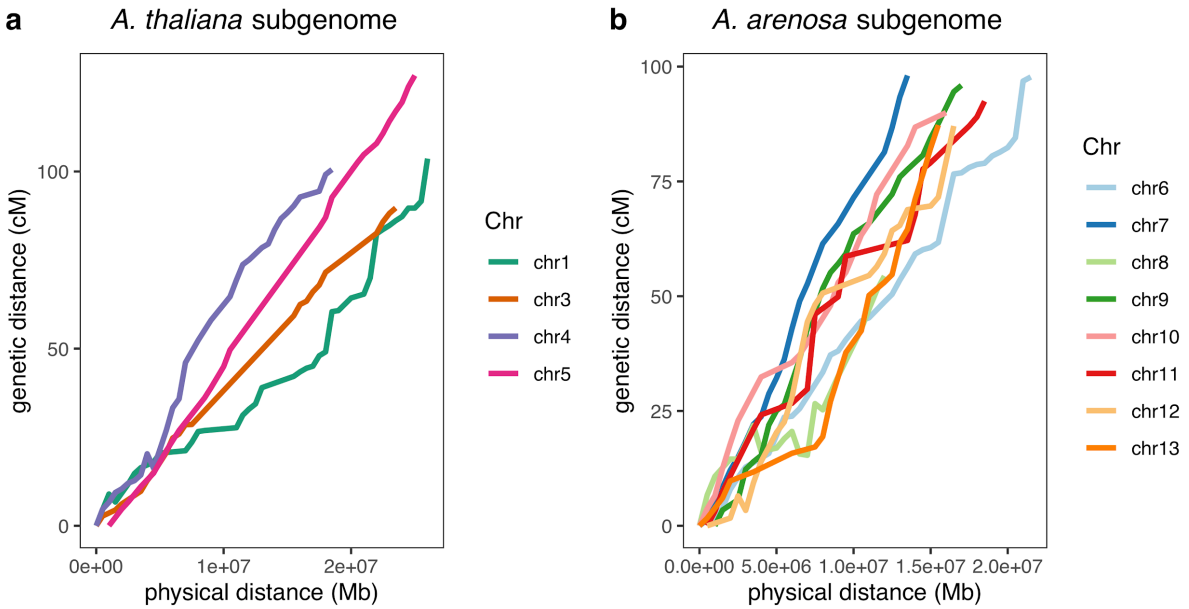

Supplementary Figure 4. A genetic map for *A. suecica*. Physical distance (Mb) vs genetic distance (cM) is plotted for each: **a** *A. thaliana* subgenome and; **b** *A. arenosa* subgenome chromosome. Chromosome 2 is not plotted as there are too few SNPs on this chromosome in our cross, due to the recent bottleneck in *A. suecica*[20]

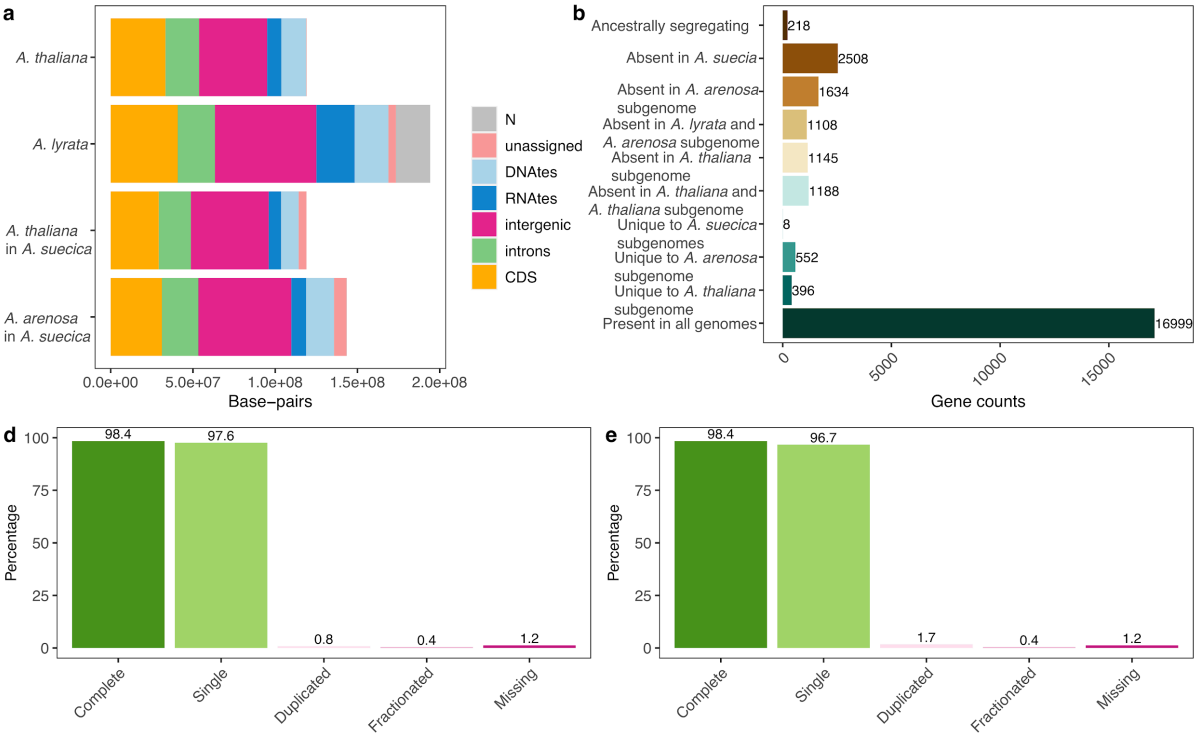

Supplementary Figure 5. Genome composition and orthologous gene relationships in *A. suecica*. a Genome composition of the *A. suecica* subgenomes and the ancestral genomes of *A. thaliana* and *A.lyrata* (here a substitute reference for *A. arenosa* because it is annotated). **b** Counts of orthologous relationships between the subgenomes of the reference *A. suecica* genome and the reference *A. thaliana* and *A. lyrata* genome. Ancestrally segregating genes are genes that are shared between the *A. thaliana* reference and the *A. arenosa* subgenome or shared between the *A. lyrata* reference and the *A. thaliana* subgenome. Therefore they most likely represent genes ancestrally segregating in the ancestor of *A. thaliana* and *A. lyrata*. BUSCO analysis of *A. suecica* using the BUSCO set for eudicots for the **d** *A. thaliana* and **e** *A. arenosa* subgenome.

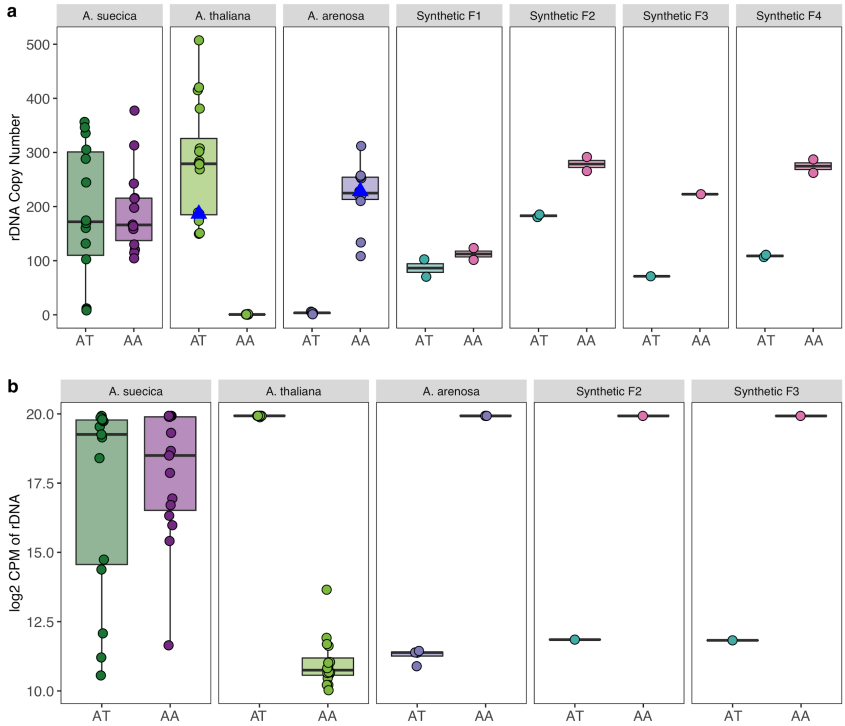

Supplementary figure 6. **rDNA copy number variation and expression. a** Copy number of *A. thaliana* and *A. arenosa* rDNA in natural *A. suecica*, ancestral species and synthetic lines. Blue triangles represent the *A. thaliana* and *A.arenosa* parent lines of the synthetic *A. suecica* cross. AT represents results when mapping to the *A. thaliana* consensus sequence and AA to the *A. arenosa* consensus sequences for the 45S rRNA **b** Expression (log2 CPM) of *A. thaliana* and *A. arenosa* rDNA in natural *A. suecica*, ancestral species and synthetic lines. Accessions with log2 CPM of >=15 was taken as evidence for expression for the *A. thaliana* and *A. arenosa* 45S rRNA in *A. suecica*, as this CPM value was above the maximum level of mis-mapping observed in the ancestral species (*A. thaliana* mapping to the *A. arenosa* 45S rRNA).

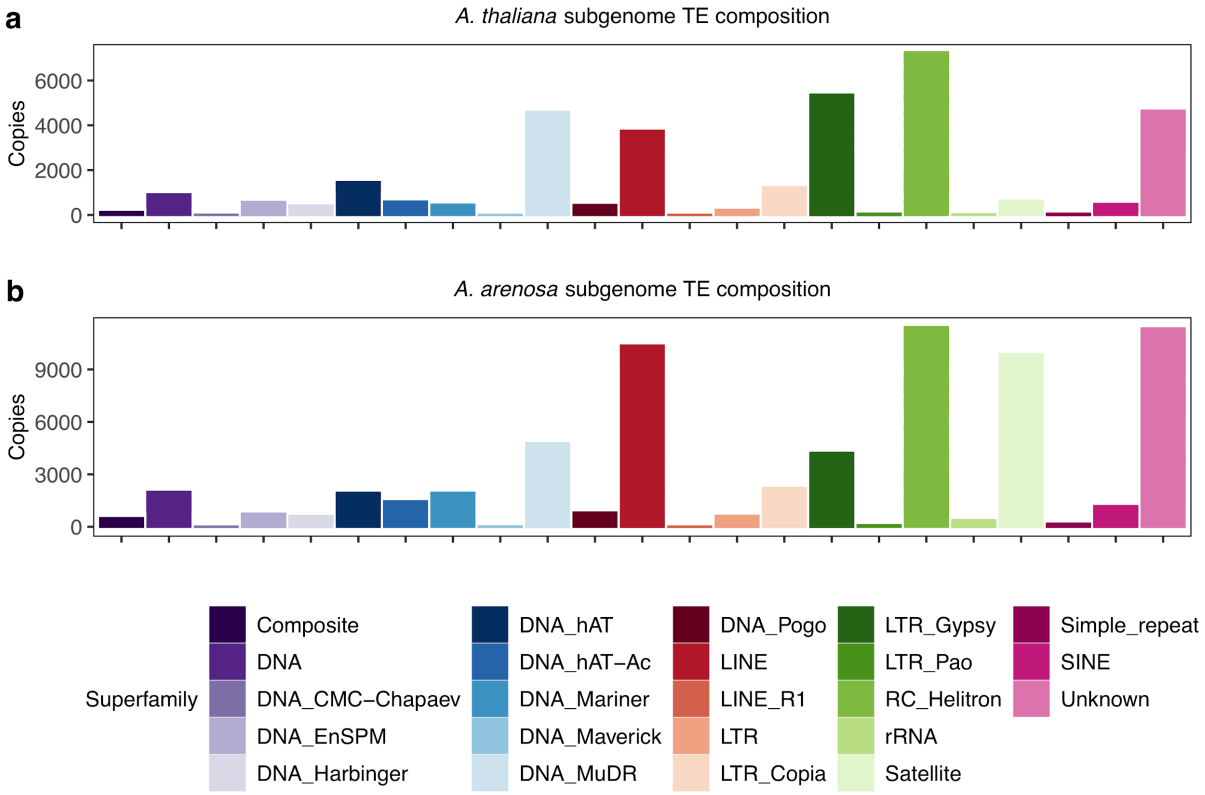

Supplementary Figure 7. TE-composition of the *A. suecica* reference genome. TE composition of the **a** *A. thaliana* and **b** *A. arenosa* subgenome of *A. suecica*.

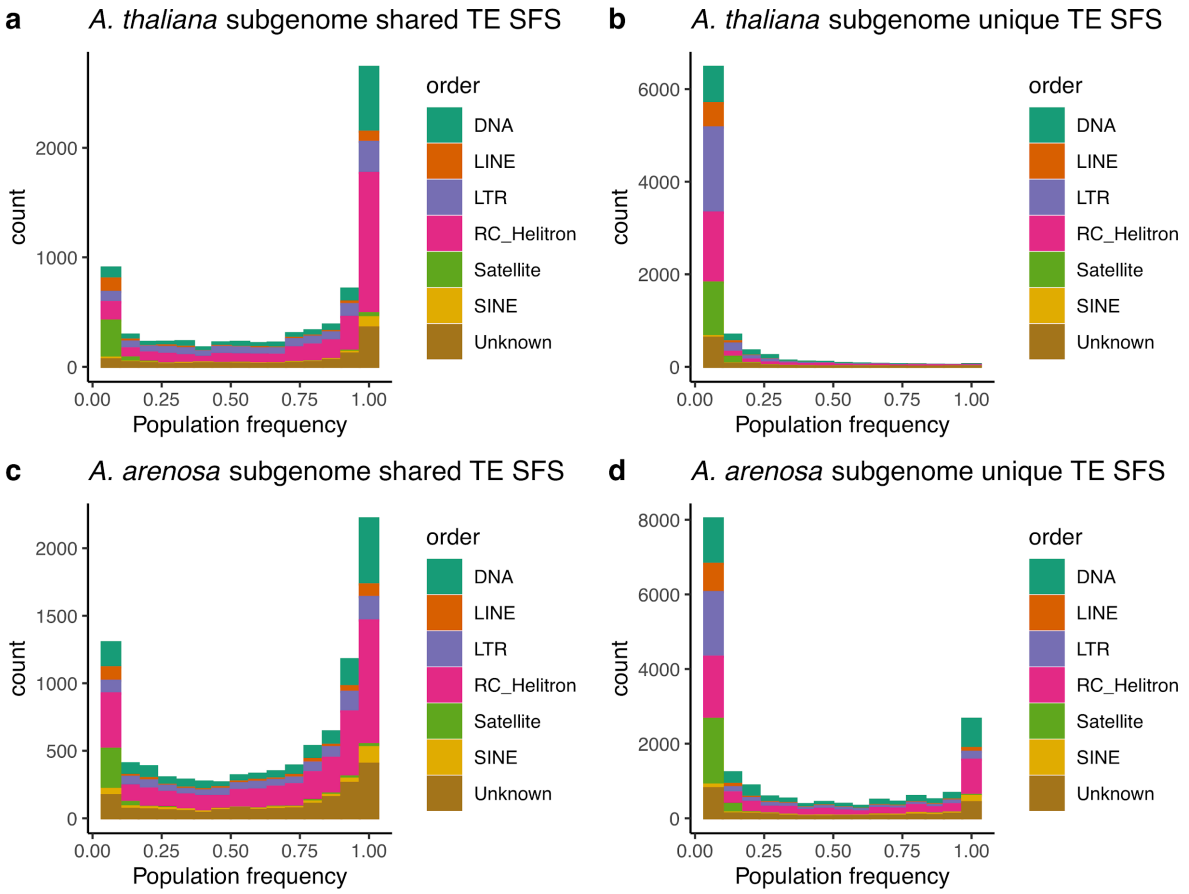

Supplementary Figure 8. Site frequency spectrum (SFS) of shared TEs and unique TEs in *A. suecica* broken down by TE family. Shared TE SFS for the **a** *A. thaliana* and **b** *A. arenosa* subgenome. Private TE SFS for the **c** *A. thaliana* and **d** *A. arenosa* subgenome.

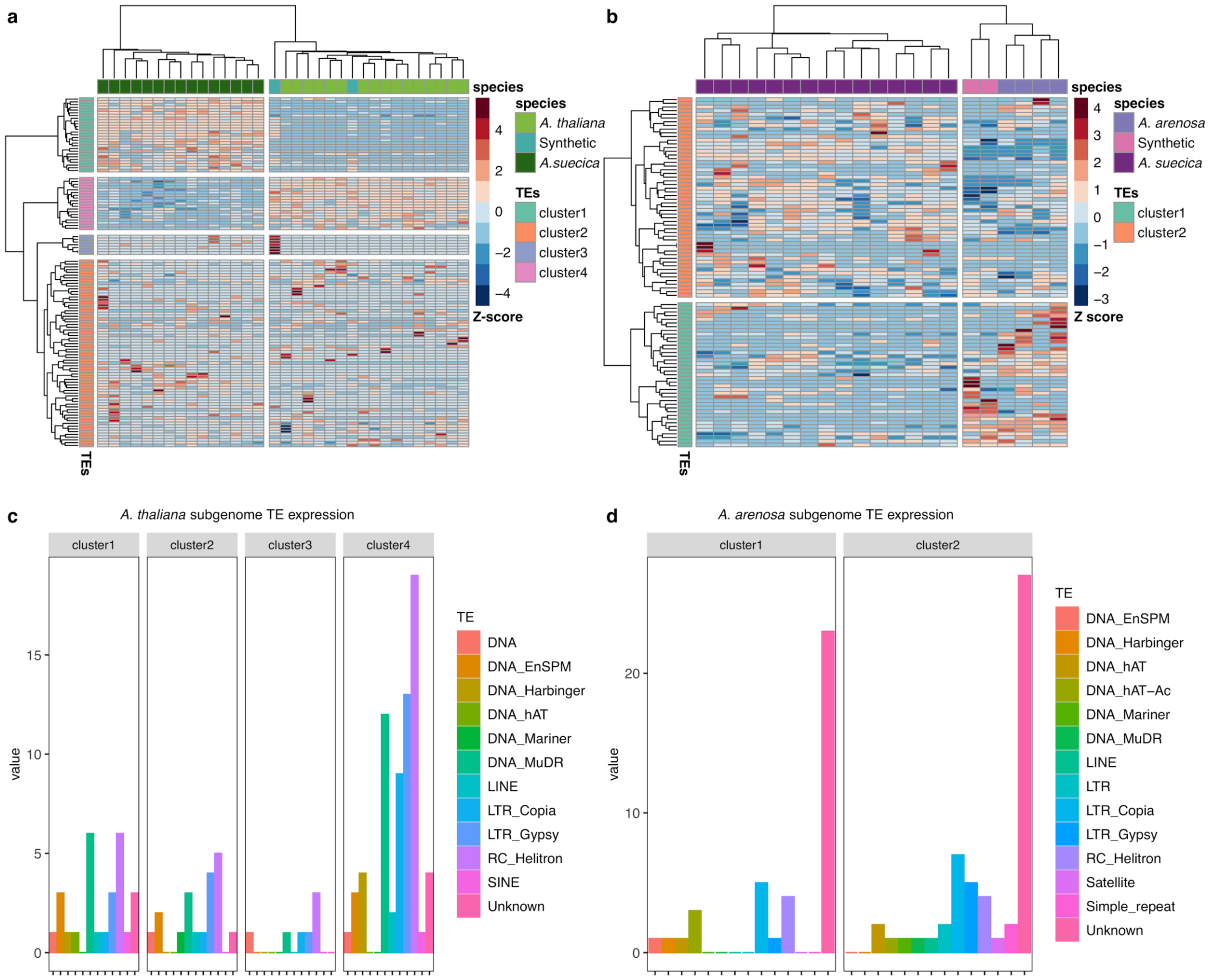

Supplementary Figure 9. Analysis of TE expression in *A. suecica*. Patterns of TE expression in natural and synthetic *A. suecica* show that allopolyploidy is not accompanied by an overall up-regulation in TE expression as predicted by the "genome shock" hypothesis. **a** Heatmap of TE expression for the *A. thaliana* subgenome of *A. suecica* (dark green) synthetic *A. suecica* (cyan) and *A. thaliana* (light green). **b** Heatmap of TE expression for the *A. arenosa* subgenome of *A. suecica* (dark purple) synthetic *A. suecica* (pink) and *A. arenosa* (light purple). **c** and **d** the breakdown of TE families expressed in each cluster, with helitrons being the most abundant class on the *A. thaliana* subgenome and TEs of an unknown family being the most abundant in the *A. arenosa* subgenome.

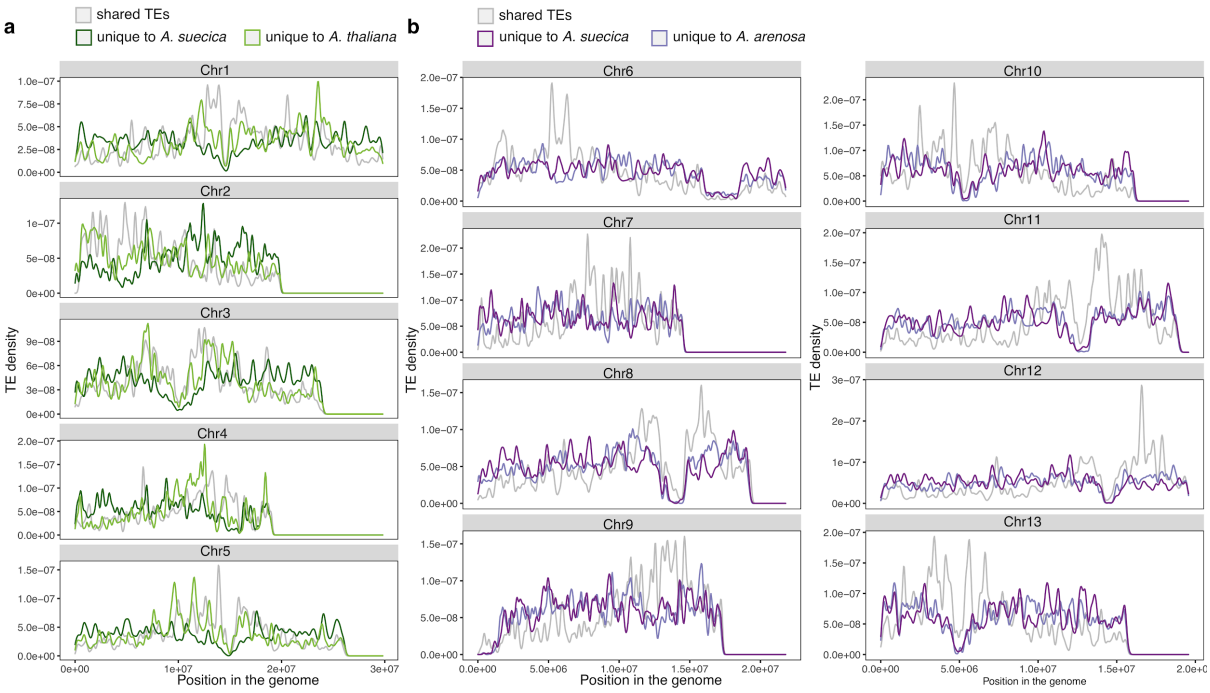

Supplementary Figure 10. Genomic distribution of TEs in the *A. suecica* genome. a Shared TEs in the population between *A. thaliana* and the *A. thaliana* subgenome of *A. suecica.* Shared TEs are likely older than private TEs and are enriched around the pericentromeric regions in the *A. thaliana* subgenome. Private TEs are enriched in the chromosomal arms for both species, where protein coding gene density is higher (Fig. 1b). **b** as in **a** but examining TEs in the population of *A. arenosa* and the *A. arenosa* part of *A. suecica*. Note the region between 5 and 10 on chromosome 2 was not included in the analysis as this region shows synteny with an unplaced contig.

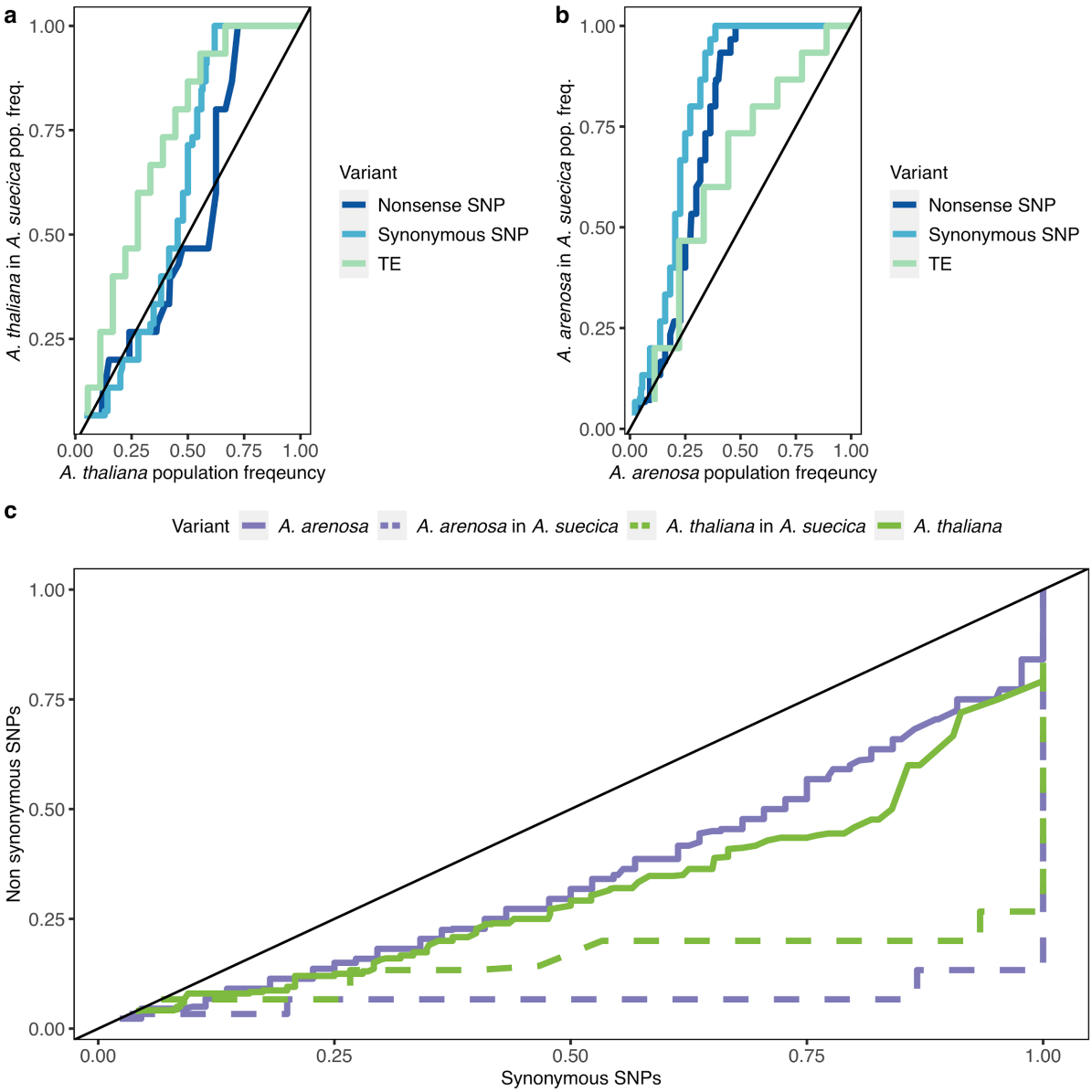

Supplementary Fig 11. Patterns of selection in *A. suecica.* **a** Comparison of shared variation (Nonsense SNPs, synonymous SNPs, and TEs) population frequencies in the *A. thaliana* subgenome of 15 natural *A. suecica* accessions and the closest 31 *A. thaliana* accessions. **b** Comparison of shared variation (Nonsense SNPs, synonymous SNPs, and TEs) frequencies in *A. arenosa* subgenome of 15 *A. suecica* accessions and 11 Swedish *A. arenosa* lines. Although results may be affected by the sampling and potential misidentification of the ancestral populations, the current data suggests a similar pattern on both of the subgenomes for TEs and SNPs showing a bottleneck effect. **c** Plotting quantile pairs of the population frequencies of private nonsynonymous and synonymous SNPs in *A. suecica* and ancestral populations against each other, each species shows evidence of evolution under purifying selection, since population frequency quantiles of nonsynonymous SNPs are skewed to lower values than population frequency quantiles of synonymous SNPS.

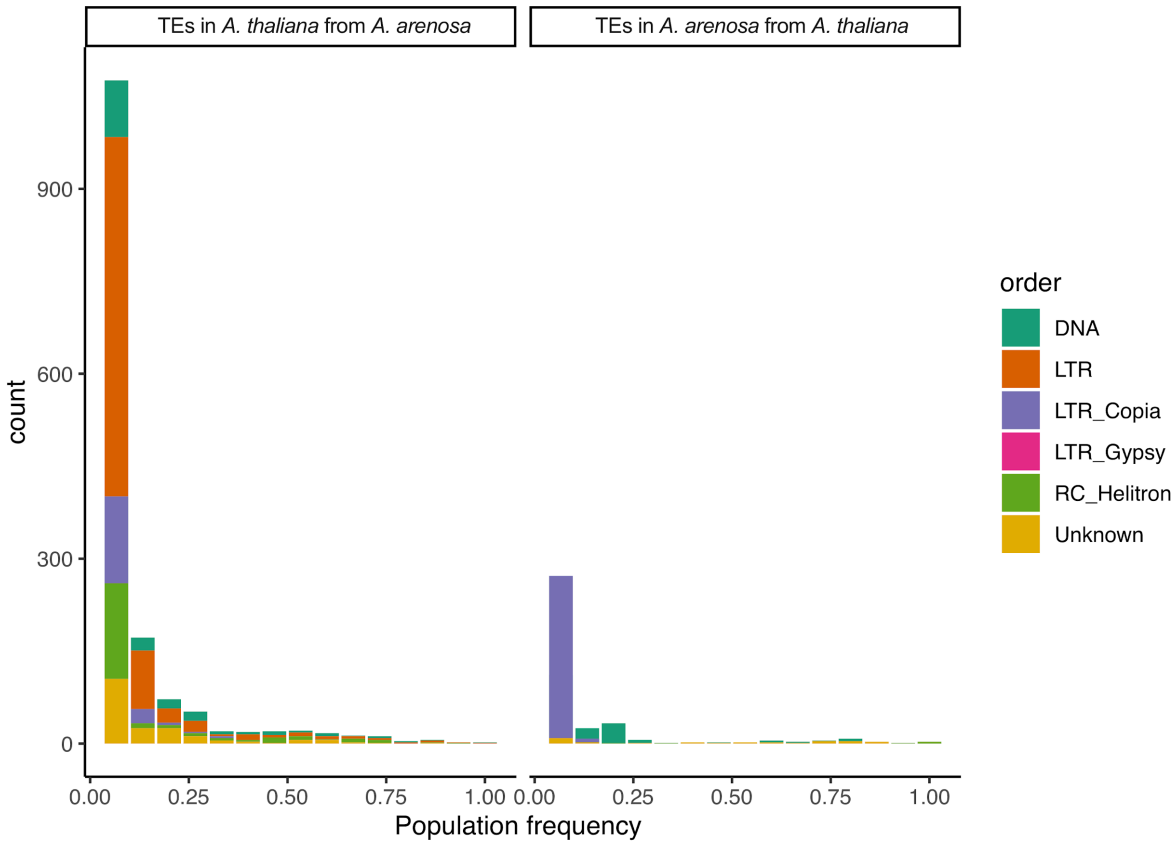

Supplementary Figure 12. Population frequencies of presence-absence calls for TEs that have mobilized between the subgenomes in *A. suecica.* **a** TEs ancestrally from *A. arenosa* that are present in the *A. thaliana* subgenome of *A. suecica* and **b** TEs ancestrally from *A. thaliana* that are present in the *A. arenosa* subgenome of *A. suecica*.

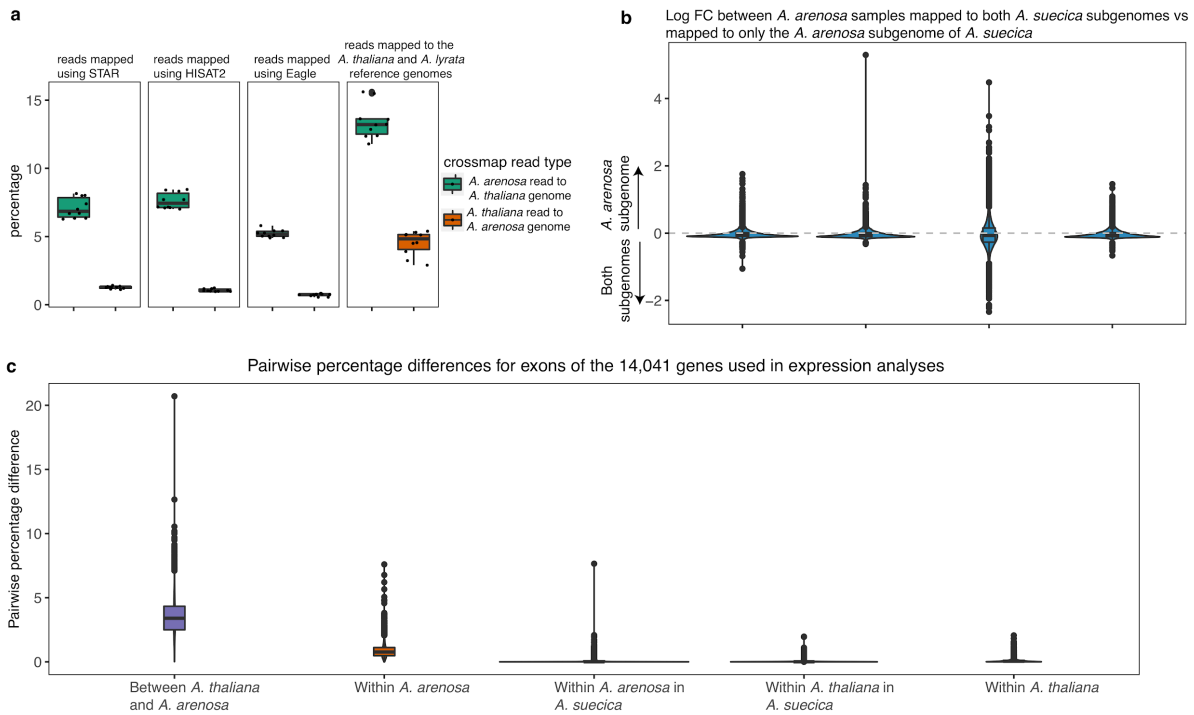

Supplementary Figure 13. Cross-mapping in RNA-seq. **a** Boxplots of cross-mapping reads. This was examined by mixing reads in-silico between *A. thaliana* and *A. arenosa*. On average ~6% of *A. arenosa* reads map to *A. thaliana* subgenome instead of the *A. arenosa* subgenome, and ~1% vice versa. Mapping these reads to the combined reference genomes of *A. thaliana* and *A. lyrata* (boxplot 4 in **a**) shows that reads map more precisely to the *A. suecica* reference and that cross-mapping is not due to unreported homeologous exchange. **b** LogFC of log2 CPM read counts for *A. arenosa* (CPM of *A. arenosa* subgenome genes when reads are mapped only to *A. arenosa* subgenome of *A. suecica*/CPM of *A. arenosa* subgenome genes when reads are mapped to the full genome) show only a small effect of mapping strategy to estimate gene expression on the *A. arenosa* subgenome. **c** Pairwise percentage differences (π) for each group measured for the exons of the 14,041 genes in the expression analysis. High levels of π in *A. arenosa* overlaps with the distribution of π between *A. thaliana* and *A. arenosa.* This explains why there is more cross-mapping for *A. arenosa* than for *A. thaliana* in **a** Importantly, lower π within *A. suecica* for both subgenomes means that measurements for subgenome dominance are not biased by cross-mapping, as we expect less cross-mapping since the distribution of π overlaps less with π between *A. thaliana* and *A. arenosa*.

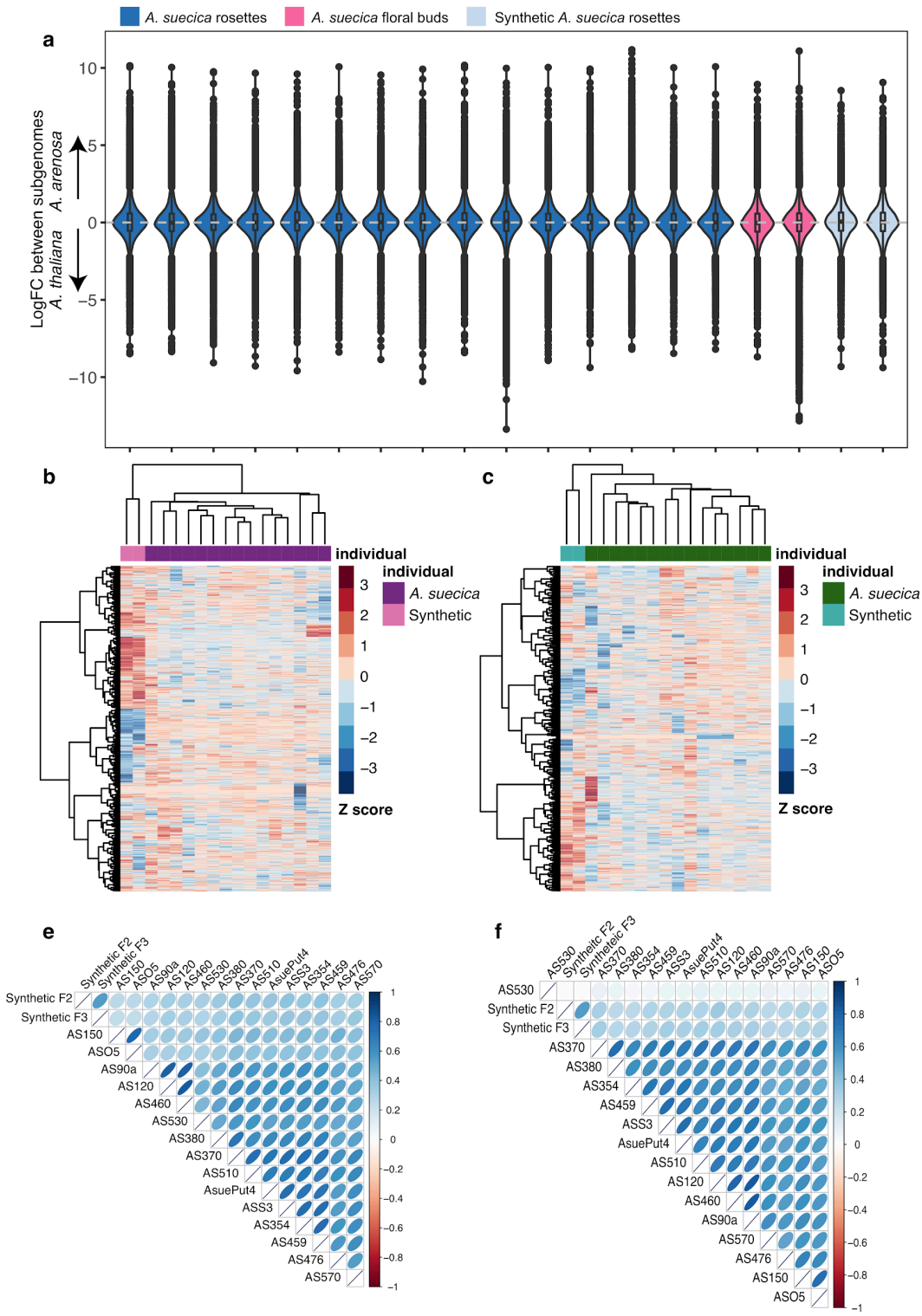

Supplemental figure 14. Expression differences between subgenomes in natural and synthetic *A. suecica*. a The distribution of expression differences across homeologous gene pairs in natural and synthetic *A. suecica*. **b** A heatmap of expression for genes in the top 5% biased toward the *A. arenosa* subgenome. The gene must be in the 5% quantile for at least 1 accession. **c** The same as in **b** but for the *A. thaliana* subgenome. Correlations of log fold change for genes in the tails of the distribution (top 5% quantile) for the *A. arenosa* subgenome **d** and the *A. thaliana* subgenome **e**

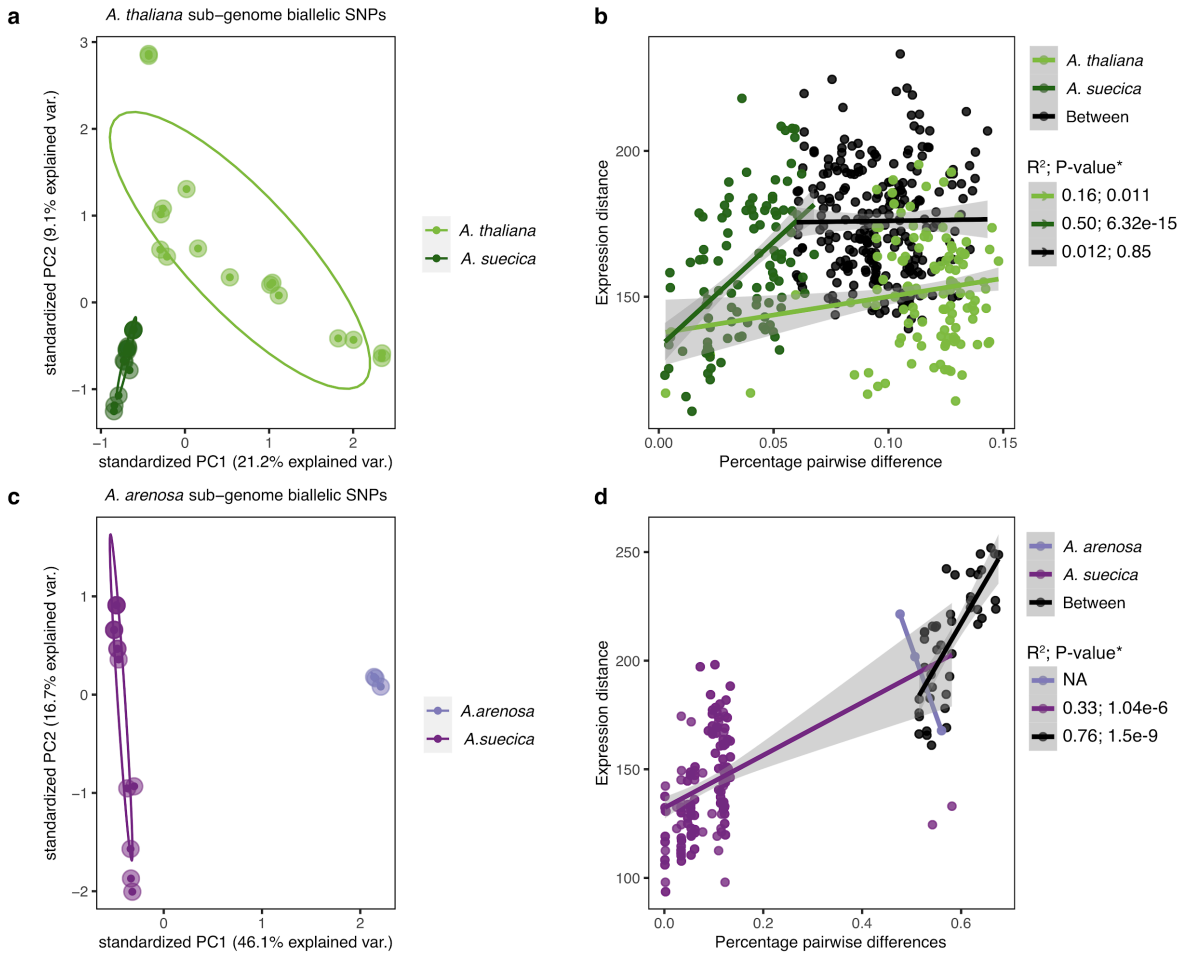

Supplementary Figure 15. Comparison of genetic and expression distance. **a** PCA plot of biallelic SNPs in the population of *A. thaliana* and *A. suecica* for the *A. thaliana* subgenome of *A. suecica* (N=345,075 biallelic SNPs), of the analyzed 13,647 genes in gene expression in addition to 500bp up and downstream of each gene sequence **b** Correlation of π (pairwise genetic differences) and expression distance (i.e. euclidean distance) for 14,041 genes (*=Bootstrapped 1000 times). **c** PCA plot of biallelic SNPs in the population of *A. arenosa* (N.B. we had DNA sequencing for only 3 of the 4 accessions used in the expression analysis) and *A. suecica* for the *A. arenosa* subgenome of *A. suecica* (N= 1,761,708 biallelic SNPs), of the analyzed 14,041 genes in gene expression in addition to 500bp up and downstream of each gene sequence **d** Correlation of Pi (pairwise genetic differences for mapped genomic regions) and expression distance (i.e. euclidean distance) for 14,041 genes (*=Bootstrapped 1000 times). *A. arenosa* was too few samples to give reliable correlations and therefore is NA. Grey bars represent the 95 confidence intervals.

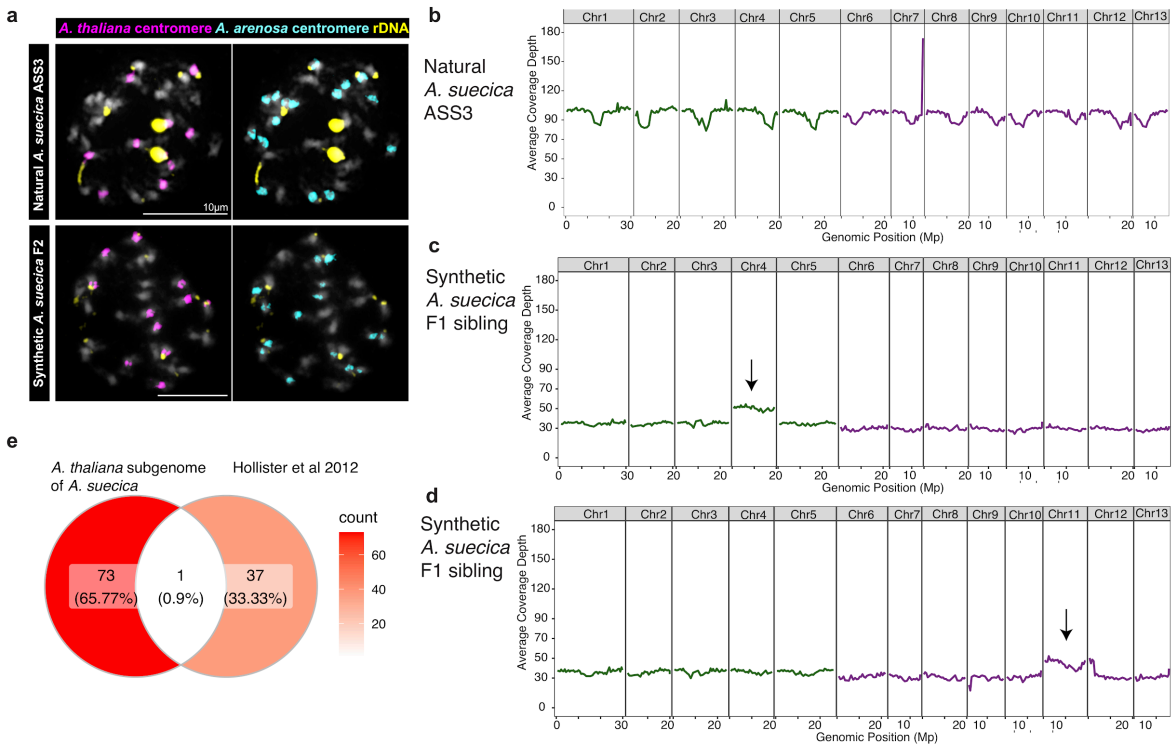

Supplementary Figure 16. **Aneuploidy is frequent in synthetic *A. suecica***. **a** Comparison of FISH analyses of the reference natural *A. suecica* "ASS3 "and synthetic *A. suecica.* Synthetic *A. suecica* shows aneuploidy in both subgenomes in the F2 generation (gain of one chromosome on the *A. thaliana* subgenome (N=11) and loss of one chromosome on the *A. arenosa* subgenome (N=15)). Natural *A. suecica* shows a stable karyotype **b** DNA sequencing coverage in the reference natural *A. suecica* accession "ASS3" **c** and **d** DNA sequencing coverage in siblings of F1 synthetic *A. suecica* show different cases of aneuploidy (indicated with arrow) in synthetic *A. suecica*, chromosome 4 in **c** and chromosome 11 in **d e** overlap of genes involved in cell division from figure 5e and genes previously shown to play a role in the adaptation to autopolyploidy in *A. arenosa*[121]. The little overlap in genes between *A. suecica* and *A. arenosa* highlights that successful meiosis in polyploids is likely a complex trait.

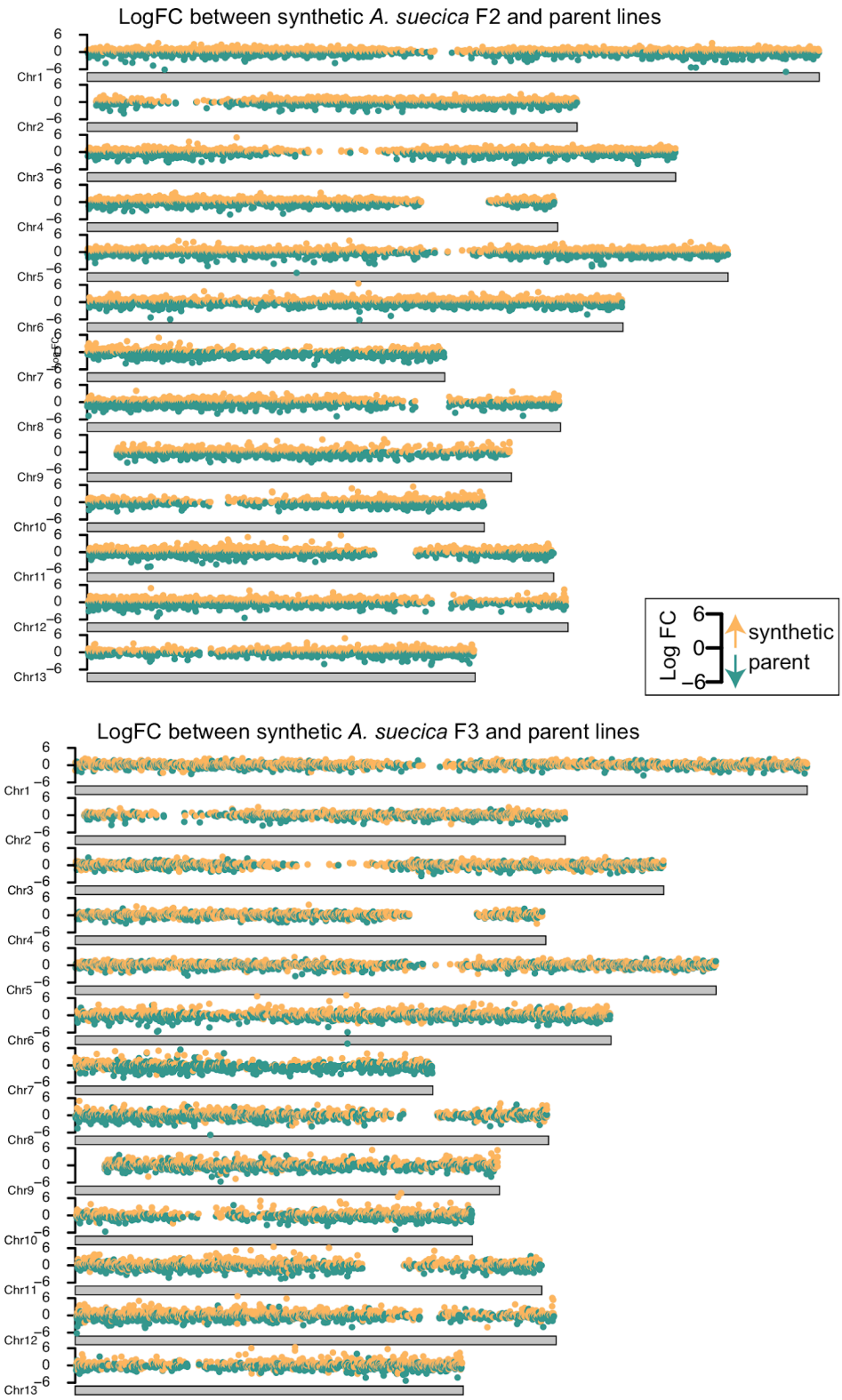

Supplementary Figure 17. No aneuploidy in synthetic *A. suecica* lines used for RNA seq based on log fold change to parent lines. Log fold change for gene expression in **a** the 2nd and **b** the 3rd generation of synthetic *A. suecica* compared to the parent lines. No clear signal of aneuploidy (i.e. an elevated increase in expression for a full chromosome) is evident.

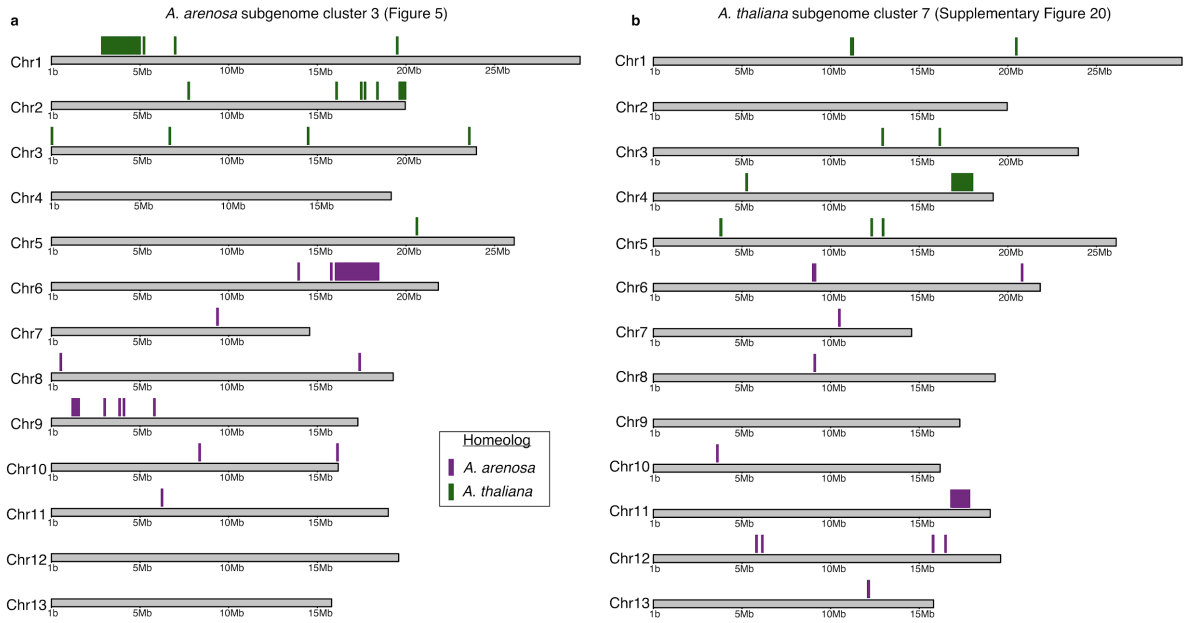

Supplementary Figure 18 Genomic locations of genes investigated for HE signatures in *A. suecica*. a Genes in cluster 3 for Figure 5 in AS530 and **b** Genes in cluster 7 from Figure 18 in AS150 and ASÖ5

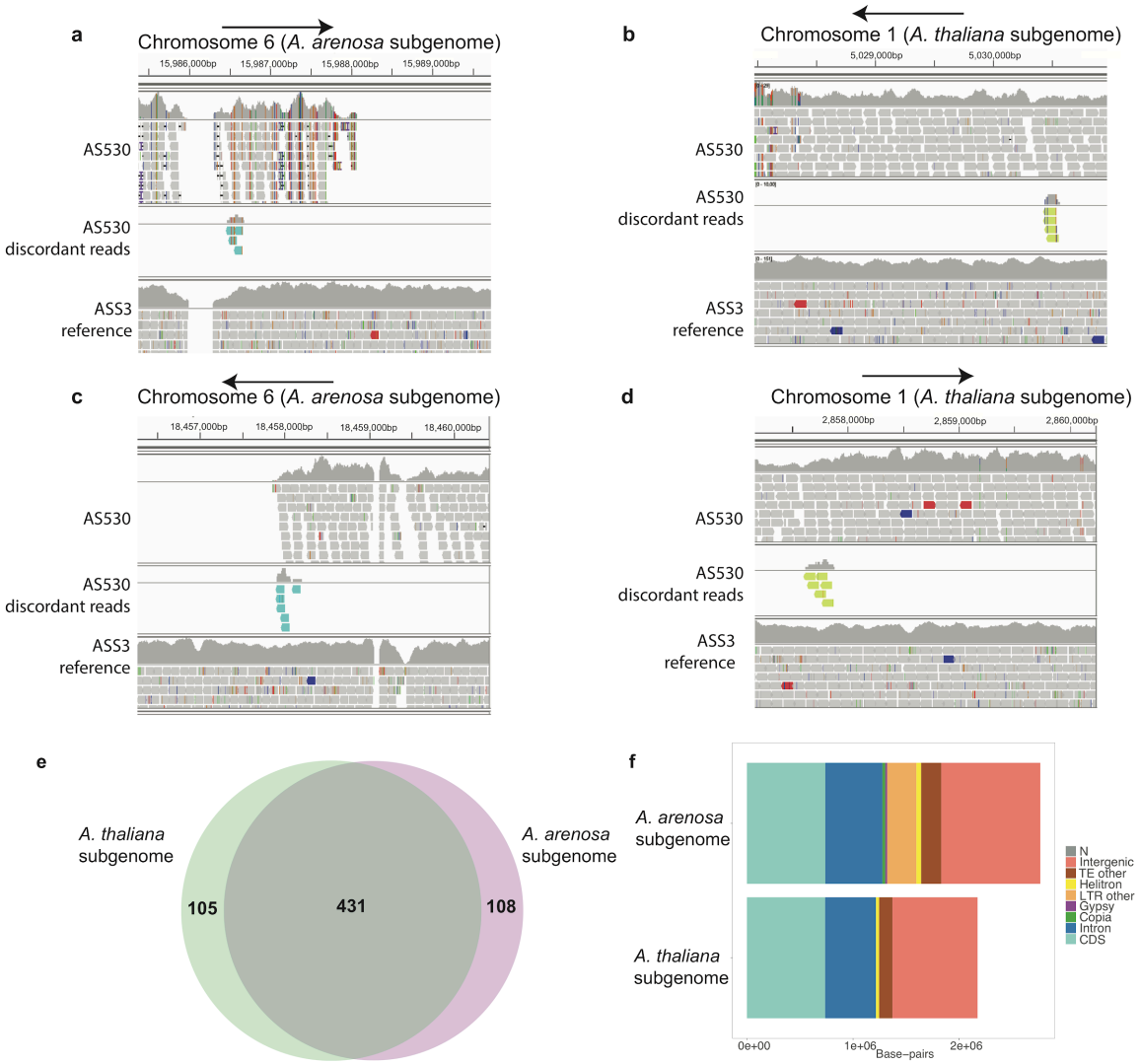

Supplementary Figure 19 Discordant read analysis supports HE in *A. suecica* **a** IGV screen grab of reads mapped to the beginning of the likely HE event in chromosome 6 (at ~ 15.9Mb) before coverage depth decreases to 0 in "AS530". Arrows point to the direction of the break along the chromosome. Discordant read pairs (cyan) map between the *A. arenosa* subgenome on chromosome 6 and the read pair (green) maps to the homeologous chromosome 1 on the *A. thaliana* subgenome (at ~5Mb) in **b**. The end of the likely HE event in chromosome 6 (at ~18.4Mb). Discordant reads (cyan) map between the *A. arenosa* subgenome in **c** and the read pair (green) maps to chromosome 1 (at ~2.8Mb) on the *A. thaliana* subgenome in **d**. **e** Gene counts between the syntenic regions. 431 have a 1:1 relationship, 108 genes are specific to the *A. arenosa* subgenome in this region and 105 genes are specific to the *A. thaliana* subgenome. **f** Composition of the syntenic regions between the two subgenomes

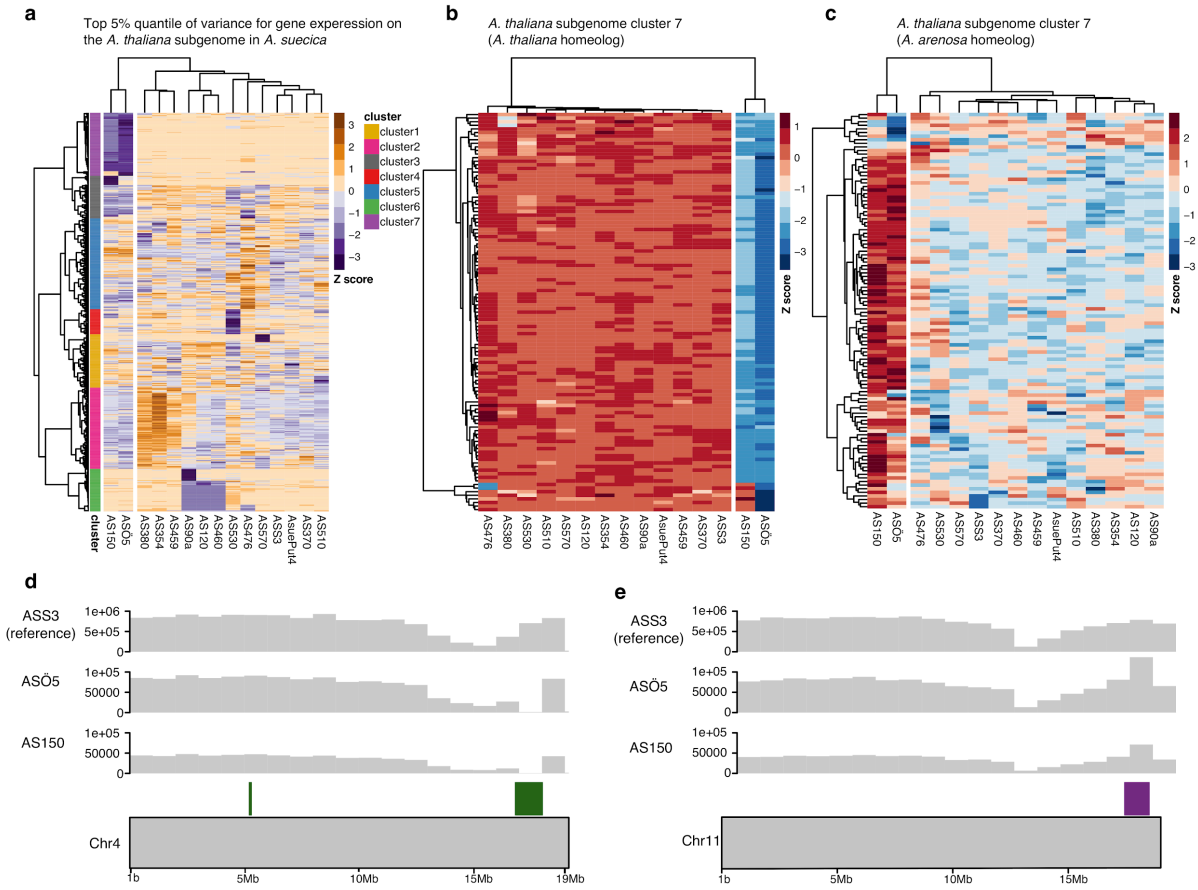

Supplementary Figure 20. Homeologous exchange contributes to expression variance within *A. suecica* on the *A. thaliana* subgenome. a Taking the top 5% quantiles (N=702) for variation in gene expression for the *A. thaliana* subgenome we find a large cluster 7 (N=111) where the two outlier accessions in our PCA ("AS150" and "ASÖ5") are expressing these genes differently to the rest of the population. **b** Homeologous genes of this cluster on the *A. thaliana* subgenome of *A. suecica* show that these genes are not expressed in these two accessions while **c** shows the opposite pattern and are higher expressed in "AS150" and "ASÖ5" compared to the rest of the population. **d** 101 of the 111 genes in cluster 7 are located on chromosome 4 in close proximity to each other on the *A. thaliana* subgenome of the *A. suecica* reference genome and appear to be deleted in "AS5Ö5" and "AS150" as they do not have DNA sequencing coverage. The *A. arenosa* subgenome homeologs (located on chromosome 11) have twice the DNA coverage, suggesting they are duplicated, in agreement with the expectations of HE event.

a Rosette specific genes expressed in both subgenomes of *A. suecica*

	GO.ID	Term	Annotated	Significant	Expected	classic
1	GO:0015995	chlorophyll biosynthetic process	57	27	3.70	4.1e−17
2	GO:0009768	photosynthesis, light harvesting in phot...	17	15	1.10	1.6e−16
3	GO:0015979	photosynthesis	187	92	12.13	1.4e−15
4	GO:0009735	response to cytokinin	178	42	11.55	1.8e−13
5	GO:0019253	reductive pentose−phosphate cycle	15	13	0.97	4.1e−13
6	GO:0055114	oxidation−reduction process	970	132	62.92	2.9e−12
7	GO:0042742	defense response to bacterium	285	52	18.49	9.4e−11
8	GO:0009409	response to cold	296	51	19.20	5.7e−10
9	GO:0019761	glucosinolate biosynthetic process	26	16	1.69	6.5e−10
10	GO:0009767	photosynthetic electron transport chain	39	23	2.53	2.4e−09
11	GO:0009773	photosynthetic electron transport in pho...	12	9	0.78	3.6e−09
12	GO:0018298	protein−chromophore linkage	43	16	2.79	4.3e−09
13	GO:0010218	response to far red light	44	13	2.85	2.6e−06
14	GO:0002239	response to oomycetes	47	16	3.05	2.6e−06
15	GO:0010114	response to red light	55	15	3.57	4.4e−06
16	GO:0010196	nonphotochemical quenching	13	7	0.84	5.7e−06
17	GO:0090391	granum assembly	6	5	0.39	6.4e−06
18	GO:0032544	plastid translation	14	7	0.91	1.1e−05
19	GO:0009645	response to low light intensity stimulus	14	7	0.91	2.1e−05
20	GO:0009416	response to light stimulus	553	82	35.87	3.8e−05
21	GO:0010206	photosystem II repair	12	6	0.78	4.8e−05
22	GO:0009625	response to insect	18	7	1.17	8.0e−05
23	GO:0110102	chloroplast ribulose bisphosphate carbox...	5	4	0.32	8.3e−05
24	GO:0009098	leucine biosynthetic process	13	6	0.84	8.5e−05
25	GO:0010200	response to chitin	98	18	6.36	8.6e−05
26	GO:0010207	photosystem II assembly	22	9	1.43	0.00012
27	GO:1901259	chloroplast rRNA processing	19	7	1.23	0.00012
28	GO:1900865	chloroplast RNA modification	13	6	0.84	0.00022
29	GO:0019464	glycine decarboxylation via glycine clea...	6	4	0.39	0.00024
30	GO:0009617	response to bacterium	330	62	21.41	0.00033
31	GO:0071456	cellular response to hypoxia	153	22	9.92	0.00035
32	GO:0009644	response to high light intensity	54	13	3.50	0.00040
33	GO:0009627	systemic acquired resistance	55	10	3.57	0.00049
34	GO:0030388	fructose 1,6−bisphosphate metabolic proc...	7	4	0.45	0.00053
35	GO:0009753	response to jasmonic acid	172	20	11.16	0.00060
36	GO:1900056	negative regulation of leaf senescence	12	5	0.78	0.00061
37	GO:0006094	gluconeogenesis	18	6	1.17	0.00069
38	GO:0098869	cellular oxidant detoxification	84	15	5.45	0.00084
39	GO:0006782	protoporphyrinogen IX biosynthetic proce...	13	5	0.84	0.00094
40	GO:0052544	defense response by callose deposition i...	13	5	0.84	0.00094
41	GO:0009695	jasmonic acid biosynthetic process	19	6	1.23	0.00095

b Floral bud specific genes expressed in both subgenomes of *A. suecica*

	GO.ID	Term	Annotated	Significant	Expected	classic
1	GO:0055085	transmembrane transport	780	187	120.20	4.6e−10
2	GO:0080167	response to karrikin	93	34	14.33	4.5e−07
3	GO:0009753	response to jasmonic acid	172	50	26.51	2.2e−06
4	GO:0009739	response to gibberellin	106	34	16.33	4.2e−06
5	GO:0009737	response to abscisic acid	443	105	68.27	2.1e−05
6	GO:0071555	cell wall organization	289	63	44.54	5.0e−05
7	GO:0009733	response to auxin	245	62	37.76	7.9e−05
8	GO:0071456	cellular response to hypoxia	153	42	23.58	0.00012
9	GO:0006995	cellular response to nitrogen starvation	23	11	3.54	0.00025
10	GO:0009749	response to glucose	48	17	7.40	0.00027
11	GO:0042908	xenobiotic transport	35	14	5.39	0.00038
12	GO:0035445	borate transmembrane transport	4	4	0.62	0.00056
13	GO:0010143	cutin biosynthetic process	18	10	2.77	0.00078
14	GO:0071577	zinc ion transmembrane transport	12	7	1.85	0.00079

c Floral bud specific genes expressed biased towards *A. arenosa*

	GO.ID	Term	Annotated	Significant	Expected	classic
1	GO:0055085	transmembrane transport	780	46	28.48	5.4e−05
2	GO:0006032	chitin catabolic process	9	4	0.33	0.00019

d Rosette specific genes expressed biased towards *A. arenosa*

	GO.ID	Term	Annotated	Significant	Expected	classic
1	GO:0010411	xyloglucan metabolic process	39	5	0.64	0.00041
2	GO:0009089	lysine biosynthetic process via diaminop...	11	3	0.18	0.00065
3	GO:0046685	response to arsenic−containing substance	11	3	0.18	0.00065
4	GO:0071456	cellular response to hypoxia	153	9	2.51	0.00093

e Rosette specific genes expressed biased towards *A. thaliana*

	GO.ID	Term	Annotated	Significant	Expected	Classic
1	GO:0031408	oxylipin biosynthetic process	20	4	0.34	0.00031

Supplementary Table 1. Gene ontology (GO) analysis for gene expression comparison between whole rosettes and floral buds in *A. suecica*. No significant GO was found for genes biased towards the *A. thaliana* subgenome of *A. suecica* for floral buds.

a

A. thaliana cluster 1

	GO.ID	Term	Annotated	Significant	Expected	classic
1	GO:0006355	regulation of transcription, DNA–templat...	1384	267	209.78	9.6e–07
2	GO:0016567	protein ubiquitination	524	107	79.43	2.5e–05
3	GO:0007623	circadian rhythm	122	34	18.49	5.0e–05
4	GO:0008645	hexose transmembrane transport	29	15	4.40	6.4e–05
5	GO:0009739	response to gibberellin	106	36	16.07	0.00015
6	GO:0010167	response to nitrate	16	9	2.43	0.00017
7	GO:0009723	response to ethylene	189	48	28.65	0.00027
8	GO:0009733	response to auxin	245	63	37.14	0.00033
9	GO:0006857	oligopeptide transport	20	12	3.03	0.00034
10	GO:1990641	response to iron ion starvation	6	5	0.91	0.00042
11	GO:0009638	phototropism	15	8	2.27	0.00065
12	GO:0071577	zinc ion transmembrane transport	12	7	1.82	0.00071
13	GO:0009741	response to brassinosteroid	82	25	12.43	0.00088

b

A. thaliana cluster 2

	GO.ID	Term	Annotated	Significant	Expected	classic
1	GO:0009735	response to cytokinin	178	43	20.09	4.4e–10
2	GO:0007018	microtubule–based movement	64	26	7.22	1.7e–09
3	GO:0006412	translation	527	97	59.48	7.4e–09
4	GO:0000911	cytokinesis by cell plate formation	55	19	6.21	3.3e–06
5	GO:0006268	DNA unwinding involved in DNA replicatio...	18	10	2.03	6.1e–06
6	GO:1901259	chloroplast rRNA processing	19	10	2.14	1.1e–05
7	GO:0009658	chloroplast organization	201	47	22.69	3.8e–05
8	GO:0032544	plastid translation	14	8	1.58	4.1e–05
9	GO:0000727	double–strand break repair via break–ind...	11	7	1.24	5.0e–05
10	GO:0000226	microtubule cytoskeleton organization	130	38	14.67	0.00013
11	GO:0045037	protein import into chloroplast stroma	23	10	2.60	0.00015
12	GO:0006880	intracellular sequestering of iron ion	7	5	0.79	0.00031
13	GO:0042793	plastid transcription	11	6	1.24	0.00057
14	GO:0007088	regulation of mitotic nuclear division	50	14	5.64	0.00061
15	GO:0010103	stomatal complex morphogenesis	16	8	1.81	0.00075
16	GO:0051301	cell division	338	74	38.15	0.00076
17	GO:0010020	chloroplast fission	20	8	2.26	0.00093

c

A. thaliana cluster 3

	GO.ID	Term	Annotated	Significant	Expected	classic
1	GO:0051028	mRNA transport	64	10	2.15	3e–05
2	GO:0042147	retrograde transport, endosome to Golgi	24	6	0.81	0.00011
3	GO:0006390	mitochondrial transcription	4	3	0.13	0.00015
4	GO:0002943	tRNA dihydrouridine synthesis	5	3	0.17	0.00036
5	GO:0006457	protein folding	140	14	4.71	0.00076

d

A. arenosa cluster 1

	GO.ID	Term	Annotated	Significant	Expected	classic
1	GO:0055114	oxidation–reduction process	970	148	86.72	2.6e–08
2	GO:0098869	cellular oxidant detoxification	84	19	7.51	6.7e–05
3	GO:0009854	oxidative photosynthetic carbon pathway	5	4	0.45	0.00030
4	GO:0006749	glutathione metabolic process	30	10	2.68	0.00057

e

A. arenosa cluster 3

	GO.ID	Term	Annotated	Significant	Expected	classic
1	GO:0006397	mRNA processing	329	128	73.49	2.8e–05
2	GO:0006606	protein import into nucleus	47	25	10.50	0.00014
3	GO:0009908	flower development	335	116	74.83	0.00025
4	GO:0051028	mRNA transport	64	25	14.30	0.00056
5	GO:0040029	regulation of gene expression, epigeneti...	152	63	33.95	0.00061
6	GO:0042176	regulation of protein catabolic process	38	18	8.49	0.00069
7	GO:0045944	positive regulation of transcription by ...	153	52	34.18	0.00090
8	GO:0009793	embryo development ending in seed dorman...	292	89	65.22	0.00095

774

775 **Supplementary Table 2. List of overrepresented gene ontologies on the Fig. 5e**

Materials & Methods

PacBio sequencing of *A. suecica*

We used genomic DNA from whole rosettes of one *A. suecica* (“ASS3”) accession to generate PacBio sequencing data. DNA was extracted using a modified PacBio protocol for preparing *Arabidopsis* genomic DNA for size-selected ~20kb SMRTbell libraries. Briefly, whole genomic DNA was extracted from 32g of 3-4 week old plants, grown at 16°C and subjected to a 2-day dark treatment. This generated 23 micrograms of purified genomic DNA with a fragment length of >40Kb for *A. suecica*. We assessed DNA quality with a Qubit fluorometer and a Nanodrop analysis, and ran the DNA on a gel to visualize fragmentation. Genomic libraries and single-molecule real-time (SMRT) sequence data were generated at the Functional Genomics Center Zurich (FGCZ), in Switzerland. The Pacbio RSII instrument was used with P6/C4 chemistry and an average movie length of 6 hours. A total of 12 SMRT cells were processed generating 16.3Gb of DNA bases with an N50 read length of 20 Kbp and median read length of 14 Kbp. Using the same genomic library, an additional 3.3 Gbp of data was generated by a Pacbio Sequel instrument at the Vienna Biocenter Core Facilities (VBCF), in Austria, with a median read length of 10Kbp.

A. suecica genome assembly

To generate the *A. suecica* assembly we first used FALCON[127] (version 0.3.0) with a length cutoff for seed reads set to 1 Kb in size. The assembly produced 828 contigs with an N50 of 5.81 Mb and a total assembly size of 271 Mb. Additionally, we generated a Canu[128] (v.1.3.0) assembly using default settings, which resulted in 260 contigs with an N50 of 6.65 Mb and a total assembly size of 267 Mb. Then we merged the two assemblies using the software quickmerge[129]. The resulting merged assembly consisted of 929 contigs with an N50 of 9.02 Mb and a total draft assembly size of 276 Mb. We polished the assembly using Arrow[130] (smrtlink release 5.0.0.6792) and Pilon (version 1.22). For Pilon[131], 100bp (with PCR duplicates removed), and a second PCR-free 250bp, Illumina paired end reads were used that had been generated from the reference *A. suecica* accession “ASS3”.

Pacbio sequencing of *A. arenosa*

A natural Swedish autotetraploid *A. arenosa* accession "Aa4" was inbred in a lab for two generations in order to reduce heterozygosity. We extracted whole genomic DNA from 64g of three week old plants in the same way as described for *A. suecica* (above), generating 50 µg of purified genomic DNA with a fragment sizes longer than 40 Kb in length. The *A. arenosa* genomic libraries and SMRT sequence data were generated at the Vienna Biocenter Core Facilities (VBCF), in Austria. A Pacbio Sequel instrument was used to generate a total of 22 Gbp of data from five SMRT cells, with an N50 of 13 Kbp and median read length 10 Kbp. In addition, two runs of Oxford Nanopore sequencing were carried out at the VBCF producing 750 Mbp in 180,000 reads (median 5 Kbp and 2.6 Kbp; N50 8.7 and 6.7 Kbp, respectively).

Assembly of autotetraploid *A. arenosa*

We assembled a draft contig assembly for the autotetraploid *A. arenosa* accession "Aa4" using FALCON (version 0.3.0) as for *A. suecica*. The assembly produced 3,629 contigs with an N50 of 331 Kb, maximum contig size of 2.5 Mb and a total assembly size of 461 Mb. The assembly size is greater than the calculated haploid size of 330 Mb using FACs (see Supplementary Figure 2) probably because of the high levels of heterozygosity in *A. arenosa*. The resulting assembly was polished as described for *A. suecica*.

HiC tissue fixation and library preparation

To generate physical scaffolds for the *A. suecica* assembly we generated proximity-ligation HiC sequencing data. We collected approximately 0.5 gram of tissue from 3-week old seedlings of the same reference *A. suecica* accession. Freshly collected plant tissue was fixed in 1% formaldehyde. Cross-linking was stopped by the addition of 0.15 M Glycine. The fixed tissue was ground to a powder in liquid nitrogen and suspended in 10 ml of nuclei isolation buffer. Nuclei was digested by adding 50 U DpnII and the digested chromatin was blunt-ended by incubation with 25 µL of 0.4 mM biotin-14-dCTP and 40 U of Klenow enzyme, as described in [ref]. 20 U of T4 DNA ligase was then added to start proximity ligation. The extracted DNA was sheared by sonication with a Covaris S220 to produce 250-500bp fragments. This was followed by size fractionation using AMPure XP beads. Biotin was then removed from unligated ends. DNA fragments were blunt-end repaired and adaptors were ligated to the DNA products following the NEBNext Ultra II RNA Library Prep Kit for Illumina.

To analyse structural rearrangements we collected tissue for 1 other natural *A. suecica* “AS530”, 1 *A. thaliana* accession ”6978”, 1 *A. arenosa* “Aa6” and 1 synthetic *A. suecica* (F3). Each sample had two replicates. We collected tissue and prepared libraries in the same manner as described above. 125bp paired-end Illumina reads were mapped using HiCUP[132] (version 0.6.1).

Reference-guided scaffolding of the *A. suecica* genome with *LACHESIS*

We sequenced 207 million pairs of 125bp paired-end Illumina reads from the HiC library of the reference accession "ASS3". We mapped reads using HiCUP (version 0.6.1) to the draft *A. suecica* contig assembly. This resulted in ~137 million read pairs with a unique alignment.

Setting an assembly threshold of >= 1 Kb in size, contigs of the draft *A. suecica* assembly were first assigned to the *A. thaliana* or *A. arenosa* subgenome. To do this, we used nucmer from the software MUMmer[133] (version 3.23) to perform whole-genome alignments. We aligned the draft *A. suecica* assembly to the *A. thaliana* TAIR10 reference and to our *A. arenosa* draft contig assembly, simultaneously. We used the MUMer command dnadiff to produce 1-to-1 alignments. As the subgenomes are only ~86% identical, the majority of contigs could be conclusively assigned to either subgenome by examining how similar the alignments were. Contigs that could not be assigned to a subgenome based on percentage identity were examined manually, and the length of the alignment was used to determine subgenome assignment.

Finally, we used the software LACHESIS[134] (version 1.0.0) to scaffold our draft assembly, using the reference genomes of *A. thaliana* and *A. lyrata as* a guide to assist with scaffolding

855 the contigs (we used *A. lyrata* here instead of our draft *A. arenosa* contig assembly, as *A.*
856 *lyrata* is a chromosome-level assembly). This produced a 13-scaffold chromosome-level
857 assembly for *A. suecica*.

858 Construction of the *A. suecica* genetic map

859 We crossed natural *A. suecica* accession "AS150" with the reference accession "ASS3". The
860 cross was uni-directional with "AS150" as the maternal and "ASS3" as the paternal plant. F1
861 plants were grown, and F2 seeds were collected, from which we grew and collected 192 F2
862 plants. We multiplexed the samples on 96 well plates using 75bp paired end reads and
863 generated data of 1-2x coverage per sample. Samples were mapped to the repeat-masked
864 scaffolds of the reference *A. suecica* genome using BWA-MEM[135] (version 0.7.15).
865 Samtools[136] (version 0.1.19) was used to filter reads for proper pairs and a minimum mapping
866 quality of 5 (-F 256 -f 3 -q 5). We called variants directly from samtools mpileup output on the
867 sequenced F2 individuals at known biallelic sites between the two accessions used to
868 generate the cross (a total of 590,537 SNPs). We required sites to have non-zero coverage in
869 a minimum of 20 individuals and filtered SNPs to have frequency between 0.45-0.55 in our F2
870 population (as the expectation is 50:50),. We removed F2 individuals that did not have
871 genotype calls for more than 90% of the data. This resulted in 183 individuals with genotype
872 calls for 334,257 SNPs.
873 Since sequencing coverage for the F2s was low this meant we had a low probability of
874 calling heterozygous SNPs, and a higher probability of calling a SNP as homozygous.
875 Therefore, we applied a Hidden Markov Model implemented in R package HMM[137] to classify
876 SNPs as homozygous or heterozygous for each of our F2 lines. We then divided the genome
877 into 500Kb non-overlapping windows, and classified each window as homozygous (here 0 or
878 1, for the reference or alternate SNP) or heterozygous (here 0.5). If the frequency of 1, 0 or
879 0.5 represented more than 50% of the SNPs in a given window, and exceeded missing calls
880 (NA), the window was designated as 1, 0 or 0.5 (otherwise it was NA). This was done per
881 chromosome and the resulting file for each chromosome and their markers were processed in
882 the R package qtl[138], in order to generate a genetic map. Markers genotyped in less than 100
883 F2s were excluded from the analysis. Linkage groups were assigned with a minimum LOD
884 score of 8 and a maximum recombination fraction of 0.35. Each chromosome was assigned
885 to one linkage group. We defined the final marker order by the best LOD score and the lowest
886 number of crossover events.
887 Notably, the assistance of a genetic map corrected the erroneous placement of a contig
888 at the beginning of chromosome 1 of the *A. arenosa* subgenome. The misplaced contig was
889 relocated from chromosome 1 to the pericentromeric region of chromosome 2 of the *A.*
890 *arenosa* subgenome in *A. suecica*. This error was a result of a mis-assembly of chromosome
891 1 in the *A. lyrata* reference, as was previously pointed out [77]. Also of note, chromosome 2 of
892 the *A. thaliana* subgenome of *A. suecica* was previously shown to be largely devoid of
893 intraspecific variation, thus we had sparse marker information for this chromosome in the
894 genetic map. Therefore, this chromosome-scale scaffold was largely assembled by the
895 manual inspection of 3D-proximity information based on our HiC sequencing and reviewing
896 contig order using the software Juicebox[139].

897 # Gene prediction and annotation of the *A. suecica* genome

898 We combined *de novo* and evidence-based approaches to predict protein coding genes. For
899 *de novo* prediction, we trained AUGUSTUS[140] on the set of conserved single copy genes using
900 BUSCO[141] separately on *A. thaliana* and *A. arenosa* subgenomes of *A. suecica*. The evidence-
901 based approach included both homology to the protein sequences of the ancestral species
902 and the transcriptome of *A. suecica*. We aligned the peptide sequences from TAIR10 *A.*
903 *thaliana* assembly to the *A. thaliana* subgenome of *A. suecica*, while the peptides from *A.*
904 *lyrata* from the second version of *A. lyrata* annotation[142] (Alyrata_384_v2.1) were aligned to
905 the *A. arenosa* subgenome of *A. suecica* using GenomeThreader[143] (1.7.0). We mapped the
906 RNAseq reads from the reference accession of *A. suecica* (ASS3) from the rosettes and flower
907 buds tissues (see above) to the reference genome using tophat[144] and generated intron hints
908 from the split reads using bam2hints extension of AUGUSTUS. We split the alignment into *A.*
909 *thaliana* and *A. arenosa* subgenomes and assembled the transcriptome of *A. suecica* for each
910 subgenome separately in the genome-guided mode with Trinity[145] (2.6.6). Separately for each
911 of the subgenomes, we filtered the assembled transcripts using tpm cutoff set to 1, collapsed
912 similar transcripts using CD-HIT[146,147] with sequence identity set to 90 percent, and chose the
913 longest open reading frame from the six-frame translation. We then aligned the proteins from
914 *A. thaliana* and *A. arenosa* parts of *A. suecica* to the corresponding subgenomes using
915 GenomeThreader (1.7.0). We ran AUGUSTUS using retrained parameters from BUSCO and
916 merged hints from all three sources, these being: (1) intron hints from *A. suecica* RNAseq, (2)
917 homology hints from ancestral proteins and (3) hints from *A. suecica* proteins.
918 RepeatModeler[148] (version 1.0.11) was used in order to build a *de novo* TE consensus
919 library for *A. suecica* and identify repetitive elements based on the genome sequence.
920 Genome locations for the identified TE repeats were determined by using RepeatMasker[149]
921 (version 4.0.7) and filtered for full length matches using a code described in Bailly-Bechet et.
922 al[150]. Helitrons are the most abundant TE family in both subgenomes (Supplementary Fig. 7).

923 # Synthetic *A. suecica* lines

924 To generate synthetic *A. suecica* we crossed a natural tetraploid *A. thaliana* accession (6978
925 aka “Wa-1”) to a natural Swedish autotetraploid *A. arenosa* (“Aa4”) accession. Similar to the
926 natural *A. suecica*, *A. thaliana* was the maternal and *A. arenosa* was the paternal plant in this
927 cross. Crosses in the opposite direction were unsuccessful. We managed to obtain very few
928 F1 hybrid plants, which after one round of selfing set higher levels of seed formation. The
929 resulting synthetic line was able to self-fertilize. F2 seeds were descended from a common F1
930 and were similar to natural *A. suecica* in appearance. We further continued the synthetic line
931 to F3 (selfed 3rd generation).

932 # Synteny analysis

933 We performed all-against-all BLASTP search using CDS sequences for the reference *A.*
934 *suecica* genome and the ancestral genomes, *A. thaliana* and *A. lyrata* (here the closest
935 substitute reference genome for *A. arenosa*, with annotation). We used the SynMap tool[151]
936 from the online CoGe portal[152]. We examined synteny using the default parameters for
937 DAGChainer (maximum distance between two matches = 20 genes; minimum number of
938 aligned pairs = 5 genes).

Estimating copy number of rDNA repeats using short DNA reads

To measure copy number of 45S rRNA repeats in our populations of different species, we aligned short DNA reads to a single reference 45S consensus sequence of *A. thaliana*[153]. An *A. arenosa* 45S rRNA consensus sequence was constructed by finding the best hit using BLAST in our draft *A. arenosa* contig assembly. This hit matched position 1571-8232 bp of the *A. thaliana* consensus sequence, was 6,647 bp in length and is 97% identical to the *A. thaliana* 45s rRNA consensus sequence. The aligned regions of these two 45S rRNA consensus sequences, determined by BLAST, were used in copy number estimates, to ensure that the size of the sequences were equal. The relative increase in sequence coverage of these loci, when compared to the mean coverage for the reference genome, was used to estimate copy number.

Plant material for RNA sequencing

Transcriptomic data generated in this study included 15 accessions of *A. suecica*, 16 accessions of *A. thaliana*, 4 accessions of *A. arenosa* and 2 generations of an artificial *A. suecica* line (the 2nd and 3rd selfed-generation). The sibling of a paternal *A. arenosa* parent (Aa4) and the maternal tetraploid *A. thaliana* parent (6978 aka “Wa-1”) of our artificial *A. suecica* line were included as part of our samples (Supplementary Data 1). Each accession was replicated 3 times. Seeds were stratified in the dark for 4 days at 4°C in 1 ml of sterilised water. Seeds were then transferred to pots in a controlled growth chamber at 21°C. Humidity was kept constant at 60%. Pots were thinned to 2-3 seedlings after 1 week. Pots were re-randomized each week in their trays. Whole rosettes were collected when plants reached the 7-9 true-leaf stage of development. Samples were collected between 14:00-17:00h and flash-frozen in liquid nitrogen.

RNA extraction and library preparation

For each accession, 2-3 whole rosettes in each pot were pooled and total RNA was extracted using the ZR Plant RNA MiniPrepTM kit. We treated the samples with DNAse, and performed purification of mRNA and polyA selection using the AMPure XP magnetic beads and the Poly(A) RNA Selection Kit from Lexogen. RNA quality and degradation were assessed using the RNA Fragment Analyzer (DNF-471 stranded sensitivity RNA analysis kit, 15nt). Concentration of RNA per sample was measured using the Qubit fluorometer. Library preparation was carried out following the NEBNext Ultra II RNA Library Prep Kit for Illumina. Barcoded adaptors were ligated using NEBNext Multiplex Oligos for Illumina (Index Primers Set 1 and 2). The libraries were PCR amplified for 7 cycles. 125bp paired-end sequencing was carried out at the VBCF on Illumina (HiSeq 2500) using multiplexing.

RNA-seq mapping and gene expression analysis

We mapped 125bp paired-end reads to the *de novo* assembled *A. suecica* reference using STAR[154] (version 2.7), we filtered for primary and uniquely aligned reads using the parameters --outfilterMultimapNmax 1 --outSamprimaryFlag OneBestScore. We quantified reads mapped to genes using --quantMode GeneCounts.

979 In order to reduce signals that are the result of cross mapping between the subgenomes
980 of *A. suecica* we used *A. thaliana* and *A. arenosa* as a control. For each gene in the *A. thaliana*
981 subgenome we compared log fold change of gene counts in our *A. thaliana* population to those
982 in our *A. arenosa* population. We filtered for genes with a $\log_2$(*A. thaliana*/*A. arenosa*) below
983 0. We applied the same filters for genes on the *A. arenosa* subgenome, here a $\log_2$(*A.*
984 *arenosa*/*A. thaliana*) below 0. This reduced the number of genes analyzed from 22,383 to
985 21,737 on the *A. thaliana* subgenome, and 23,353 to 23,221 on the *A. arenosa* subgenome
986 Expression analysis was then further restricted to 1:1 unique homeologous gene pairs
987 between the subgenomes of *A. suecica* (17,881 gene pairs). Gene counts were normalized
988 for gene size by calculating Transcripts Per Million (TPM). The effective library sizes were
989 calculated by computing a scaling factor based on the trimmed mean of M-values (TMM) in
990 edgeR[155], separately for each subgenome. Lowly expressed genes were removed from the
991 analysis by keeping genes that were expressed in at least 3 individuals of *A. thaliana* and *A.*
992 *suecica*, at least 1 individual of *A. arenosa* and at least 1 individual of synthetic *A. suecica*.
993 14,041 homeologous gene pairs satisfied our expression criteria. Since *A. suecica* is
994 expressing both subgenomes, in order to correctly normalize the effective library size in *A.*
995 *suecica* accessions, the effective library size was calculated as a mean of TPM counts for both
996 subgenomes. The effective library size of *A. thaliana* accessions was calculated for TPM
997 counts using the *A. thaliana* subgenome of the reference genome, as genes from this
998 subgenome will be expressed in *A. thaliana*, and the effective library size of *A. arenosa* lines
999 using the *A. arenosa* subgenome of the reference *A. suecica* genome. Gene counts were
1000 transformed to count per million (CPM) with a prior count of 1, and were $\log_2$-transformed. We
1001 used the mean of replicates per accession for downstream analyses.
1002 To compare homeologous genes between the subgenomes in *A. suecica* we computed a
1003 log-fold change using $\log_2$(*A. arenosa* homeolog/*A. thaliana* homeolog). For tissue-specific
1004 genes we took genes that showed a log-fold change >=2 in expression between two tissues.
1005 For comparing homologous genes between the (sub-)genomes of *A. suecica* and the
1006 ancestral species *A. thaliana* and *A. arenosa*, we performed a Wilcoxon test independently for
1007 each of the 14,041 homeologous gene-pairs. Using the normalised CPM values, we compared
1008 the relative expression level of a gene on the *A. thaliana* subgenome between our population
1009 of *A. thaliana* and *A. suecica*. We performed the same test on the *A. arenosa* subgenome
1010 comparing relative expression of a gene between our population of *A. arenosa* and *A. suecica*.
1011 We filtered for genes with an adjusted p-value below <0.05 (using FDR correction). This
1012 amounted to 4,186 and 4,571 DEGs for the *A. thaliana* and *A. arenosa* subgenomes,
1013 respectively.
1014 Cross-mapping between subgenomes was measured by mixing RNA reads between
1015 *A. thaliana* and *A. arenosa* and mapping to the *A. suecica* genome. ~1% of A. thaliana reads
1016 map to the A. arenosa subgenome and ~6% of the *A. arenosa* reads map to the *A. thaliana*
1017 subgenome, regardless of mapping strategy or pipeline (see Supplementary Figure 13). This
1018 can be explained by pairwise percentage differences or π within *A. arenosa* overlapping this
1019 distribution of π between *A. thaliana* and *A. arenosa* such that some exons on the *A. thaliana*
1020 subgenome are in fact closer to a particular *A. arenosa* individual than those on the *A. arenosa*
1021 subgenome of *A. suecica*. However lower π in *A. suecica* suggest this observation will not affect
1022 estimates of subgenome dominance for *A. suecica*.

1023 # Expression analysis of rRNA

1024 RNA reads were mapped in a similar manner as DNA reads for the analysis of rDNA copy
1025 number (above). Expression analysis was performed in a similar manner to protein coding
1026 genes, in edgeR. We defined the exclusive expression of a particular 45S rRNA gene by taking
1027 a cut-off of 15 for $\log_2$(CPM) as this was the maximum level of cross-mapping we observed
1028 for the ancestral species (see Supplementary Fig. 6).

1029 # Expression analysis of transposable elements

1030 To analyse the expression of transposable elements between species, the annotated TE
1031 consensus sequences in *A. suecica* were aligned using BLAST all vs all. Highly similar TE
1032 sequences (more than 85% similar for more than 85% percent of the TE sequence length),
1033 were removed, leaving 813 TE families out of 1213. Filtered *A. suecica* TEs were aligned to
1034 annotated *A. thaliana* (TAIR10) and *A. arenosa* (the PacBio contig assembly presented in
1035 this study) TE sequences to assign each family to an ancestral species using BLAST. 208
1036 TE families were assigned to the *A. thaliana* parent and 171 TE families were assigned to
1037 the *A. arenosa* parent.
1038 RNA reads were mapped to TE sequences using a similar approach as for gene
1039 expression analysis using edgeR. TEs that showed expression using a cut-off of $\log_2$CPM >
1040 2 were kept. 121 *A. thaliana* TE sequences and 93 *A. arenosa* TE sequences passed this
1041 threshold. We took the mean of replicates per accession for further downstream analyses.

1042 # Gene ontology (GO) enrichment analysis

1043 We used the R package TopGO[156] to conduct gene ontology enrichment analysis. We used
1044 the “weight01” algorithm when running TopGO which accounts for the hierarchical structure
1045 of GO terms and thus implicitly corrects for multiple testing. GO annotations were based on
1046 the *A. thaliana* ortholog of *A. suecica* genes. Gene annotations for *A. thaliana* were obtained
1047 using the R package biomaRt[157] from Ensembl ‘biomaRt::useMart(biomart = "plants_mart",
1048 dataset = "athaliana_eg_gene", host = 'plants.ensembl.org').

1049 # Genome sizes measurements

1050 We measured genome size for the reference *A. suecica* accession “ASS3” and the *A. arenosa*
1051 accession used for PacBio “Aa4”, using *Solanum lycopersicum* cv. Stupicke (2C = 1.96 pg
1052 DNA) as the standard. The reference *A. lyrata* accession “MN47” and the *A. thaliana*
1053 accession “CVI” were used as additional controls. Each sample had 2 replicates.
1054 In brief, the leaves from three week old fresh tissue were chopped using a razor blade in 500
1055 µl of UV Precise P extraction buffer + 10 µl mercaptoethanol per ml (kit PARTEC CyStain PI
1056 Absolute P no. 05- 5022) to isolate nuclei. Instead of the Partec UV Precise P staining buffer,
1057 however, 1 ml of a 5 mg DAPI solution was used, as DAPI provides DNA content histograms
1058 with high resolution. The suspension was then passed through a 30 µm filter (Partec CellTrics
1059 no. 04-0042-2316) and incubated for 15 minutes on ice before FACs.
1060 Genome size was measured using flow cytometry and a FACS Aria III sorter with near UV
1061 375nm laser for DAPI. Debris was excluded by selecting peaks when plotting DAPI-W against
1062 DAPI-A for 20,000 events.

1063 The data were analyzed using the flowCore[158] package in R. Genome size was estimated
1064 by comparing the mean G1 of the standard *Solanum lycopersicum* to that of each sample to
1065 calculate the 2C DNA content of that sample using the equation:

1066 $$Sample\ 2C\ DNA\ content\ =\ [(sample\ G1\ peak\ mean)/(standard\ G1\ peak\ mean)]$$
1067 $$*\ standard\ 2C\ DNA\ content$$

1068 We also measured genome size for the reference *A. suecica* accession "ASS3" using the
1069 software jellyfish[159] and findGSE[160] using kmers (21mers). The genome size estimated was
1070 312Mb, compared to the 305Mb estimated using FACs (see Supplementary Fig 1).

1071 Mapping of TE insertions

1072 We used PopoolationTE2[100] (version v1.10.04) to identify TE insertions. The advantage of this
1073 TE-calling software to others is that it avoids a reference bias by treating all TEs as *de-novo*
1074 insertions. Briefly, it works by using discordant read pairs to calculate the location and
1075 abundance of a TE in the genome for an accession of interest.

1076 We mapped 100 bp Illumina DNA reads from [20,76,161], in addition to our newly generated
1077 synthetic *A. suecica* using BWA MEM[135] (version 0.7.15) to a repeat-masked version of the *A.*
1078 *suecica* reference genome, concatenated with our annotated repeat sequences (see 'Genome
1079 annotation'), as this is the data format required by PopoolationTE2. Reads were given an
1080 increased penalty of 15 for being unpaired. Reads were de-duplicated using Samtools[136]
1081 rmdup (version 1.9). The resulting bam files were then provided to PopoolationTE2 to identify
1082 TE insertions in the genome of each of our *A. suecica*, *A. thaliana* and *A. arenosa* accessions.
1083 We used a mapping quality of 10 for the read in the discordant read pair mapping to the
1084 genome. We used the 'separate' mode in the 'identify TE signatures' step and a '--min-
1085 distance -200 --max-distance 500' in the 'pairupsignatues' step of the pipeline. TE counts
1086 within each accession were merged if they fell within 400 bp of each other and if they mapped
1087 to the same TE sequence. All TE counts (i.e. the processed TE counts for each accession)
1088 were then combined to produce a population-wide count estimate. Population wide TE
1089 insertions were merged if they mapped to the same TE sequence and fell within 400 bp of
1090 each other. Coverage of each TE insertion in the population was also calculated for each
1091 accession. The final file was a list TE insertions present in the population and the presence or
1092 absence (or "NA" if there was no coverage to support the presence or absence of a TE
1093 insertion) in each accession analyzed (Supplementary Data 1).

1094 Assigning ancestry to TE sequences

1095 In order to examine TE consensus sequences that have mobilized between the subgenomes
1096 of *A. suecica*, we first examined which of our TE consensus sequences (N=1152) have at
1097 least the potential to mobilize (i.e. have full length TE copies in the genome of *A. suecica)*. We
1098 filtered for TE consensus sequences that had TE copies in the genome of *A. suecica* that are
1099 more than 80% similar in identity for more than 80% of the consensus sequence length
1100 (N=936). Of these, 188 consensus sequences were private to the *A. thaliana* subgenome, 460
1101 were private to the *A. arenosa* subgenome, and 288 TE consensus sequences were present
1102 in both subgenomes of *A. suecica*. To determine if TEs have jumped from the *A. thaliana*
1103 subgenome to the *A. arenosa* subgenome and vice versa we next needed to assign ancestry
1104 to these 288 TE consensus sequences. To do this we used BLAST to search for these
1105 consensus sequences in the ancestral genomes of *A. suecica*, using the TAIR10 *A. thaliana*

1106 reference and our *A. arenosa* PacBio contig assembly. Using the same 80%-80% rule we
1107 assigned 55 TEs to *A. arenosa* and 15 TEs to *A. thaliana* ancestry.

1108 Read mapping and SNP calling

1109 To call biallelic SNPs we mapped reads to the *A. suecica* reference genome using the same
1110 filtering parameters described in "Mapping of TE insertions". Biallelic SNPs were called using
1111 HaplotypeCaller from GATK[162] (version 3.8) using default quality thresholds. SNPs were
1112 annotated using SnpEff[163]. Biallelic SNPs on the *A. thaliana* sub-genome were polarized using
1113 38 diploid *A. lyrata* lines[76] and biallelic SNPS on the *A. arenosa* sub-genome were polarized
1114 using 30 *A. thaliana* accessions[161] closely related to *A. suecica*[20].

1115 Chromosome preparation and FISH

1116 Whole inflorescences of *A. arenosa*, *A. suecica* and *A. thaliana* were fixed in freshly prepared
1117 ethanol:acetic acid fixative (3:1) overnight, transferred into 70% ethanol and stored at -20°C
1118 until use. Selected inflorescences were rinsed in distilled water and citrate buffer (10 mM
1119 sodium citrate, pH 4.8), and digested by a 0.3% mix of pectolytic enzymes (cellulase,
1120 cytohelicase, pectolyase; all from Sigma-Aldrich) in citrate buffer for c. 3 hrs. Mitotic
1121 chromosome spreads were prepared from pistils as previously described[164] by Mandáková
1122 and Lysak and suitable slides pretreated by RNase (100 µg/ml, AppliChem) and pepsin (0.1
1123 mg/ml, Sigma-Aldrich).
1124 For identification of *A. thaliana* and *A. arenosa* subgenomes in the allotetraploid
1125 genome of *A. suecica*, FISH probes were made from plasmids pARR20–1 or pAaCEN
1126 containing 180 bp of *A. thaliana* (pAL; Vongs et al. 1993) or ~250 bp of *A. arenosa* (pAa;
1127 Kamm et al. 1995) pericentromeric repeats, respectively. The *A. thaliana* BAC clone T15P10
1128 (AF167571) bearing 45S rRNA gene repeats was used for in situ localization of NORs.
1129 Individual probes were labeled with biotin-dUTP, digoxigenin-dUTP and Cy3-dUTP by nick
1130 translation, pooled, precipitated, and resuspended in 20 µl of hybridization mixture [50%
1131 formamide and 10% dextran sulfate in 2× saline sodium citrate (2× SSC)] per slide as
1132 previously described[96].
1133 Probes and chromosomes were denatured together on a hot plate at 80°C for 2 min
1134 and incubated in a moist chamber at 37°C overnight. Post hybridization washing was
1135 performed in 20% formamide in 2× SSC at 42°C. Fluorescent detection was as follows: biotin-
1136 dUTP was detected by avidin–Texas Red (Vector Laboratories) and amplified by goat anti-
1137 avidin–biotin (Vector Laboratories) and avidin–Texas Red; digoxigenin-dUTP was detected by
1138 mouse anti-digoxigenin (Jackson ImmunoResearch) and goat anti-mouse Alexa Fluor 488
1139 (Molecular Probes). Chromosomes were counterstained with DAPI (4',6-diamidino-2-
1140 phenylindole; 2 µg/ml) in Vectashield (Vector Laboratories). Fluorescent signals were
1141 analyzed and photographed using a Zeiss Axioimager epifluorescence microscope and a
1142 CoolCube camera (MetaSystems). Images were acquired separately for the four
1143 fluorochromes using appropriate excitation and emission filters (AHF Analysentechnik). The
1144 monochromatic images were pseudo colored and merged using Adobe Photoshop CS6
1145 software (Adobe Systems).

DAP-seq enrichment analysis for transcription factor target genes

We downloaded the target genes of transcription factors from the plant cistrome database (http://neomorph.salk.edu/dap_web/pages/index.php), which is a collection of transcription factor binding sites and their target genes, in *A. thaliana*, based on DAP-seq[165]. To test for enrichment of a gene set (for example the genes in *A. thaliana* cluster 2 on Fig. 5) for target genes of a particular transcription factor, we performed a hyper-geometric test in R. As a background we used the total 14,041 genes used in our gene expression analysis. We then performed FDR correction for multiple testing to calculate an accurate p-value of the enrichment.

Data Availability

Genome assemblies and raw short reads can be found in the European Nucleotide Archive (ENA) (https://www.ebi.ac.uk/ena/browser/home).
The genome assembly for *A. suecica* ASS3 can be found under the BioProject number PRJEB42198, assembly accession GCA_905175345. The raw reads for the *A. suecica* genome assembly generated by Pacbio RSII can be found under ERR5037702 and those from Sequel under ERR5031296. The HiC reads used for scaffolding the *A. suecica* assembly can be found under ERR5032369.
The contig assembly for tetraploid *A. arenosa (ssp. arenosa)* can be found under the BioProject number PRJEB42276, assembly accession GCA_905175405. The raw reads for the *A. arenosa* Aa4 contig assembly generated by Sequel can be found under ERR5031542 and the reads generated by Nanopore under ERR5031541. HiC reads for the *A. arenosa* assembly can be found under ERR5032370.
HiC sequencing data for the ancestral species, the outlier accession AS530 and synthetic *A. suecica* can be found under the BioProject PRJEB42290.
DNA resequencing of synthetic *A. suecica* and parents generated in this study can be found under the BioProject PRJEB42291.
The RNA-seq reads are under the BioProject number PRJEB42277.
TE presence/absence calls for *A. suecica* and the ancestral species can be found in Supplementary Data 1.
A list of DEGs, orthologs, enriched DAP-seq transcription factors, CyMIRA gene overlaps and RNA-seq mapping statistics can be found in Supplementary Data 2.
Log fold change and CPM (counts per million) for genes on the *A. thaliana* and *A. arenosa* subgenome can be found in Supplementary Data 3.
The gene annotation (gff3 file) of the *A. suecica* genome can be found in Supplementary Data 4.
TE consensus sequences and a hierarchy file of TE order for *A. suecica* can be found in Supplementary Data 5.

Acknowledgments

This work was supported, in part, by DFG SPP 1529 to M.N. and Detlef Weigel. T.M. and M.A.L. were supported by the Czech Science Foundation (grant no. 19-03442S) and the CEITEC 2020 project (grant no. LQ1601). P.Y.N. acknowledges postdoctoral fellowship of the

Research Foundation–Flanders (12S9618N). We thank the Next Generation Sequencing Unit of the Vienna Biocenter Core Facilities (VBCF) for assistance. We thank Svante Holm and Torbjörn Säll for material collections and helpful discussions throughout. We also thank Yves Van de Peer for providing useful feedback on the manuscript, and Joel Sharbrough for pointing us to the CyMIRA database

References

1 Van de Peer Y, Mizrachi E, Marchal K. The evolutionary significance of polyploidy. *Nat Rev Genet* 2017; **18**: 411–424.

2 Soltis PS, Soltis DE. Ancient WGD events as drivers of key innovations in angiosperms. *Curr Opin Plant Biol* 2016; **30**: 159–165.

3 Dehal P, Boore JL. Two rounds of whole genome duplication in the ancestral vertebrate. *PLoS Biol* 2005; **3**: e314.

4 Li Z, Tiley GP, Galuska SR, Reardon CR, Kidder TI, Rundell RJ *et al.* Multiple large-scale gene and genome duplications during the evolution of hexapods. *Proc Natl Acad Sci U S A* 2018; **115**: 4713–4718.

5 Chen ZJ, Sreedasyam A, Ando A, Song Q, De Santiago LM, Hulse-Kemp AM *et al.* Genomic diversifications of five Gossypium allopolyploid species and their impact on cotton improvement. *Nat Genet* 2020; **52**: 525–533.

6 Edger PP, Poorten TJ, VanBuren R, Hardigan MA, Colle M, McKain MR *et al.* Origin and evolution of the octoploid strawberry genome. *Nat Genet* 2019; **51**: 541–547.

7 Ramírez-González RH, Borrill P, Lang D, Harrington SA, Brinton J, Venturini L *et al.* The transcriptional landscape of polyploid wheat. *Science* 2018; **361**. doi:10.1126/science.aar6089.

8 Zhuang W, Chen H, Yang M, Wang J, Pandey MK, Zhang C *et al.* The genome of cultivated peanut provides insight into legume karyotypes, polyploid evolution and crop domestication. Nature Genetics. 2019; **51**: 865–876.

9 Bertioli DJ, Jenkins J, Clevenger J, Dudchenko O, Gao D, Seijo G *et al.* The genome sequence of segmental allotetraploid peanut Arachis hypogaea. *Nat Genet* 2019; **51**: 877–884.

10 Kasianov AS, Klepikova AV, Kulakovskiy IV, Gerasimov ES, Fedotova AV, Besedina EG *et al.* High-quality genome assembly of Capsella bursa-pastoris reveals asymmetry of regulatory elements at early stages of polyploid genome evolution. *Plant J* 2017; **91**: 278–291.

11 Kryvokhyzha D, Milesi P, Duan T, Orsucci M, Wright SI, Glémin S *et al.* Towards the new normal: Transcriptomic convergence and genomic legacy of the two subgenomes of an allopolyploid weed (Capsella bursa-pastoris). *PLoS Genet* 2019; **15**: e1008131.

1226 12 Douglas GM, Gos G, Steige KA, Salcedo A, Holm K, Josephs EB *et al.* Hybrid
1227 origins and the earliest stages of diploidization in the highly successful recent
1228 polyploid Capsella bursa-pastoris. *Proc Natl Acad Sci U S A* 2015; **112**: 2806–
1229 2811.

1230 13 Griffiths AG, Moraga R, Tausen M, Gupta V, Bilton TP, Campbell MA *et al.*
1231 Breaking Free: The Genomics of Allopolyploidy-Facilitated Niche Expansion in
1232 White Clover. *Plant Cell* 2019; **31**: 1466–1487.

1233 14 Gordon SP, Contreras-Moreira B, Levy JJ, Djamei A, Czedik-Eysenberg A,
1234 Tartaglio VS *et al.* Gradual polyploid genome evolution revealed by pan-
1235 genomic analysis of Brachypodium hybridum and its diploid progenitors. *Nat*
1236 *Commun* 2020; **11**: 3670.

1237 15 Catalán P, López-Álvarez D, Bellosta C, Villar L. Updated taxonomic
1238 descriptions, iconography, and habitat preferences of Brachypodium distachyon,
1239 B. stacei , and B. hybridum (Poaceae). *An Jard Bot Madr* 2016; **73**: 028.

1240 16 Paape T, Briskine RV, Halstead-Nussloch G, Lischer HEL, Shimizu-Inatsugi R,
1241 Hatakeyama M *et al.* Patterns of polymorphism and selection in the
1242 subgenomes of the allopolyploid Arabidopsis kamchatica. *Nat Commun* 2018; **9**:
1243 3909.

1244 17 Edger PP, Smith R, McKain MR, Cooley AM, Vallejo-Marin M, Yuan Y *et al.*
1245 Subgenome Dominance in an Interspecific Hybrid, Synthetic Allopolyploid, and a
1246 140-Year-Old Naturally Established Neo-Allopolyploid Monkeyflower. *Plant Cell*
1247 2017; **29**: 2150–2167.

1248 18 Soltis DE, Soltis PS, Pires JC, Kovarik A, Tate JA, Mavrodiev E. Recent and
1249 recurrent polyploidy in Tragopogon (Asteraceae): cytogenetic, genomic and
1250 genetic comparisons. *Biol J Linn Soc Lond* 2004; **82**: 485–501.

1251 19 te Beest M, Le Roux JJ, Richardson DM, Brysting AK, Suda J, Kubesová M *et*
1252 *al.* The more the better? The role of polyploidy in facilitating plant invasions. *Ann*
1253 *Bot* 2012; **109**: 19–45.

1254 20 Novikova PY, Tsuchimatsu T, Simon S, Nizhynska V, Voronin V, Burns R *et al.*
1255 Genome Sequencing Reveals the Origin of the Allotetraploid Arabidopsis
1256 suecica. *Mol Biol Evol* 2017; **34**: 957–968.

1257 21 Fowler NL, Levin DA. Ecological Constraints on the Establishment of a Novel
1258 Polyploid in Competition with Its Diploid Progenitor. *Am Nat* 1984; **124**: 703–
1259 711.

1260 22 Bomblies K, Madlung A. Polyploidy in the Arabidopsis genus. *Chromosome Res*
1261 2014; **22**: 117–134.

1262 23 Hollister JD, Arnold BJ, Svedin E, Xue KS, Dilkes BP, Bomblies K. Genetic
1263 adaptation associated with genome-doubling in autotetraploid Arabidopsis
1264 arenosa. *PLoS Genet* 2012; **8**: e1003093.

1265 24 Bomblies K, Jones G, Franklin C, Zickler D, Kleckner N. The challenge of

1266 evolving stable polyploidy: could an increase in ‘crossover interference distance’
1267 play a central role? *Chromosoma* 2016; **125**: 287–300.

1268 25 Leitch AR, Leitch IJ. Genomic plasticity and the diversity of polyploid plants.
1269 *Science* 2008; **320**: 481–483.

1270 26 Bottani S, Zabet NR, Wendel JF, Veitia RA. Gene Expression Dominance in
1271 Allopolyploids: Hypotheses and Models. *Trends Plant Sci* 2018; **23**: 393–402.

1272 27 Parisod C, Alix K, Just J, Petit M, Sarilar V, Mhiri C *et al.* Impact of transposable
1273 elements on the organization and function of allopolyploid genomes. *New Phytol*
1274 2010; **186**: 37–45.

1275 28 McClintock B. The significance of responses of the genome to challenge.
1276 Science. 1984; **226**: 792–801.

1277 29 Feldman M, Liu B, Segal G, Abbo S, Levy AA, Vega JM. Rapid elimination of
1278 low-copy DNA sequences in polyploid wheat: a possible mechanism for
1279 differentiation of homoeologous chromosomes. *Genetics* 1997; **147**: 1381–1387.

1280 30 Zhang H, Gou X, Zhang A, Wang X, Zhao N, Dong Y *et al.* Transcriptome shock
1281 invokes disruption of parental expression-conserved genes in tetraploid wheat.
1282 *Sci Rep* 2016; **6**: 26363.

1283 31 Wang X, Zhang H, Li Y, Zhang Z, Li L, Liu B. Transcriptome asymmetry in
1284 synthetic and natural allotetraploid wheats, revealed by RNA-sequencing. *New*
1285 *Phytol* 2016; **209**: 1264–1277.

1286 32 Zhang H, Bian Y, Gou X, Zhu B, Xu C, Qi B *et al.* Persistent whole-chromosome
1287 aneuploidy is generally associated with nascent allohexaploid wheat. *Proc Natl*
1288 *Acad Sci U S A* 2013; **110**: 3447–3452.

1289 33 Kashkush K, Feldman M, Levy AA. Gene loss, silencing and activation in a
1290 newly synthesized wheat allotetraploid. *Genetics* 2002; **160**: 1651–1659.

1291 34 Shaked H, Kashkush K, Ozkan H, Feldman M, Levy AA. Sequence elimination
1292 and cytosine methylation are rapid and reproducible responses of the genome
1293 to wide hybridization and allopolyploidy in wheat. *Plant Cell* 2001; **13**: 1749–
1294 1759.

1295 35 Ozkan H, Levy AA, Feldman M. Allopolyploidy-Induced Rapid Genome
1296 Evolution in the Wheat (Aegilops–Triticum) Group. *Plant Cell* 2001; **13**: 1735–
1297 1747.

1298 36 Xiong Z, Gaeta RT, Pires JC. Homoeologous shuffling and chromosome
1299 compensation maintain genome balance in resynthesized allopolyploid Brassica
1300 napus. *Proc Natl Acad Sci U S A* 2011; **108**: 7908–7913.

1301 37 Wu J, Lin L, Xu M, Chen P, Liu D, Sun Q *et al.* Homoeolog expression bias and
1302 expression level dominance in resynthesized allopolyploid Brassica napus. *BMC*
1303 *Genomics* 2018; **19**: 586.

1304 38 Szadkowski E, Eber F, Huteau V, Lodé M, Huneau C, Belcram H *et al.* The first
1305 meiosis of resynthesized Brassica napus, a genome blender. *New Phytol* 2010;
1306 **186**: 102–112.

1307 39 Zhao T, Tao X, Feng S, Wang L, Hong H, Ma W *et al.* LncRNAs in polyploid
1308 cotton interspecific hybrids are derived from transposon neofunctionalization.
1309 *Genome Biol* 2018; **19**: 195.

1310 40 Yoo M-J, Szadkowski E, Wendel JF. Homoeolog expression bias and
1311 expression level dominance in allopolyploid cotton. *Heredity* 2013; **110**: 171–
1312 180.

1313 41 Li A, Liu D, Wu J, Zhao X, Hao M, Geng S *et al.* mRNA and Small RNA
1314 Transcriptomes Reveal Insights into Dynamic Homoeolog Regulation of
1315 Allopolyploid Heterosis in Nascent Hexaploid Wheat. *Plant Cell* 2014; **26**: 1878–
1316 1900.

1317 42 Flagel LE, Wendel JF. Evolutionary rate variation, genomic dominance and
1318 duplicate gene expression evolution during allotetraploid cotton speciation. *New*
1319 *Phytol* 2010; **186**: 184–193.

1320 43 Liu B, Brubaker CL, Mergeai G, Cronn RC, Wendel JF. Polyploid formation in
1321 cotton is not accompanied by rapid genomic changes. *Genome* 2001; **44**: 321–
1322 330.

1323 44 Kashkush K, Feldman M, Levy AA. Transcriptional activation of
1324 retrotransposons alters the expression of adjacent genes in wheat. *Nat Genet*
1325 2003; **33**: 102–106.

1326 45 Kraitshtein Z, Yaakov B, Khasdan V, Kashkush K. Genetic and epigenetic
1327 dynamics of a retrotransposon after allopolyploidization of wheat. *Genetics*
1328 2010; **186**: 801–812.

1329 46 Yaakov B, Kashkush K. Mobilization of Stowaway-like MITEs in newly formed
1330 allohexaploid wheat species. *Plant Mol Biol* 2012; **80**: 419–427.

1331 47 International Wheat Genome Sequencing Consortium (IWGSC), IWGSC
1332 RefSeq principal investigators:, Appels R, Eversole K, Feuillet C, Keller B *et al.*
1333 Shifting the limits in wheat research and breeding using a fully annotated
1334 reference genome. *Science* 2018; **361**. doi:10.1126/science.aar7191.

1335 48 Wang M, Tu L, Yuan D, Zhu D, Shen C, Li J *et al.* Reference genome
1336 sequences of two cultivated allotetraploid cottons, Gossypium hirsutum and
1337 Gossypium barbadense. *Nat Genet* 2019; **51**: 224–229.

1338 49 Yang Z, Ge X, Yang Z, Qin W, Sun G, Wang Z *et al.* Extensive intraspecific
1339 gene order and gene structural variations in upland cotton cultivars. *Nat*
1340 *Commun* 2019; **10**: 2989.

1341 50 Huang G, Wu Z, Percy RG, Bai M, Li Y, Frelichowski JE *et al.* Genome
1342 sequence of Gossypium herbaceum and genome updates of Gossypium
1343 arboreum and Gossypium hirsutum provide insights into cotton A-genome

1344 evolution. *Nat Genet* 2020; **52**: 516–524.

1345 51 Zhang T, Hu Y, Jiang W, Fang L, Guan X, Chen J *et al.* Sequencing of
1346 allotetraploid cotton (Gossypium hirsutum L. acc. TM-1) provides a resource for
1347 fiber improvement. *Nat Biotechnol* 2015; **33**: 531–537.

1348 52 Han J, Masonbrink RE, Shan W, Song F, Zhang J, Yu W *et al.* Rapid
1349 proliferation and nucleolar organizer targeting centromeric retrotransposons in
1350 cotton. *Plant J* 2016; **88**: 992–1005.

1351 53 Wang M, Wang P, Lin M, Ye Z, Li G, Tu L *et al.* Evolutionary dynamics of 3D
1352 genome architecture following polyploidization in cotton. *Nat Plants* 2018; **4**: 90–
1353 97.

1354 54 Cheng F, Wu J, Fang L, Sun S, Liu B, Lin K *et al.* Biased gene fractionation and
1355 dominant gene expression among the subgenomes of Brassica rapa. *PLoS One*
1356 2012; **7**: e36442.

1357 55 Schnable JC, Springer NM, Freeling M. Differentiation of the maize subgenomes
1358 by genome dominance and both ancient and ongoing gene loss. *Proc Natl Acad*
1359 *Sci U S A* 2011; **108**: 4069–4074.

1360 56 International Wheat Genome Sequencing Consortium (IWGSC). A
1361 chromosome-based draft sequence of the hexaploid bread wheat (Triticum
1362 aestivum) genome. *Science* 2014; **345**: 1251788.

1363 57 Chalhoub B, Denoeud F, Liu S, Parkin IAP, Tang H, Wang X *et al.* Plant
1364 genetics. Early allopolyploid evolution in the post-Neolithic Brassica napus
1365 oilseed genome. *Science* 2014; **345**: 950–953.

1366 58 Wang M, Tu L, Lin M, Lin Z, Wang P, Yang Q *et al.* Asymmetric subgenome
1367 selection and cis-regulatory divergence during cotton domestication. *Nat Genet*
1368 2017; **49**: 579–587.

1369 59 Gaut BS, Seymour DK, Liu Q, Zhou Y. Demography and its effects on genomic
1370 variation in crop domestication. *Nat Plants* 2018; **4**: 512–520.

1371 60 Kremling KAG, Chen S-Y, Su M-H, Lepak NK, Romay MC, Swarts KL *et al.*
1372 Dysregulation of expression correlates with rare-allele burden and fitness loss in
1373 maize. *Nature* 2018; **555**: 520–523.

1374 61 Qian L, Qian W, Snowdon RJ. Sub-genomic selection patterns as a signature of
1375 breeding in the allopolyploid Brassica napus genome. *BMC Genomics* 2014; **15**:
1376 1170.

1377 62 Wang L, Beissinger TM, Lorant A, Ross-Ibarra C, Ross-Ibarra J, Hufford MB.
1378 The interplay of demography and selection during maize domestication and
1379 expansion. *Genome Biol* 2017; **18**: 215.

1380 63 Alonge M, Wang X, Benoit M, Soyk S, Pereira L, Zhang L *et al.* Major Impacts of
1381 Widespread Structural Variation on Gene Expression and Crop Improvement in
1382 Tomato. *Cell* 2020; **182**: 145–161.e23.

1383 64 Liu Y, Du H, Li P, Shen Y, Peng H, Liu S *et al.* Pan-Genome of Wild and
1384 Cultivated Soybeans. *Cell* 2020; **182**: 162–176.e13.

1385 65 Zhou Y, Minio A, Massonnet M, Solares E, Lv Y, Beridze T *et al.* The population
1386 genetics of structural variants in grapevine domestication. *Nat Plants* 2019; **5**:
1387 965–979.

1388 66 Buggs RJA, Zhang L, Miles N, Tate JA, Gao L, Wei W *et al.* Transcriptomic
1389 shock generates evolutionary novelty in a newly formed, natural allopolyploid
1390 plant. *Curr Biol* 2011; **21**: 551–556.

1391 67 Chester M, Gallagher JP, Symonds VV, Cruz da Silva AV, Mavrodiev EV, Leitch
1392 AR *et al.* Extensive chromosomal variation in a recently formed natural
1393 allopolyploid species, Tragopogon miscellus (Asteraceae). *Proc Natl Acad Sci U*
1394 *S A* 2012; **109**: 1176–1181.

1395 68 Chelaifa H, Monnier A, Ainouche M. Transcriptomic changes following recent
1396 natural hybridization and allopolyploidy in the salt marsh species Spartina ×
1397 townsendii and Spartina anglica (Poaceae). *New Phytol* 2010; **186**: 161–174.

1398 69 Kryvokhyzha D, Salcedo A, Eriksson MC, Duan T, Tawari N, Chen J *et al.*
1399 Parental legacy, demography, and admixture influenced the evolution of the two
1400 subgenomes of the tetraploid Capsella bursa-pastoris (Brassicaceae). *PLoS*
1401 *Genet* 2019; **15**: e1007949.

1402 70 Akama S, Shimizu-Inatsugi R, Shimizu KK, Sese J. Genome-wide quantification
1403 of homeolog expression ratio revealed nonstochastic gene regulation in
1404 synthetic allopolyploid Arabidopsis. *Nucleic Acids Res* 2014; **42**: e46.

1405 71 Wu H, Yu Q, Ran J-H, Wang X-Q. Unbiased subgenome evolution in
1406 allotetraploid species of Ephedra and its implications for the evolution of large
1407 genomes in gymnosperms. *Genome Biol Evol* 2020. doi:10.1093/gbe/evaa236.

1408 72 Säll T, Lind-Halldén C, Jakobsson M, Halldén C. Mode of reproduction in
1409 Arabidopsis suecica. *Hereditas* 2004; **141**: 313–317.

1410 73 Hohmann N, Wolf EM, Lysak MA, Koch MA. A Time-Calibrated Road Map of
1411 Brassicaceae Species Radiation and Evolutionary History. *Plant Cell* 2015; **27**:
1412 2770–2784.

1413 74 O'Kane SL, Schaal BA, Al-Shehbaz IA. The Origins of Arabidopsis suecica
1414 (Brassicaceae) as Indicated by Nuclear rDNA Sequences. *Syst Bot* 1996; **21**:
1415 559–566.

1416 75 Jakobsson M, Hagenblad J, Tavaré S, Säll T, Halldén C, Lind-Halldén C *et al.* A
1417 unique recent origin of the allotetraploid species Arabidopsis suecica: Evidence
1418 from nuclear DNA markers. *Mol Biol Evol* 2006; **23**: 1217–1231.

1419 76 Novikova PY, Hohmann N, Nizhynska V, Tsuchimatsu T, Ali J, Muir G *et al.*
1420 Sequencing of the genus Arabidopsis identifies a complex history of
1421 nonbifurcating speciation and abundant trans-specific polymorphism. *Nat Genet*
1422 2016; **48**: 1077–1082.

1423 77 Slotte T, Hazzouri KM, Ågren JA, Koenig D, Maumus F, Guo Y-L *et al.* The
1424 Capsella rubella genome and the genomic consequences of rapid mating
1425 system evolution. *Nat Genet* 2013; **45**: 831–835.

1426 78 Liu S, Liu Y, Yang X, Tong C, Edwards D, Parkin IAP *et al.* The Brassica
1427 oleracea genome reveals the asymmetrical evolution of polyploid genomes. *Nat*
1428 *Commun* 2014; **5**: 3930.

1429 79 Madlung A, Tyagi AP, Watson B, Jiang H, Kagochi T, Doerge RW *et al.*
1430 Genomic changes in synthetic Arabidopsis polyploids. *Plant J* 2005; **41**: 221–
1431 230.

1432 80 Copenhaver GP, Pikaard CS. Two-dimensional RFLP analyses reveal
1433 megabase-sized clusters of rRNA gene variants in Arabidopsis thaliana,
1434 suggesting local spreading of variants as the mode for gene homogenization
1435 during concerted evolution. The Plant Journal. 1996; **9**: 273–282.

1436 81 Navashin M. Chromosome Alterations Caused by Hybridization and Their
1437 Bearing upon Certain General Genetic Problems. *Cytologia* 1934; **5**: 169–203.

1438 82 Tucker S, Vitins A, Pikaard CS. Nucleolar dominance and ribosomal RNA gene
1439 silencing. *Curr Opin Cell Biol* 2010; **22**: 351–356.

1440 83 Maciak S, Michalak K, Kale SD, Michalak P. Nucleolar Dominance and
1441 Repression of 45S Ribosomal RNA Genes in Hybrids between Xenopus
1442 borealis and X. muelleri (2n = 36). Cytogenetic and Genome Research. 2016;
1443 **149**: 290–296.

1444 84 Książczyk T, Kovarik A, Eber F, Huteau V, Khaitova L, Tesarikova Z *et al.*
1445 Immediate unidirectional epigenetic reprogramming of NORs occurs
1446 independently of rDNA rearrangements in synthetic and natural forms of a
1447 polyploid species Brassica napus. Chromosoma. 2011; **120**: 557–571.

1448 85 Chen ZJ, Comai L, Pikaard CS. Gene dosage and stochastic effects determine
1449 the severity and direction of uniparental ribosomal RNA gene silencing
1450 (nucleolar dominance) in Arabidopsis allopolyploids. *Proc Natl Acad Sci U S A*
1451 1998; **95**: 14891–14896.

1452 86 Pontes O, Lawrence RJ, Silva M, Preuss S, Costa-Nunes P, Earley K *et al.*
1453 Postembryonic establishment of megabase-scale gene silencing in nucleolar
1454 dominance. *PLoS One* 2007; **2**: e1157.

1455 87 Lewis MS, Pikaard CS. Restricted chromosomal silencing in nucleolar
1456 dominance. *Proc Natl Acad Sci U S A* 2001; **98**: 14536–14540.

1457 88 Pontes O, Neves N, Silva M, Lewis MS, Madlung A, Comai L *et al.*
1458 Chromosomal locus rearrangements are a rapid response to formation of the
1459 allotetraploid Arabidopsis suecica genome. Proceedings of the National
1460 Academy of Sciences. 2004; **101**: 18240–18245.

1461 89 Long Q, Rabanal FA, Meng D, Huber CD, Farlow A, Platzer A *et al.* Massive
1462 genomic variation and strong selection in Arabidopsis thaliana lines from

1463 Sweden. *Nat Genet* 2013; **45**: 884–890.

1464 90 Rabanal FA, Mandáková T, Soto-Jiménez LM, Greenhalgh R, Parrott DL,
1465 Lutzmayer S *et al.* Epistatic and allelic interactions control expression of
1466 ribosomal RNA gene clusters in Arabidopsis thaliana. *Genome Biol* 2017; **18**:
1467 75.

1468 91 Pontes O, Lawrence RJ, Neves N, Silva M, Lee J-H, Chen ZJ *et al.* Natural
1469 variation in nucleolar dominance reveals the relationship between nucleolus
1470 organizer chromatin topology and rRNA gene transcription in Arabidopsis. *Proc*
1471 *Natl Acad Sci U S A* 2003; **100**: 11418–11423.

1472 92 Guo X, Han F. Asymmetric epigenetic modification and elimination of rDNA
1473 sequences by polyploidization in wheat. *Plant Cell* 2014; **26**: 4311–4327.

1474 93 Liu B, Davis TM. Conservation and loss of ribosomal RNA gene sites in diploid
1475 and polyploid Fragaria (Rosaceae). *BMC Plant Biol* 2011; **11**: 1–13.

1476 94 Steige KA, Slotte T. Genomic legacies of the progenitors and the evolutionary
1477 consequences of allopolyploidy. *Curr Opin Plant Biol* 2016; **30**: 88–93.

1478 95 Vicient CM, Casacuberta JM. Impact of transposable elements on polyploid
1479 plant genomes. *Ann Bot* 2017; **120**: 195–207.

1480 96 Ungerer MC, Strakosh SC, Zhen Y. Genome expansion in three hybrid
1481 sunflower species is associated with retrotransposon proliferation. *Curr Biol*
1482 2006; **16**: R872–3.

1483 97 Rieseberg LH, Raymond O, Rosenthal DM, Lai Z, Livingstone K, Nakazato T *et*
1484 *al.* Major ecological transitions in wild sunflowers facilitated by hybridization.
1485 *Science* 2003; **301**: 1211–1216.

1486 98 Cavrak VV, Lettner N, Jamge S, Kosarewicz A, Bayer LM, Mittelsten Scheid O.
1487 How a retrotransposon exploits the plant's heat stress response for its
1488 activation. *PLoS Genet* 2014; **10**: e1004115.

1489 99 Göbel U, Arce AL, He F, Rico A, Schmitz G, de Meaux J. Robustness of
1490 Transposable Element Regulation but No Genomic Shock Observed in
1491 Interspecific Arabidopsis Hybrids. *Genome Biol Evol* 2018; **10**: 1403–1415.

1492 100 Kofler R, Gomez-Sanchez D, Schlotterer C. PoPoolationTE2: Comparative
1493 Population Genomics of Transposable Elements Using Pool-Seq. *Mol Biol Evol*
1494 2016; **33**: 2759–2764.

1495 101 Lockton S, Gaut BS. The evolution of transposable elements in natural
1496 populations of self-fertilizing Arabidopsis thaliana and its outcrossing relative
1497 Arabidopsis lyrata. *BMC Evol Biol* 2010; **10**: 10.

1498 102 Quadrana L, Bortolini Silveira A, Mayhew GF, LeBlanc C, Martienssen RA,
1499 Jeddeloh JA *et al.* The Arabidopsis thaliana mobilome and its impact at the
1500 species level. *Elife* 2016; **5**. doi:10.7554/eLife.15716.

1501 103 Stuart T, Eichten SR, Cahn J, Karpievitch YV, Borevitz JO, Lister R. Population
1502 scale mapping of transposable element diversity reveals links to gene regulation
1503 and epigenomic variation. *Elife* 2016; **5**. doi:10.7554/eLife.20777.

1504 104 Wolfe KH. Yesterday's polyploids and the mystery of diploidization. *Nat Rev*
1505 *Genet* 2001; **2**: 333–341.

1506 105 Conant GC, Birchler JA, Pires JC. Dosage, duplication, and diploidization:
1507 clarifying the interplay of multiple models for duplicate gene evolution over time.
1508 *Curr Opin Plant Biol* 2014; **19**: 91–98.

1509 106 Aköz G, Nordborg M. The Aquilegia genome reveals a hybrid origin of core
1510 eudicots. *Genome Biol* 2019; **20**: 256.

1511 107 Jiao Y, Wickett NJ, Ayyampalayam S, Chanderbali AS, Landherr L, Ralph PE *et*
1512 *al.* Ancestral polyploidy in seed plants and angiosperms. *Nature* 2011; **473**: 97–
1513 100.

1514 108 Soltis PS, Marchant DB, Van de Peer Y, Soltis DE. Polyploidy and genome
1515 evolution in plants. *Curr Opin Genet Dev* 2015; **35**: 119–125.

1516 109 Thomas BC, Pedersen B, Freeling M. Following tetraploidy in an Arabidopsis
1517 ancestor, genes were removed preferentially from one homeolog leaving
1518 clusters enriched in dose-sensitive genes. *Genome Res* 2006; **16**: 934–946.

1519 110 Renny-Byfield S, Gong L, Gallagher JP, Wendel JF. Persistence of subgenomes
1520 in paleopolyploid cotton after 60 my of evolution. *Mol Biol Evol* 2015; **32**: 1063–
1521 1071.

1522 111 Garsmeur O, Schnable JC, Almeida A, Jourda C, D'Hont A, Freeling M. Two
1523 evolutionarily distinct classes of paleopolyploidy. *Mol Biol Evol* 2014; **31**: 448–
1524 454.

1525 112 Li Q, Qiao X, Yin H, Zhou Y, Dong H, Qi K *et al.* Unbiased subgenome evolution
1526 following a recent whole-genome duplication in pear (Pyrus bretschneideri
1527 Rehd.). *Hortic Res* 2019; **6**: 34.

1528 113 Shan S, Boatwright JL, Liu X, Chanderbali AS, Fu C, Soltis PS *et al.*
1529 Transcriptome Dynamics of the Inflorescence in Reciprocally Formed
1530 Allopolyploid Tragopogon miscellus (Asteraceae). *Front Genet* 2020; **11**: 888.

1531 114 Bird KA, Niederhuth C, Ou S, Gehan M, Chris Pires J, Xiong Z *et al.* Replaying
1532 the evolutionary tape to investigate subgenome dominance in allopolyploid
1533 Brassica napus. doi:10.1101/814491.

1534 115 Alger EI, Edger PP. One subgenome to rule them all: underlying mechanisms of
1535 subgenome dominance. *Curr Opin Plant Biol* 2020; **54**: 108–113.

1536 116 Carlson KD, Fernandez-Pozo N, Bombarely A, Pisupati R, Mueller LA, Madlung
1537 A. Natural variation in stress response gene activity in the allopolyploid
1538 Arabidopsis suecica. *BMC Genomics* 2017; **18**: 653.

1539 117 Chang PL, Dilkes BP, McMahon M, Comai L, Nuzhdin SV. Homoeolog-specific
1540 retention and use in allotetraploid Arabidopsis suecica depends on parent of
1541 origin and network partners. *Genome Biol* 2010; **11**: R125.

1542 118 Adams KL, Percifield R, Wendel JF. Organ-specific silencing of duplicated
1543 genes in a newly synthesized cotton allotetraploid. *Genetics* 2004; **168**: 2217–
1544 2226.

1545 119 Sicard A, Lenhard M. The selfing syndrome: a model for studying the genetic
1546 and evolutionary basis of morphological adaptation in plants. *Ann Bot* 2011;
1547 **107**: 1433–1443.

1548 120 Lu Y-J, Swamy KBS, Leu J-Y. Experimental Evolution Reveals Interplay
1549 between Sch9 and Polyploid Stability in Yeast. *PLoS Genet* 2016; **12**:
1550 e1006409.

1551 121 Yant L, Hollister JD, Wright KM, Arnold BJ, Higgins JD, Franklin FC *et al.*
1552 Meiotic adaptation to genome duplication in Arabidopsis arenosa. *Curr Biol*
1553 2013; **23**: 2151–2156.

1554 122 Morgan C, Zhang H, Henry CE, Franklin FCH, Bomblies K. Derived alleles of
1555 two axis proteins affect meiotic traits in autotetraploid Arabidopsis arenosa. *Proc*
1556 *Natl Acad Sci U S A* 2020; **117**: 8980–8988.

1557 123 Haga N, Kobayashi K, Suzuki T, Maeo K, Kubo M, Ohtani M *et al.* Mutations in
1558 MYB3R1 and MYB3R4 cause pleiotropic developmental defects and preferential
1559 down-regulation of multiple G2/M-specific genes in Arabidopsis. *Plant Physiol*
1560 2011; **157**: 706–717.

1561 124 Forsythe ES, Sharbrough J, Havird JC, Warren JM, Sloan DB. CyMIRA: The
1562 Cytonuclear Molecular Interactions Reference for Arabidopsis. *Genome Biol*
1563 *Evol* 2019; **11**: 2194–2202.

1564 125 Wu Y, Lin F, Zhou Y, Wang J, Sun S, Wang B *et al.* Genomic mosaicism due to
1565 homoeologous exchange generates extensive phenotypic diversity in nascent
1566 allopolyploids. *Natl Sci Rev* 2020. doi:10.1093/nsr/nwaa277.

1567 126 Darwin C. The origin of species by means of natural selection : or The
1568 preservation of favored races in the struggle for life / by Charles Darwin. 1872.
1569 doi:10.5962/bhl.title.2106.

1570 127 Chin C-S, Peluso P, Sedlazeck FJ, Nattestad M, Concepcion GT, Clum A *et al.*
1571 Phased diploid genome assembly with single-molecule real-time sequencing.
1572 *Nat Methods* 2016; **13**: 1050–1054.

1573 128 Koren S, Walenz BP, Berlin K, Miller JR, Bergman NH, Phillippy AM. Canu:
1574 scalable and accurate long-read assembly via adaptive k-mer weighting and
1575 repeat separation. *Genome Res* 2017; **27**: 722–736.

1576 129 Chakraborty M, Baldwin-Brown JG, Long AD, Emerson JJ. Contiguous and
1577 accurate de novo assembly of metazoan genomes with modest long read
1578 coverage. *Nucleic Acids Res* 2016; **44**: e147.

130 Chin C-S, Alexander DH, Marks P, Klammer AA, Drake J, Heiner C *et al.* Nonhybrid, finished microbial genome assemblies from long-read SMRT sequencing data. Nature Methods. 2013; **10**: 563–569.

131 Walker BJ, Abeel T, Shea T, Priest M, Abouelliel A, Sakthikumar S *et al.* Pilon: an integrated tool for comprehensive microbial variant detection and genome assembly improvement. *PLoS One* 2014; **9**: e112963.

132 Wingett S, Ewels P, Furlan-Magaril M, Nagano T, Schoenfelder S, Fraser P *et al.* HiCUP: pipeline for mapping and processing Hi-C data. *F1000Res* 2015; **4**: 1310.

133 Marçais G, Delcher AL, Phillippy AM, Coston R, Salzberg SL, Zimin A. MUMmer4: A fast and versatile genome alignment system. *PLoS Comput Biol* 2018; **14**: e1005944.

134 Burton JN, Adey A, Patwardhan RP, Qiu R, Kitzman JO, Shendure J. Chromosome-scale scaffolding of de novo genome assemblies based on chromatin interactions. *Nat Biotechnol* 2013; **31**: 1119–1125.

135 Li H, Durbin R. Fast and accurate short read alignment with Burrows-Wheeler transform. *Bioinformatics* 2009; **25**: 1754–1760.

136 Li H, Handsaker B, Wysoker A, Fennell T, Ruan J, Homer N *et al.* The Sequence Alignment/Map format and SAMtools. *Bioinformatics* 2009; **25**: 2078–2079.

137 Himmelmann L. HMM: Hidden Markov Models. *R package version* 2010; **1**.

138 Broman KW, Wu H, Sen S, Churchill GA. R/qtl: QTL mapping in experimental crosses. *Bioinformatics* 2003; **19**: 889–890.

139 Durand NC, Shamim MS, Machol I, Rao SSP, Huntley MH, Lander ES *et al.* Juicer Provides a One-Click System for Analyzing Loop-Resolution Hi-C Experiments. *Cell Syst* 2016; **3**: 95–98.

140 Stanke M, Morgenstern B. AUGUSTUS: a web server for gene prediction in eukaryotes that allows user-defined constraints. *Nucleic Acids Res* 2005; **33**: W465–7.

141 Seppey M, Manni M, Zdobnov EM. BUSCO: Assessing Genome Assembly and Annotation Completeness. In: Kollmar M (ed). *Gene Prediction: Methods and Protocols*. Springer New York: New York, NY, 2019, pp 227–245.

142 Rawat V, Abdelsamad A, Pietzenuk B, Seymour DK, Koenig D, Weigel D *et al.* Improving the Annotation of Arabidopsis lyrata Using RNA-Seq Data. *PLoS One* 2015; **10**: e0137391.

143 Gremme G, Brendel V, Sparks ME, Kurtz S. Engineering a software tool for gene structure prediction in higher organisms. *Information and Software Technology* 2005; **47**: 965–978.

1617 144 Kim D, Pertea G, Trapnell C, Pimentel H, Kelley R, Salzberg SL. TopHat2:
1618 accurate alignment of transcriptomes in the presence of insertions, deletions
1619 and gene fusions. *Genome Biol* 2013; **14**: R36.

1620 145 Grabherr MG, Haas BJ, Yassour M, Levin JZ, Thompson DA, Amit I *et al.* Full-
1621 length transcriptome assembly from RNA-Seq data without a reference genome.
1622 *Nat Biotechnol* 2011; **29**: 644–652.

1623 146 Fu L, Niu B, Zhu Z, Wu S, Li W. CD-HIT: accelerated for clustering the next-
1624 generation sequencing data. *Bioinformatics* 2012; **28**: 3150–3152.

1625 147 Li W, Godzik A. Cd-hit: a fast program for clustering and comparing large sets of
1626 protein or nucleotide sequences. *Bioinformatics* 2006; **22**: 1658–1659.

1627 148 Smit AFA, Hubley R. RepeatModeler Open-1.0 http://www.repeatmasker.org.
1628 2008-2015.

1629 149 Smit AFA, Hubley R, Green P. RepeatMasker Open-4.0. . 2013-2015.

1630 150 Bailly-Bechet M, Haudry A, Lerat E. 'One code to find them all': a perl tool to
1631 conveniently parse RepeatMasker output files. *Mob DNA* 2014; **5**: 13.

1632 151 Lyons E, Pedersen B, Kane J, Freeling M. The value of nonmodel genomes and
1633 an example using SynMap within CoGe to dissect the hexaploidy that predates
1634 the rosids. *Trop Plant Biol* 2008; **1**: 181–190.

1635 152 Lyons E, Freeling M. How to usefully compare homologous plant genes and
1636 chromosomes as DNA sequences. *Plant J* 2008; **53**: 661–673.

1637 153 Rabanal FA, Nizhynska V, Mandáková T, Novikova PY, Lysak MA, Mott R *et al.*
1638 Unstable Inheritance of 45S rRNA Genes in Arabidopsis thaliana. *G3* 2017; **7**:
1639 1201–1209.

1640 154 Dobin A, Davis CA, Schlesinger F, Drenkow J, Zaleski C, Jha S *et al.* STAR:
1641 ultrafast universal RNA-seq aligner. *Bioinformatics* 2013; **29**: 15–21.

1642 155 Robinson MD, McCarthy DJ, Smyth GK. edgeR: a Bioconductor package for
1643 differential expression analysis of digital gene expression data. *Bioinformatics*
1644 2010; **26**: 139–140.

1645 156 Alexa A, Rahnenfuhrer J. topGO: enrichment analysis for gene ontology. *R*
1646 *package version* 2010; **2**: 2010.

1647 157 Durinck S, Spellman PT, Birney E, Huber W. Mapping identifiers for the
1648 integration of genomic datasets with the R/Bioconductor package biomaRt. *Nat*
1649 *Protoc* 2009; **4**: 1184–1191.

1650 158 Hahne F, LeMeur N, Brinkman RR, Ellis B, Haaland P, Sarkar D *et al.* flowCore:
1651 a Bioconductor package for high throughput flow cytometry. *BMC Bioinformatics*
1652 2009; **10**: 106.

1653 159 Marçais G, Kingsford C. A fast, lock-free approach for efficient parallel counting

of occurrences of k-mers. *Bioinformatics* 2011; **27**: 764–770.

160 Sun H, Ding J, Piednoël M, Schneeberger K. findGSE: estimating genome size variation within human and Arabidopsis using k-mer frequencies. *Bioinformatics* 2018; **34**: 550–557.

161 Genomes Consortium. Electronic address, magnus nordborg gmi oeaw ac at, Genomes, Consortium. 1,135 Genomes Reveal the Global Pattern of Polymorphism in Arabidopsis thaliana. *Cell* 2016; **166**: 481–491.

162 McKenna A, Hanna M, Banks E, Sivachenko A, Cibulskis K, Kernytsky A *et al.* The Genome Analysis Toolkit: a MapReduce framework for analyzing next-generation DNA sequencing data. *Genome Res* 2010; **20**: 1297–1303.

163 Cingolani P, Platts A, Wang LL, Coon M, Nguyen T, Wang L *et al.* A program for annotating and predicting the effects of single nucleotide polymorphisms, SnpEff: SNPs in the genome of Drosophila melanogaster strain w1118; iso-2; iso-3. *Fly* 2012; **6**: 80–92.

164 Mandáková T, Lysak MA. Chromosome Preparation for Cytogenetic Analyses in Arabidopsis. *Curr Protoc Plant Biol* 2016; **1**: 43–51.

165 O'Malley RC, Huang S-SC, Song L, Lewsey MG, Bartlett A, Nery JR *et al.* Cistrome and Epicistrome Features Shape the Regulatory DNA Landscape. *Cell* 2016; **165**: 1280–1292.